A POWER QUALITY MONITORING SYSTEM FOR A 20 kW OCEAN TURBINE

By
Kevin Cook

A Thesis Submitted to the Faculty of

The College of Engineering and Computer Science

in Partial Fulfillment of the Requirements for the Degree of

Master of Science

Florida Atlantic University SeaTech Campus

Dania Beach, FL.

July 2010

A POWER QUALITY MONITORING SYSTE FOR THE CENTER OF OCEAN AND ENERGY TECHNOLOGY'S OCEAN TURBINE

By

Kevin Cook

This thesis was prepared under the direction of the candidate's thesis advisor, Dr. Nikolas I. Xiros. Department of Ocean and Mechanical Engineering, and has been approved by the members of his supervisory committee. It was submitted to the faculty of the College of Engineering and Computer Science and was accepted in partial fulfillment of the requirements for the degree of Master of Science.

SUPERVISORY COMMITTEE:

_____
Nikolas I. Xiros, Ph. D,
Thesis Advisor

_____
Manhar Dhanak, Ph. D,

_____
Pierre-Philippe Beaujean, Ph. D.

_____
Mohammad Ilyas, Ph. D,
Chairman, Department of Ocean and Mechanical Engineering

_____
Karl K. Stevens, Ph.D., P.E.
Dean, College of Engineering and Computer Science

_____ _____
Barry T. Rosson, Ph.D. Date
Dean, Graduate College

ACKNOWLEDGEMENTS

First of all I would like my gratitude express appreciation to my committee members, Dr. Nikolaos Xiros, Dr. Pierre-Philippe Beaujean and Dr.Manhar Dhanak under whose supervision this work was completed.

I would like to express to the supervisor of this work Dr. Nikolaos Xiros for his guidance and effort in this work. I would also like to express appreciation to Dr. Beaujean for his counsel and care and for his help in getting projects pushed along so that this work could be completed.

Special thanks are also owed to the staff at FAU, in particular, Caitlin Slezycki, Tom Pantelakis, Ed Henderson, John Kielbasa, and Beatriz Gomez. Thank you for your constant willingness to share your expertise and for your help with the technical aspects of this work.

To my parents I give thanks for their lessons in life that taught me the value of hard work and to never give up.

Last but not least, I would like to give a special thanks to my wife Krissie who let me move her across the country so that I could achieve my Master's degree. Also thanks to my children Stellan and Rachelle along with their mother, who are my inspiration and have provided all of the motivation for my success

ABSTRACT

Author: Kevin Cook

Title: A power quality monitoring system for the Center of Ocean Energy and Technology's ocean turbine.

Institution: Florida Atlantic University

Thesis Advisor: Dr. Nikolaos I Xiros

Degree: Master of Science in Ocean Engineering

Year: 2010

This thesis explores an approach for the measurement of the quality of power generated by the Center of Ocean and Energy Technology's prototype ocean turbine. The work includes the development of a system that measures the current and voltage waveforms for all three phases of power created by the induction generator and quantifies power variations and events that occur within the system. These so called "power quality indices" are discussed in detail including the definition of each and how they are calculated using LabView. The results of various tests demonstrate that this system is accurate and may be implemented in the ocean turbine system to measure the quality of power produced by the turbine. The work then explores a dynamic model of the ocean turbine system that can be used to simulate the response of the turbine to varying conditions.

Table of Contents

List of Figures

List of Tables

1 Introduction and objectives.

1.1 Motivation

With the price of oil consistently increasing and the spending power of the general population decreasing, it is getting more and more important to find alternative sources of energy. This is especially important in Florida where the demands in energy are expected to grow by at least 30 % in the next 10 years.[1] To meet this need the Center for Ocean Energy and Technology (COET) at Florida Atlantic University (FAU) is developing an ocean turbine that will be used to harness the energy of the Gulf Stream Current and convert it to electrical energy that can be used to meet the future demands of Florida.

"On the other hand, the increased use of sensitive electronic circuitry by industrial, commercial and residential customers, as well as the progress of utility deregulation and competition has imposed greater demand on the quality" of [2] power that is delivered by the energy grid. As such in order to be considered a viable source of energy, the COET ocean turbine must be able to supply power that is considered by standards to be high quality. If the power developed is not high quality then the result will be the creation of voltage variation, flicker and waveform distortion of the energy delivered to the power grid.[3] Meeting the standards is especially important because utility companies such as Florida Power and Light (FPL) want to see that the ocean turbine can produce enough high quality power before they will invest in implementing this technology which is the overall goal of the research into the ocean turbine.[4] This thesis focuses on the

development of a system that will monitor certain power quality parameters and send a warning when these parameters fall below power quality standards. Although the equipment and means to measure power quality are available due to extensive research for wind turbines, the devices that measure power quality are relatively expensive. The goal of this thesis is the development of a monitoring system that will be precise in measuring power quality as well as being cost effective.

The design includes a list of all sensors needed as well as their setup configuration. It also includes the algorithms that were developed in LabView to calculate power quality values as well as monitoring when power values fall outside of threshold levels. This power quality monitoring system can also be used in the development of a fault analysis system as changes in power quality can be linked to the wearing of the motor windings as well as other faults that may occur within the ocean turbine system.

1.2 System description

The 20 kW ocean energy turbine developed by the Center of Ocean Energy and Technology at FAU (COET) is designed to produce energy by rotation of a three-blade propeller connected to an asynchronous electric motor/generator through a shaft supported by needle bearing and a planetary gear reduction box. The turbine is tethered to a barge and anchored to the seafloor via a towline

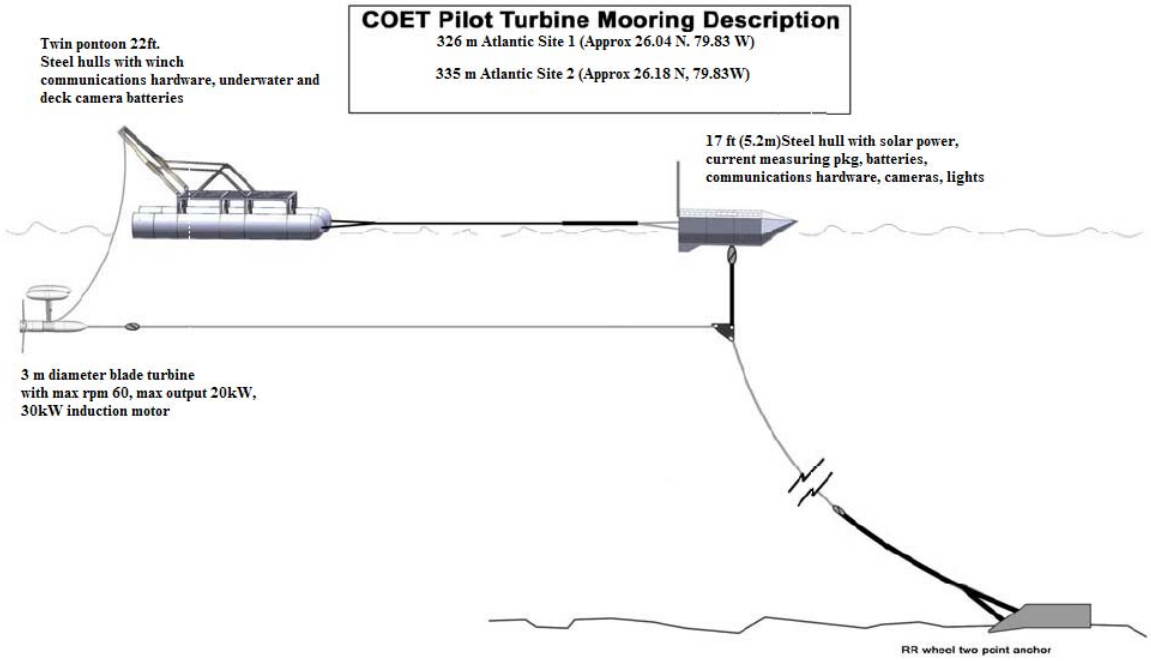

Figure 1 Ocean Turbine Configuration (Courtesy of Driscoll).

As the propeller turns, an AC induction generator converts mechanical energy into electrical energy. This energy will then be conducted to a resistor bank located on the barge. The electrical system is shown below in Figure 2 and is the central focus of this thesis.

1.3 The ocean turbine electrical system

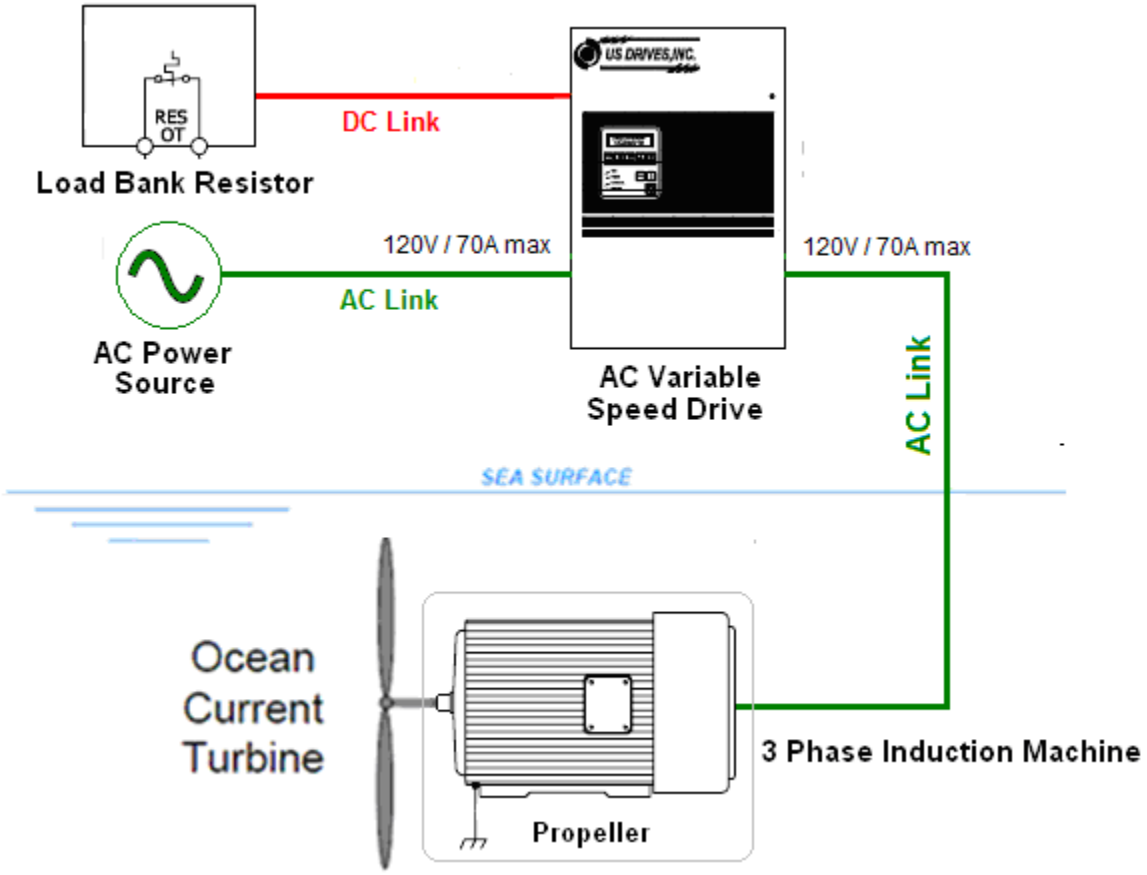

Figure 2: Schematic of the ocean turbine electrical system.

As Figure 2 shows, the electrical system is made up of the following components:

- AC voltage source
- Resistor load bank
- AC variable speed drive
- 3 phase induction machine

AC Voltage Source: Initially the ocean current will not provide enough torque to begin rotating the turbine blades. Instead, an AC source will be employed that will provide the initial momentum.

Resistor Load Bank: The power produced by the turbine will eventually be supplied to the power grid. However, for the prototype application the energy will be converted to heat as the power is passed through a bank of resistors.

AC Variable Speed Drive: The AC drive is used to control the speed of the induction motor as well as the current through the resistor bank for any given period of time. To accomplish this, the AC drive receives AC power as an input. It then can control the amount of power by converting it to an adjustable frequency and adjustable voltage output for controlling the operation of the induction motor.[5] For this project the Phoenix EX Vector AC Drive manufactured by US drives, Inc. will be used. The schematic of the drive is shown here in Figure 3.

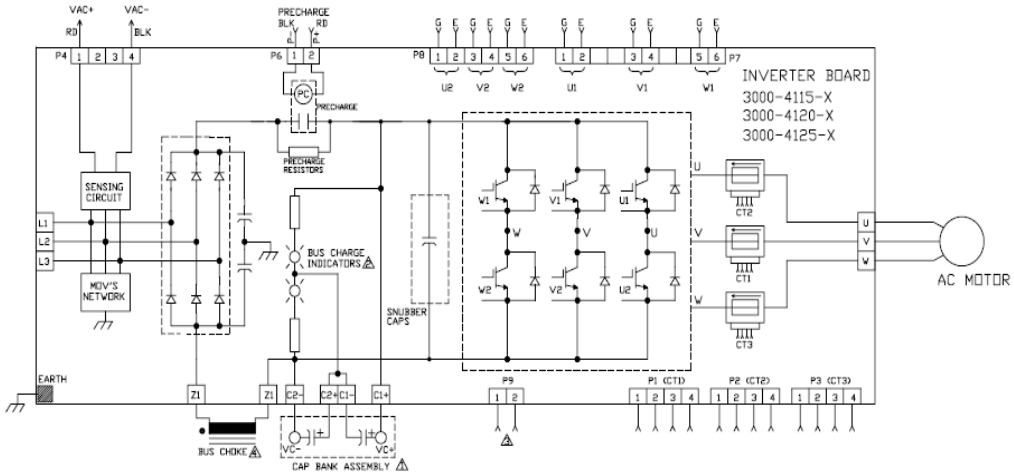

Figure 3: Schematic of Phoenix EX Vector AC Drive.[6]

Figure 3 shows the diode rectifier in series with the transistor inverter. The voltages across the gates of the transistor are controlled by a PID controller.

Diode Rectifier: The Phoenix EX AC drive uses a 3 phase diode-bridge rectifier to convert the incoming AC voltage into a DC voltage that is approximately equal to the magnitude of the input AC voltage. The output of the rectifier makes up the DC link that runs to the load bank resistor as well as the inverter part of the AC drive.

Switch Inverter: Figure 2 illustrates that at all times the DC link will be connected to two voltage sources. The first source is the AC power supply that is represented in Figure 2. The second source is the induction generator. With two sources supplying voltage to the resistor bank it is necessary to have a control over the amount of voltage across the resistor bank at any time. This is the function of the inverter which is composed of a series of transistor switches. When the voltage across the resistor bank is too high, the inverter switches can be opened so that no current flows from the induction machine. Likewise if the voltage is too low the switches can be closed in order to bring the voltage level up to the correct value. The inverter used in the Phoenix EX AC drive uses a 3 phase full bridge inverter to control this voltage.

3 Phase Induction Machine: The 3 Phase induction machine is a rotating electric machine that can either convert electrical energy into mechanical energy or vice versa depending on the setting of the device. As the rotor of the induction machine spins the

mechanical energy of the motion of the blades will be turned into electrical energy which will then be supplied to the resistor bank.

1.4 Thesis contributions

This thesis presents the system that will be used to monitor power quality while the turbine is in operation. Chapter 2 begins by defining power quality and discusses the parameters needed in order for it to be measured. This Chapter then discusses the hardware that will be used and how it will be implemented in the ocean turbine electrical system. In Chapter 3 a detailed definition of power quality and how power quality parameters are quantified is discussed. This Chapter also explains how each parameter will be calculated and is concluded with a discussion of how these calculations are implemented in National Instruments LabView software package. The next step of this thesis is the development of a model of the ocean turbine system. Chapter 4 discusses the design of this model and provides an analysis of simulated data. Next this paper discusses in Chapter 5 how the system was verified and proven to be accurate in calculating power quality parameters. Chapter 6 and 7 then discuss future work that may be done as well as presenting conclusions from this work.

2 The power quality monitoring system

2.1 Parameters

The International Electrotechnical Commission (IEC) defines power quality as "Characteristics of the electricity at a given point on an electrical system evaluated against a set of reference technical parameters[7]." This definition can be simplified to be "the combination of voltage and current quality[8]." The terms voltage and current quality refer to how much each waveform deviates from their ideal forms. For simplicity the ideal form can be defined as a sinusoidal wave. As voltage and current waveforms are the basis for power quality, this thesis was developed to capture the voltage and current waveforms produced by this system and to analyze them.

There are three locations in the ocean turbine system where voltage and current waveforms are measured. The first is between the AC power and the AC drive controller. If any fluctuations occur within this line they will be manifest on the total power output of the resistor load bank. To be able to account for any power quality issues that arise from the AC power source the waveforms are collected from this power line. As the turbine itself is the focus of this work, the voltage and current waveforms will also be measured between the turbine and the AC drive. These waveforms will give the best indication as to the quality of power that is generated by the ocean turbine. Lastly, because power quality is ultimately a consumer driven issue[9] the power must also be monitored across the load bank resistor.

It should be noted that the purpose of this thesis is not to create a power quality monitoring that will be used for an automatic intervention in the system, but instead the measurements will be used to send alerts when values fall under accepted levels. When this occurs the data will be recorded and used to diagnose equipment malfunction, the cause of power quality problems and to provide statistical information on the power system. It should also be noted that this thesis will focus strictly on the monitoring of stationary signals as they have the greatest effect on power quality. This work, however does provide a basis for research to be continued in the area of monitoring non-stationary signals.

There have been many studies that have introduced various methods for measuring and quantifying power quality. From these it has been found that the most important aspects in measuring Power Quality are the requirements for data acquisition. The analog to digital converter that will be used to measure the waveforms has enough range to accommodate the highest value of the sample while at the same time maintaining enough resolution to achieve the necessary accuracy[10]. Some of the resolution limits for odd-order harmonics are shown below in Table 1. To account for these values sensors were selected that have 24 bit resolution.

Table 1: Resolution needed for measuring harmonic voltages.

Systems	Limit	Accuracy	Resolution
Distribution	3.0%	± 0.150%	≥ 11 bits
Subtransmission	1.5%	± 0.075%	≥ 12 bits
Transmission	1.0%	± 0.050%	≥ 12 bits

2.2 Hardware setup

A general scheme for monitoring the power quality of the turbine is shown in Figure 4.

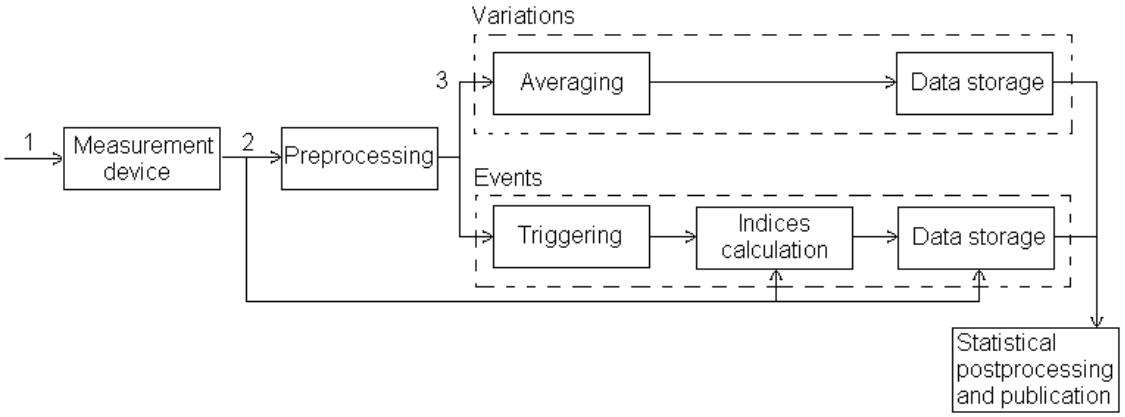

Figure 4: General Scheme of power quality measurements: Voltage or current in the system: Sampled and digitized voltage or current: Quantify data for further processing. [8]

From Figure 4 the first step in the development of the power quality monitoring system was to select sensors and find where they should be placed within the electrical system of the ocean turbine. As discussed previously there are three locations where the power quality should be measured. First the power from the AC source is measured. Second the power from the ocean turbine is measured and third the power across the resistor load bank is also measured. The general setup of the monitoring system is shown here in Figure 5.

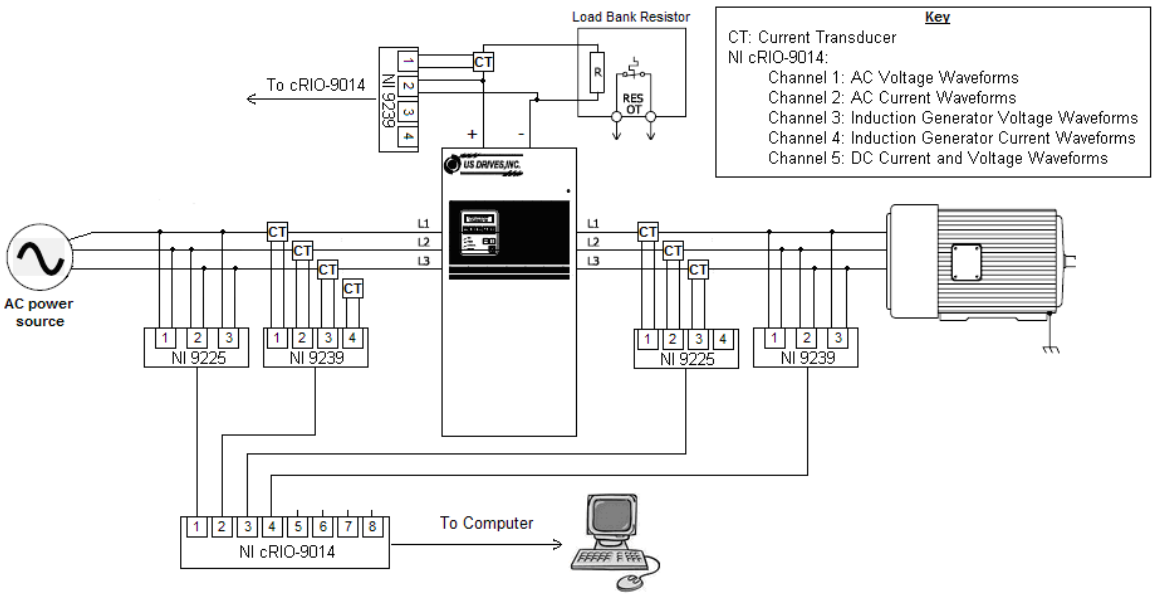

Figure 5: Power Quality Monitoring System.

2.2.1 Measurement devices

The voltage and current waveforms produced by the induction machine will be recorded using sensors created by National instruments (NI). These sensors are connected to the NI cRIO-9014 Real-Time PowerPC Embedded Controller which will collect the data and transfer it to a PC via an Ethernet connection. The analysis and processing of the waveform data will be performed using National Instrument (NI) LabView environment. The analysis of the data will be used to quantify the power quality indices which will lead to the detection of events or variations that occur while the system is in operation. Each sensor is discussed in detail below.

Measuring Voltage Waveform: The NI 9225 300 Vrms C Series analog input module is designed for the waveform measurements of high-voltage signals. It also has three

channels so it is ideal for the monitoring of the 3 phase induction motor. Because this system will be in water it is also necessary to ensure that each line be isolated from the others in order to prevent the short circuiting of the equipment. The NI 9225 has 600 V of continuous channel-to-channel isolation for measurements with differing potentials, as well as 2,300 Vrms transient withstand for protection from sudden voltage spikes that may occur. The NI 9225 also uses four 24-bit analog-to-digital converters (ADCs) for true simultaneous sampling at 50 kS/s. This means that we can take samples simultaneously with a current waveform device and monitor the phase offset between current and voltage which in turn provides the power factor of the system.

Measuring Current Waveform: To measure high currents safely, the typical practice is to use a special purpose Current Transformer (CT) or transducer which reduces the magnitude of the current in the circuit to a more manageable level. The power quality monitoring system uses LEM HTB 100-P current transducer to measure the current waveforms. These devices convert the current waveform to voltage using the Hall Effect. The conversion is rated at .08 volts per amp. This means that if there is 1 Amp running through the line that the input module will see .08 volts. The voltage waveform will be read by the NI 9239 device which has the same specs as the NI 9225 except that its max voltage is 10 V which is well within design parameters as the maximum voltage that can be expected is 5.8V

RMS Values: The NI 9225 and the NI 9239 will input waveforms into the software package LabView. There the rms values of each signal will be calculated. To ensure the

validity of these calculations the rms values will be compared to rms values monitored in the safety system of the Ocean Turbine[11].

Data Collection: The National Instruments cRIO-9014 controller features an industrial 400 MHz real-time processor for deterministic and reliable real-time applications.[12] Because of this feature the manipulation of data will be performed within this unit which saves memory for other applications. The controller is also designed for extreme ruggedness and reliability which makes it ideal for this application. This device collects the data from each module and will send the data via an Ethernet port to a computer where the results of the data processing may be viewed.

2.2.2 Power quality monitoring sensor board

With the sensors and their configuration chosen the next step was to develop a sensor board that runs the sensors and collects data. The sensor board consists of the current transducers, a terminal block and a power source for the transducers. It also has built in fuses to protect the NI devices and a led to show when the board is powered.

2.2.2.1 Sensor board design

The design of the board consisted of several steps. The first was the development of the footprints for the circuit board so that each part could be placed. To do this each part had

to be created using PCAD's library executive program. A sample of the current transducers is shown here in Figure 6.

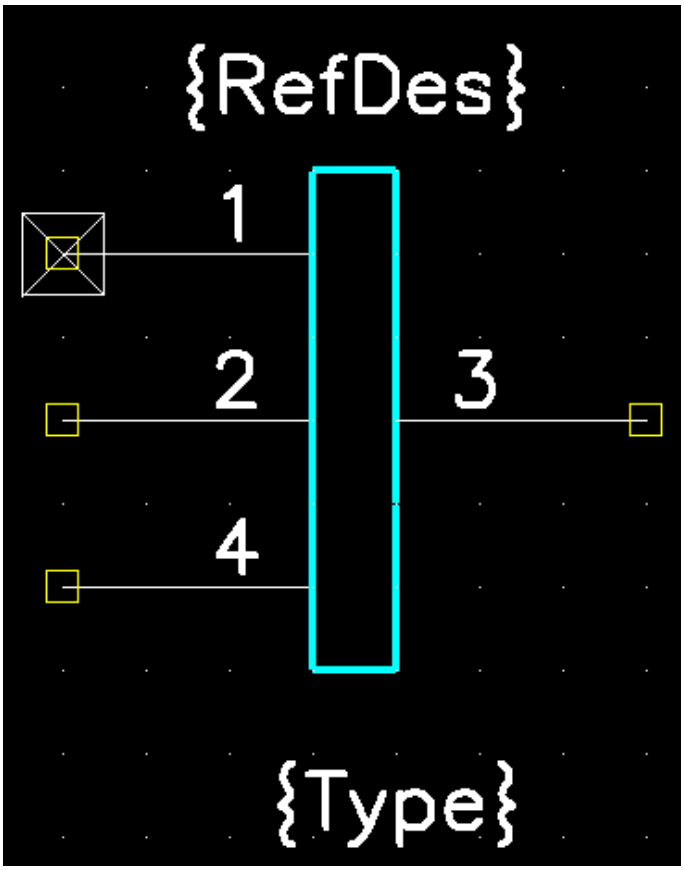

Figure 6: Current Transducer Symbol.

This step consisted of defining each wire to match the terminals of each device. Once the part was created the next step was to develop a footprint of each part for the PCB board. These footprints are used to drill holes in the PCB board so that each part may be mounted. The footprint for the current transducer is shown below in Figure 7. The footprints were designed so that the green line represents the actual size of the part and

the white line will be a little outline of the part. This is done so that they may be easily placed on the board.

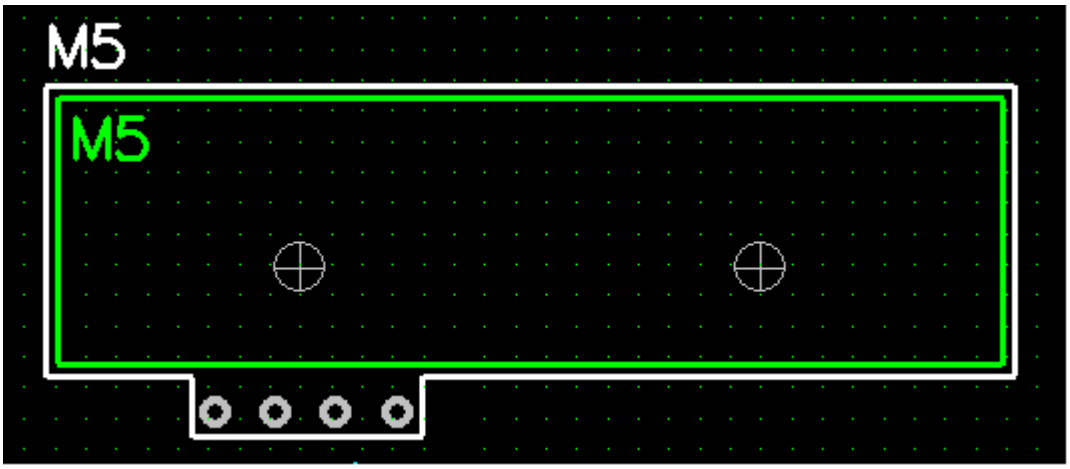

Figure 7: Footprint of Current Transducer.

2.2.2.2 Sensor board schematic

Once all of the parts and their footprints were developed the next step was to create a schematic of how the power quality sensor board is wired. The schematic is shown here in the following 3 figures and was designed using the PCAD schematic program.

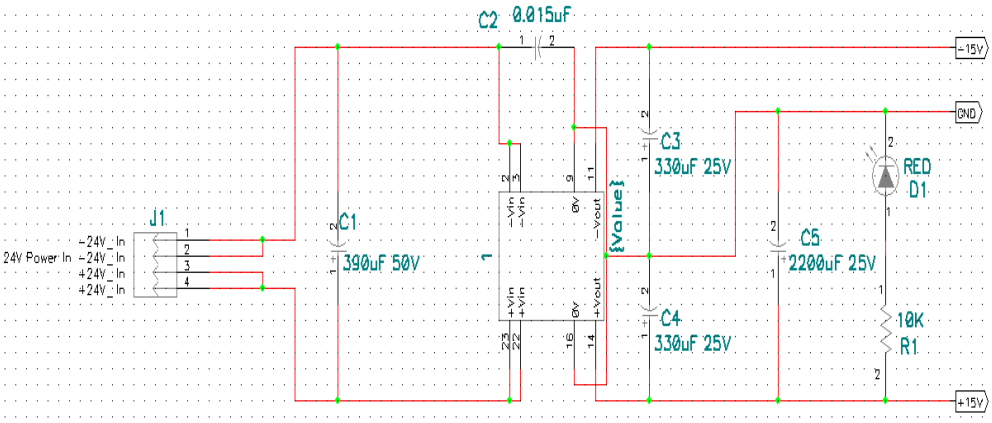

Figure 8: Schematic 1: Power supply of sensor board.

Most of the machine condition monitoring hardware for the ocean turbine, as well as the cRIO-9014 controller is powered by a 24 volt source. The current transducers however, have an input power of 15V. Rather than have a separate power source for the transducers the sensor board uses a 24 to 15V DC to DC converter to power the current transducers. This device is represented as "1" on the schematic shown above. "J1" represents the 24V input. The rest of the schematic shows several resistors that are used to isolate this power from the rest of the board. It shows that red led (D1) that lights up whenever the board is powered. The schematic also shows the positive and negative 15V that are used to power the current transducers.

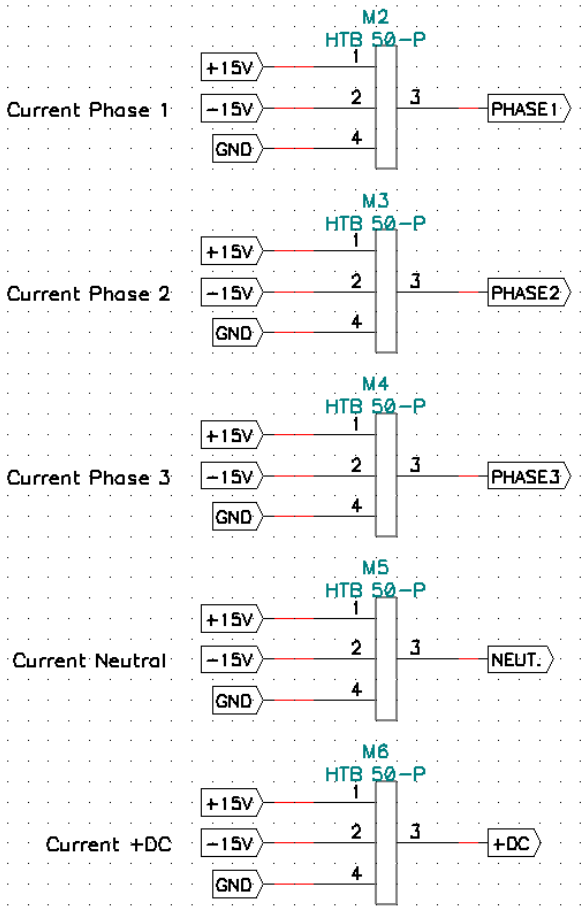

Figure 9: Schematic 2: Current transducer setup.

Figure 9 shows the inputs and outputs of the current sensors. This illustrates that each phase is monitored including the ground wire of the 3 phase generator. This is done to monitor any current that may leak out of the system. The output signals from the current transducers are sent to connectors as shown in Figure 10.

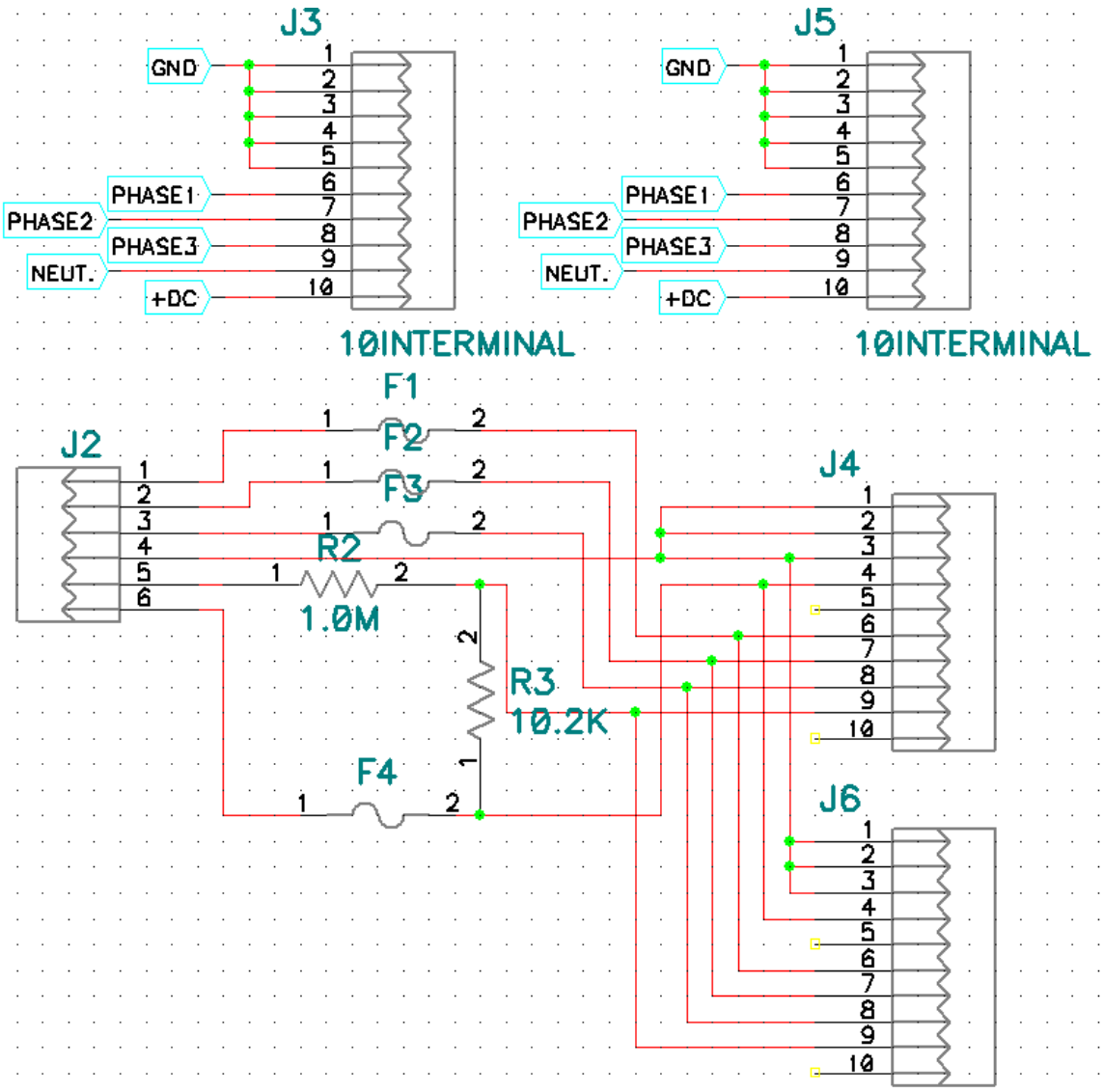

Figure 10: Schematic 3, output connections of sensor board.

Figure 10 shows the output configuration for the sensor board. J2 represents the terminal block that connects each phase of the ocean turbine electrical system to the voltage and current sensors. The voltage waveforms are taken from the terminal block and are measured between each phase. Voltage 1 represents the potential between phase 1 and phase 2. Voltage 2 is the potential between phase 2 and phase 3. And voltage 3 is the potential between phase 1 and phase 3. The DC voltage is measured between the positive and negative sides of the resistor load.

In order to provide safety into this system, fuses were placed on each voltage line to break the signal in cased of a short. These are set to break if the current from to the NI sensors is higher than 1A. The current waveforms are measured directly from the current transducers. Also shown in this Figure 10 are the output connectors for the voltage and current signals. There are two connectors for each. One set of connectors is wired to the NI input modules and will be used for the collection and calculation of power quality information. The other set were placed for the use of the safety system.[11]

The DC voltage also needed to be stepped down so that the NI module will be able to support the signal. To do this a voltage divider[13] was built to step down the voltage across the DC load bank by a factor of 100. This step is compensated for in the data processing section of this thesis. The full schematic of the power quality sensor board is shown in Figure 11.

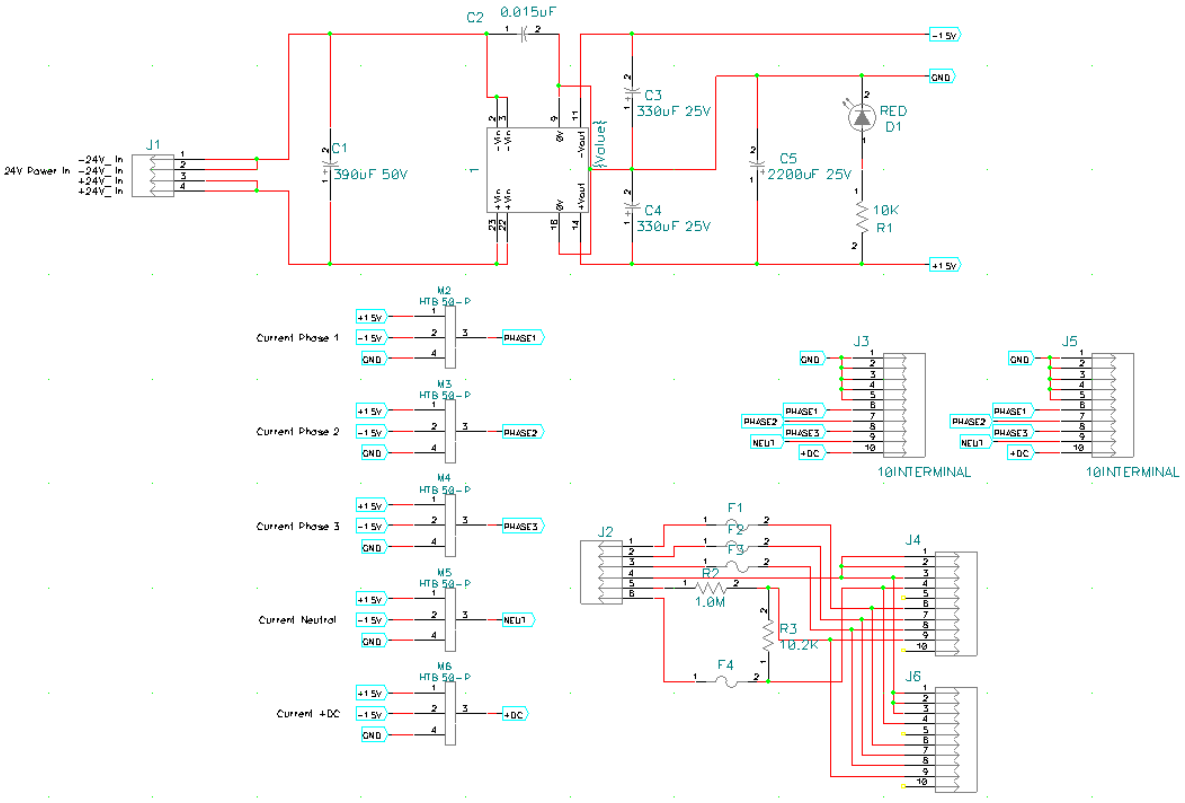

Figure 11: Full schematic of power quality sensor board.

2.2.2.1 Sensor board layout

The final step in the design of the sensor board was to lay out the wiring diagram for the printed circuit board. This was completed using PCAD 2004 PCB. The final layout is shown here in Figure 12.

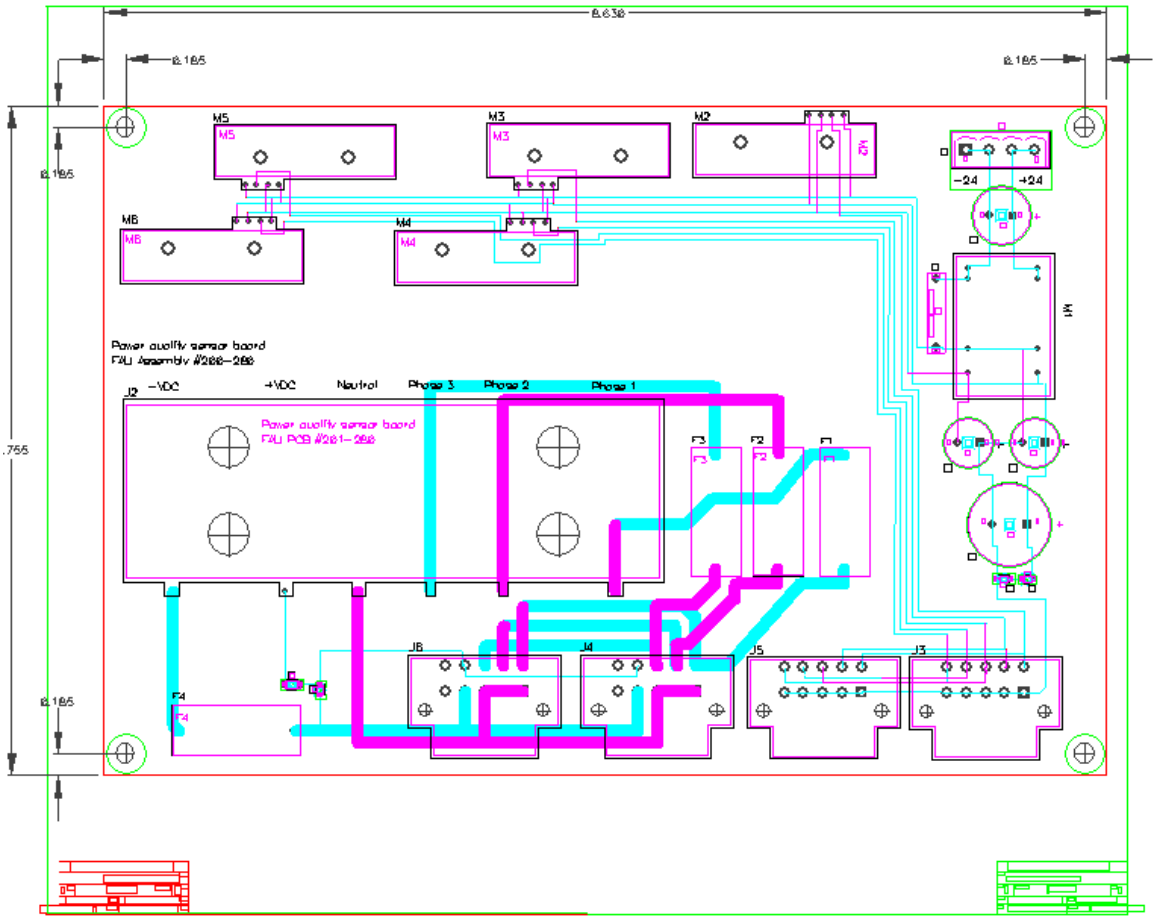

Figure 12: PCB layout of power quality sensor board.

All files used in the development of the board were integrated into the Ocean Eng. Electronics Lab parts library. The part number for the assembly is 200-280. A full bill of materials is shown below in Table 2.

Table 2: Bill of materials for power quality sensor board.

Parts List						
200-280						
Power Quality sensor Board Assembly						
Item	**Quantity**	**Part Number**	**Type**	**Title Detail**		**Reference**
		Vendor	Rev	Vendor P/N	Mfr Name	Mfr P/N
1	1	300-103	PS	Resistor, Chip, 0805, CF, 5%, 1/10W		R1
				10K Ohm		
		Digi-Key Corp.		P10KACT-ND	Panasonic	
2	1	301-1022	PS	Resistor, Chip, 0805, MF, 1%, 1/10W		R3
				10.2K Ohm		
		Digi-Key Corp.		P10.2KCCT-ND	Panasonic	
3	1	304-038	PS	Resistor, Flip Chip 300mW, 1500 Volts, 1206		R2
				1.0 Mohms 1%		
		Digi-Key Corp.		HVF1206T1004FE	Ohmite	HVF1206T1004FE
4	1	326-011	PS	Capacitor, alum-elec., radial		C1
				390uF, 50V, FA series		
				12.5X30		
				CAP-ALUM-FA12		
				obsolete. Use FC series		
		Digi-Key Corp.		P5654A-ND	Panasonic	
5	2	326-018	PS	Capacitor, alum-elec., radial		C3,C4
				330uF, 25V FA/FC series		
				size 10x12.5		
				CAP-ALUM-FA10		
				obsolete. Use FC series		
		Digi-Key Corp.		P10273-ND	Panasonic	EEU-FC1E331
6	1	326-039	PS	Capacitor, alum-elec., radial		C5
			A	2200uF, 25V		
		Digi-Key Corp.		493-1565-ND	Nichicon	UHE1E222MHD6
7	1	329-012	PS	Capacitor, Interference Suppressor Cap		C2
				0.015uF 250VAC		
				X-Y Series Metallized Film		
		Digi-Key Corp.		P4631-ND	Panasonic	ECQ-U2A153MV
8	1	480-001	PS	LED		D1
				Ultra Bright Red, Gull Wing-S type, IF=10mA		
				NOTE wider gull wing lead is the Anode for this		
				device		
		Digi-Key Corp.		P493CT-ND	Panasonic	LN1271RAL
9	1	502-030	PS	Header, Vertical		J1
				5mm, 4 pos		
		Digi-Key Corp.		ED1835-ND	On-Shore Technology, Inc	EDSTL955/4
10	1	502-040	PS	Plug		
				5mm, 4 pos		
		Digi-Key Corp.		ED1703-ND	On-Shore Technology, Inc	ED950/4
11	40	508-013-G	PS	Terminals, Mini-Fit Jr., Female, socket		used on J3,J4,J5
			0	Socket, 18-24awg, Gold over bronze		J6 mate
				CRIMP tool is p/n 730-002		
				Extraction tool 730-006		
		Mouser Electronics	PS	538-39-00-0182	Molex	39-00-0182
12	4	508-067	A	Receptacle, Mini-Fit Jr., Dual Row		mates with J3,J4
				10 pos., 18-24awg		J5, J6
				Mates with 508-063		
				Use terminal 508-013 or-G (socket)		
		Mouser Electronics		538-39-01-2100	Molex	39-01-2100
13	4	508-072	PS	Header, Mini-Fit Jr., Right Angle		J3,J4,J5,J6
				10 pos., Screw Mount Flange		
		Digi-Key Corp.		WM3924-ND	Molex	39-29-5103
14	1	509-013	PS	Terminal Block, Screw Type		J2
			0	6pos, 24.38 mm 600V 115A		
		Mouser Electronics		504-14002-6	Cooper-Bussmann	14002-6
15	1	550-040	PS	FUSE 5X20 FAST GLASS		mates with F1,F2
				250MA 250V		F3, F4
		Digi-Key Corp.		486-1230-ND	Schurter Inc.	0034.121
16	4	550-041	PS	FUSEHOLDER 25MM PCB 5X20MM BLACK		F1, F2, F3, F4
			0			
		Digi-Key Corp.		486-1259-ND	Schurter Inc.	0031.8211
17	5	571-008	PS	SENSOR CURRENT 50A BI TH		M2,M3,M4,M5,M6
		LEM USA		398-1040-ND	LEM USA	HTB 50-P
18	1	582-081	PS	DC/DC, 6W Dual 24Vin +/-15Vout		M1
		Mouser Electronics		580-NDS6D2415C	Murata	NDS6D2415C

2.3 System implementation

The wiring configuration for installing the sensor board is shown below. Table 3 describes how each electrical phase of the power system is connected to the sensor board.

Table 3: Wiring configuration for sensor board.

Terminal Block connector	Wire connection
1	phase 1
2	phase 2
3	phase 3
5	DC positive
6	DC negative

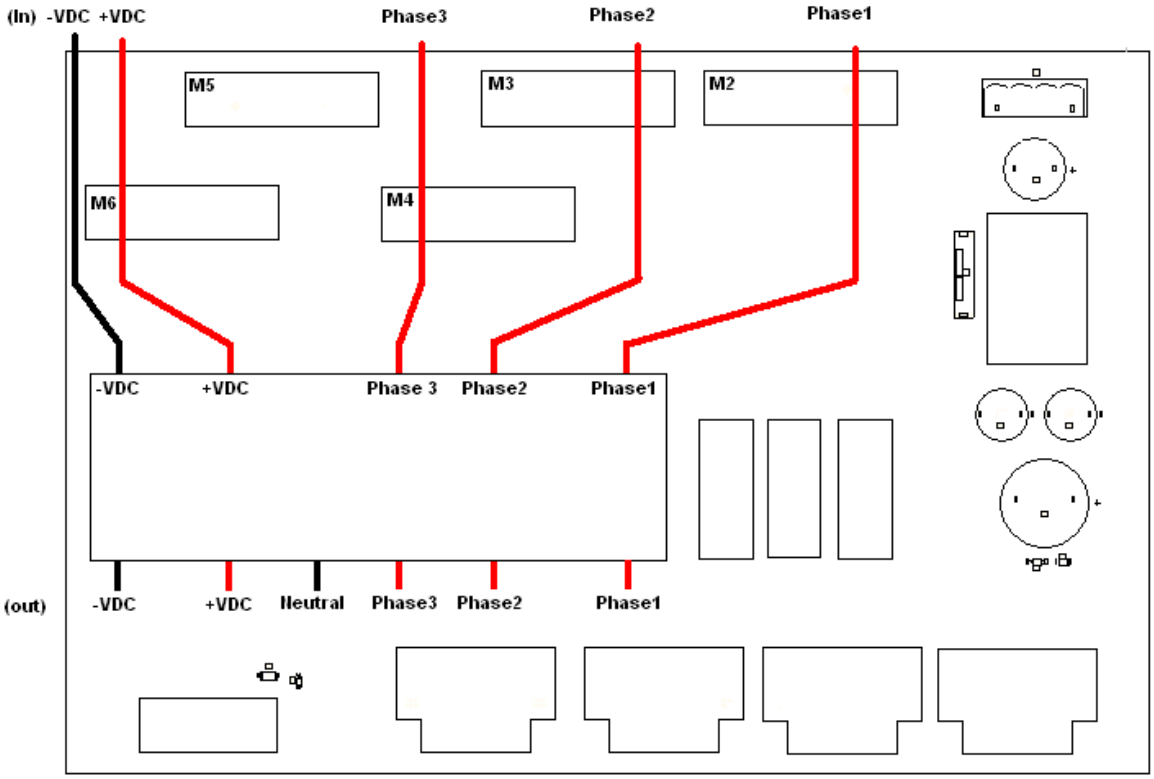

Figure 13: Wiring diagram for power quality sensor board.

Figure 13 shows how the actual connections should be made. At the top of the diagram the positive side of each phase is passed through each current transducer as shown. These transducers are represented as M2-M6. These phases are then each connected to one of the terminals of the terminal block. On the other side of the terminal block a wire for each phase is then wired back into the system. This board is physically located within the AC drive and is wired between the induction generator and the drive. The DC blocks are connected from the wires that connect the drive to the resistor bank.

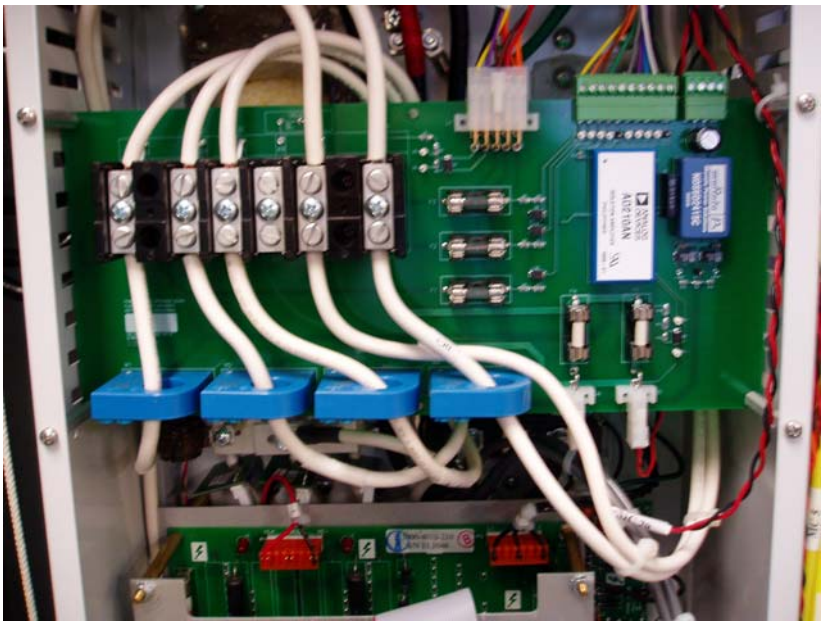

Figure 14: PQ sensor board installed in the system.

Each current and voltage waveform signal is sent to the connectors labeled J3-J6. J3 and J5 represent the current signals while J4 and J6 are the voltage waveforms. Each NI module is connected to a twisted pair of wires from these connectors. The wire configuration for each is shown in Figure 15.

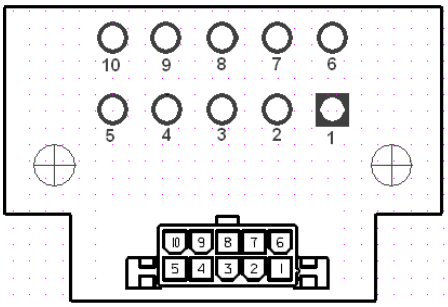

Connection Configuration					
Channel	Connector/Pin	Channel	Connector/Pin	Channel	Connector/Pin
Mod 1 0+	J4/6	Mod 2 0+	J3/6	Mod 5 0+	J3/10
Mod 1 0-	J4/7	Mod 2 0-	J3/1	Mod 5 0-	J3/5
Mod 1 1+	J4/7	Mod 2 1+	J3/7	Mod 5 1+	J4/10
Mod 1 1-	J4/8	Mod 2 1-	J3/2	Mod 5 1-	J4/5
Mod 1 2+	J4/8	Mod 2 2+	J3/8		
Mod 1 2-	J4/6	Mod 2 2-	J3/3		

Figure 15: Connection configuration for NI chassis.

Figure 15 illustrates the configuration for the sensors that collect data between the induction generator and the AC drive. For the sensors between the AC drive and the AC power source the DC channels will not be used. Also module 1 will be replaced with module 3 while module 2 will be replaced with module 4.

3 Power quality

3.1 Motivation for power quality monitoring

The term "power quality" refers to the voltage stability, frequency stability, and the absence of various forms of electrical noise (e.g. flicker or harmonic distortion) on the electrical grid. These variations in output power of the ocean turbine may be caused by changes in current speed, turbulence and other phenomena and have the potential to degrade the power quality of the distribution feeder.[14] This means that the condition of the induction generator affects the power quality and the availability of useable or reactive power.[15]

3.2 Calculating waveforms values

3.2.1 RMS and power values

The Measuring Network of Wind Energy Institutes (MEASNET) has defined the procedure for calculating active power, reactive power and rms voltage based on the measurement of instantaneous voltages and currents[16]. It states that once the phase voltage and currents are measured the fundamental Fourier coefficients should first be calculated over one cycle according to:

$$u_{\mathrm{a,cos}} = \frac{2}{T}\int_{t-T}^{t} u_{\mathrm{a}}(t)\cos(2\pi f_1 t)\,\mathrm{d}t \tag{3.1}$$

$$u_{\mathrm{a,sin}} = \frac{2}{T}\int_{t-T}^{t} u_{\mathrm{a}}(t)\sin(2\pi f_1 t)\,\mathrm{d}t \tag{3.2}$$

The effective value of the fundamental phase voltage is calculated as:

$$U_{\mathrm{a1}} = \sqrt{\frac{u_{\mathrm{a,cos}}^2 + u_{\mathrm{a,sin}}^2}{2}} \tag{3.3}$$

The voltage and current vector components of the fundamental positive sequence are calculated using:

$$u_{1+,\mathrm{cos}} = \frac{1}{6}\left[2u_{\mathrm{a,cos}} - u_{\mathrm{b,cos}} - u_{\mathrm{c,cos}} - \sqrt{3}\left(u_{\mathrm{c,sin}} - u_{\mathrm{b,sin}}\right)\right] \tag{3.4}$$

$$u_{1+,\mathrm{sin}} = \frac{1}{6}\left[2u_{\mathrm{a,sin}} - u_{\mathrm{b,sin}} - u_{\mathrm{c,sin}} - \sqrt{3}\left(u_{\mathrm{b,cos}} - u_{\mathrm{c,cos}}\right)\right] \tag{3.5}$$

$$i_{1+,\mathrm{cos}} = \frac{1}{6}\left[2i_{\mathrm{a,cos}} - i_{\mathrm{b,cos}} - i_{\mathrm{c,cos}} - \sqrt{3}\left(i_{\mathrm{c,sin}} - i_{\mathrm{b,sin}}\right)\right] \tag{3.6}$$

$$i_{1+,\mathrm{sin}} = \frac{1}{6}\left[2i_{\mathrm{a,sin}} - i_{\mathrm{b,sin}} - i_{\mathrm{c,sin}} - \sqrt{3}\left(i_{\mathrm{b,cos}} - i_{\mathrm{c,cos}}\right)\right] \tag{3.7}$$

The active and reactive powers of the fundamental positive sequence are then

$$P_{1+} = \frac{3}{2}\left(u_{1+,\mathrm{cos}} i_{1+,\mathrm{cos}} + u_{1+,\mathrm{sin}} i_{1+,\mathrm{sin}}\right) \tag{3.8}$$

$$Q_{1+} = \frac{3}{2}\left(u_{1+,\cos} i_{1+,\sin} - u_{1+,\sin} i_{1+,\cos}\right) \tag{3.9}$$

and the effective phase-to-phase voltage of the fundamental positive sequence is

$$U_{1+} = \sqrt{\frac{3}{2}\left(u_{1+,\sin}^2 + u_{1+,\cos}^2\right)} \tag{3.10}$$

The effective active and reactive currents of the fundamental positive sequence are

$$I_{\mathrm{P1+}} = \frac{P_{1+}}{\sqrt{3}U_{1+}} \tag{3.11}$$

$$I_{\mathrm{Q1+}} = \frac{Q_{1+}}{\sqrt{3}U_{1+}} \tag{3.12}$$

The power factor of the fundamental positive sequence is

$$\cos\varphi_{1+} = \frac{P_{1+}}{\sqrt{P_{1+}^2 + Q_{1+}^2}} \tag{3.13}$$

3.2.2 Methods used to calculate rms and power values

For this thesis the standards set by IEC 61000-4-30 were used for the calculation of power quality values. This standard states that in order to calculate the rms value, the waveform should be measured over a 12-cycle interval. The rms value can then be calculated from the equation: [8]

$$V = \sqrt{\frac{1}{N}\sum_{i=1}^{N} v_i^2} \tag{3.14}$$

In this equation N represents the number of integer samples in a cycle and v represents the instantaneous value of the waveform at a point of time in the sample period. A monitoring sensor will be used in order to record the rms value of the voltage, current and power generated by the induction turbine.

The fundamental power measurements, as seen in Figure 16, are represented in what is known as the power triangle. Using the three measurements of voltage, current, and the phase offset between the voltage and current waveforms, the entire triangle can be computed.

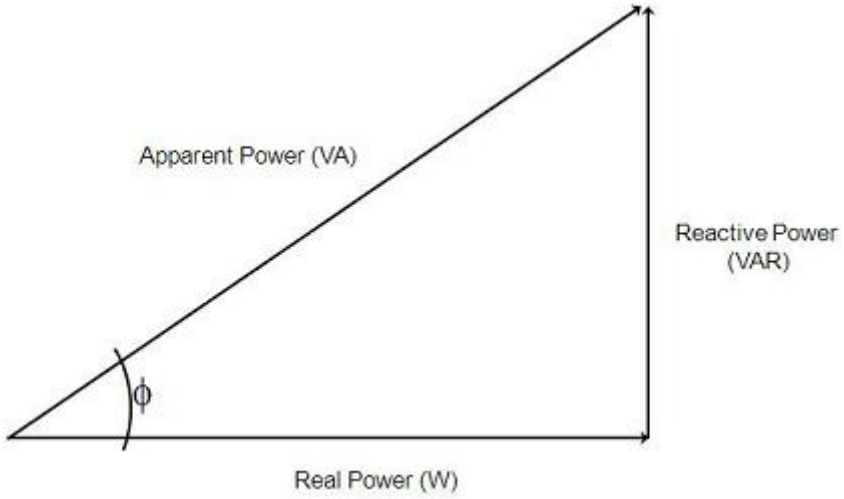

Figure 16: The power triangle.

To measure these power types, an FIR filter is implemented using the Hamming window method in order to measure the magnitude of the real and complex values that make up the voltage and current waveforms. This filter is defined as:

$$w(n) = .54 + .46\cos(2\pi m / N)\{\begin{matrix} -(N-2)/2 \le n \le (N-1)/2(Nodd) \\ -N/2 \le n \le N/2(Neven) \end{matrix} \quad (3.15)$$

This method calculates the real and complex series representations of the waveforms. Once obtained the magnitude or rms values of the real and complex parts can be found using the equations for calculating rms values. The real power is defined as the magnitude of the real part of the waveform and the complex power is the magnitude of the complex representation. For example the rms value of the current waveform can be shown as:

$$I = re(i) + imag(i) \quad (3.16)$$

In phasor form this equation becomes:

$$I = \sqrt{(re(i))^2 + (imag(i))^2}\, e^{j\sigma} \quad (3.17)$$

The phase of the waveform is found from the equation:

$$\sigma = \arctan\left(\frac{imag}{real}\right) \quad (3.18)$$

The Apparent Power is then calculated as:

$$S = VI^* \quad (3.19)$$

In this equation, * denotes that the conjugate current should be multiplied with voltage. Once the apparent power in a single phase is known the total power in a balanced three phase system is

$$S_{3\phi} = 3S_{1\phi} \tag{3.20}$$

While the induction generator that will be used in the ocean turbine is designed to be balanced it is unreasonable to assume that it will constantly be balanced while in operation. For this reason the 3 phase power will be calculated by summing the power calculated from each electrical phase.

The real power is found from the equation:

$$P = S\cos\theta \tag{3.21}$$

Where θ represents the angle between the current and voltage.

Likewise the reactive power is calculated from the equation:

$$Q = S\sin\theta \tag{3.22}$$

The power factor of the system is a measure of how much of the power has the capacity of performing work in a particular time. “One way to understand power factor is think about a horse pulling a barge along a canal. The horse must pull the barge from the shore; therefore it is pulling the barge at an angle to the direction of travel. Because the horse is

pulling at an angle, not all of the horse's effort is used to move the barge along the canal. The effort of the horse is the total power or apparent power (kVA), the power used to move the barge is the working power or real power (kW), and the power that is trying to pull the barge to the side of the canal is nonworking power or reactive power (kVAR).[17]

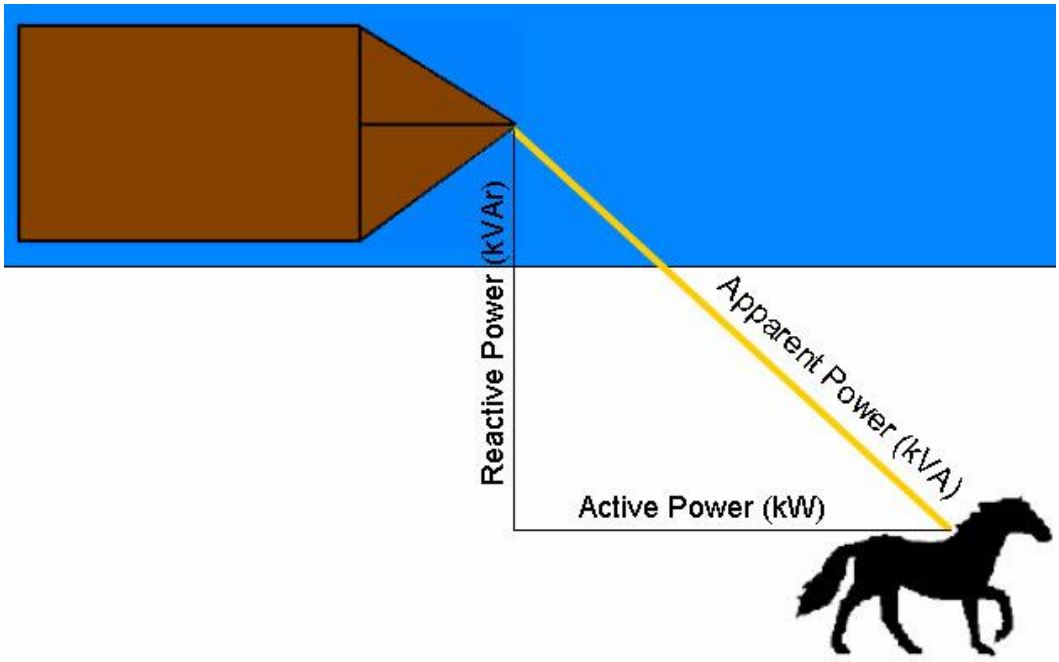

Figure 17: Explanation of the differences in power values.

The power factor is calculated from the equation:

$$PF = \cos\theta \tag{3.23}$$

This method will be used to calculate the power factor using the measurements that will be obtained by the monitoring system. FPL standards require that the power factor be .95 or greater leading or lagging[4]

3.3 Measuring power quality

There are several parameters to consider when measuring power quality. Each of these can be classified as a variation, an event or sometimes both. A variation is a steady-state disturbance that requires continuous measurements. An event on the other hand is classified as a sudden disturbance with a beginning and an ending.[8] This section describes the origins of some power quality variations and events as well as the methods that are used to analyze them.

3.3.1 Variations

3.3.1.1 Voltage frequency variations

Voltage frequency variations originate when the rate of power generation is not equal to the rate of power consumption. When an unbalance of energy occurs there is a change in the amount of rotational energy in the system and effectively the frequency of the generators. The change in frequency is calculated by the following expression:

$$\frac{df}{dt} = \frac{f_0}{2H}(P_g - P_c) \tag{3.24}$$

where H represents the inertia constant of the motor and Pg, Pc represent the power generated and power consumed in the system.

While there are no reported equipment problems due to frequency variations there are some potential consequences of frequency variation that could lead to problems. These include time deviation of clocks, variations in motor speed and variations in flux. Although these could potentially be problematic, it would require a large change in the frequency of the generators to create any type of problem making this very unlikely[18].

One of the functions of the AC drive is to ensure that the power being generated stays equivalent to the power being consumed. The drive will measure voltage on both sides and will use those measurements to control the speed of the turbine.

If the value of the frequency changes more than a desired amount then the power quality monitor should set off some type of advisory that there is a problem in the system. For generators FPL has standards in place for how the system should operate while the system frequency varies. The system response to frequency variations should include[19]:

- No tripping results with frequency excursions between 60.5 Hz and 61.8 Hz from 0 to 10 seconds.

- No tripping results with frequency excursions between 59.5 Hz and 60.5 Hz.

- No tripping results with frequency excursions between 58.5 Hz and 59.5 Hz from 0 to 60 seconds.

- No tripping results with frequency excursions between 58.0 Hz and 58.5 Hz from 0 to 10 seconds.

- No tripping results with frequency excursions between 57.5 Hz and 58.0 Hz from 0 to 1 second.

3.3.1.2 Voltage magnitude variations

Voltage variations can have serious effects on the lifetime of the induction generator. An under-voltage can lead to a reduced starting torque which will increase the full load temperature. A reduction in the starting torque may also cause the motor to stall. When the motor stalls there will be a high amount of current running through it as the torque is increased to try and restart the rotation. Because the machine is not rotating the high current will cause the motor to overheat. If the engine is in a system of turbines then the resulting voltage drop could spread to the other turbines causing them to stall as well. An overvoltage will lead to an increase in torque, starting current and a decreased power factor. This will increase the voltage dip seen by loads close to the motor[3]. These voltage variations will lead to adverse affects on any electronic device that the power supply may be operating.

If the monitoring system picks up a large voltage variation then it may be a signal that something is wrong with the system. The monitoring system will be set to signal when variations become larger than 10% of normal as specified in the IEC standards[15]. FPL standards require that the Generator terminal voltages stay within 5 % of the rated nominal design voltage or that the generator terminal voltage deviations that exceed 5%

but are within 10% of the rated nominal design voltage persist for less than 10.0 seconds. Based on these regulations the power quality monitoring system will send a warning signal if the magnitude of the voltage changes by 10% or if it changes by more that 5% for longer than 10 seconds.

3.3.1.3 Voltage fluctuations and flicker

Although voltage fluctuations and flicker will not be a factor in the prototype ocean turbine they are still important to mention. These fluctuations are generally due to load variations. These variations can be from a large machine starting up or the variation of load on the power grid. It will be important to take into account the variation of the grid load when the turbine is connected to the power grid.

3.3.1.4 Waveform distortion

Waveform distortion can be defined as the varying of any waveform from the ideal sine wave. There are three types of waveform distortion and this thesis will focus on harmonic distortion because it is the most dominant. The consequences reported from waveform distortion are[20]:

- Inadvertent tripping of circuit breakers
- Overheating of transformers and cables
- Malfunctioning of electronic devices

All of these stem from the fact that when there is waveform distortion the rms value of the voltage or current is higher than normal. When a waveform is non-sinusoidal but

periodic it can be split into a sum of harmonic components. The presence of different harmonics provides information on the origin of the disturbance making the calculation of these harmonic frequencies essential for troubleshooting.

Waveform distortion can be caused by a multiple number of variables including: distortion of transformer voltages and currents, conductors in the induction machine that overheat and supply current, changing magnetic fields. In the case of the ocean turbine the main cause of waveform distortion will probably stem from the cables that run from the water to the surface. It is unknown how the environment the changing environment will affect the heating losses of the cables. This is an area that should be studied closely once the ocean turbine prototype is operational.

While the most common method for evaluating the harmonic distortion of both current and voltage waveforms is the design of harmonic filters based on the discrete Fourier transform (DFT) or on the fast Fourier transform (FFT) to obtain the voltage and current frequency spectra from the waveforms, there are several other methods that are used in the calculation of power quality indices.

Min[21] describes the use of the Fourier transform to evaluate the harmonic distortion in both current and voltage waveforms, but suggests that while these methods can be useful in determining distortion in current and voltage waveforms, their blind use may be limiting. The use of the FFT may lead to incorrect results in harmonic analysis and also requires that the number of samples needs to be an integer power of two.

As a substitute for the Fourier transform the paper introduces the estimation algorithm based on Kalman filtering. "The Kalman filter is a recursive optimal estimator, well suited for on-line applications. It requires a state variable model for the parameters to be estimated and a measurement equation that relates the discrete measurement to the state variables (parameters)[22]." This paper also introduces the use of combinations of Fourier transforms and wavelet transforms to analyze power quality problems.

While this method is useful the calculation of total harmonic distortion (THD) using Fourier transforms will be adequate for the purpose of the ocean turbine. The first step in calculating the total harmonic distortion is to express the total waveform as a sum of sinusoidal waveforms.

The current waveforms can be written as[23]:

$$i(t) = I_0 + \sum_{h=1}^{H} I_h \sqrt{2} \cos(h\omega t - \beta_h) \tag{3.25}$$

Similarly the voltage waveform can be written as:

$$v(t) = V_0 + \sum_{h=1}^{H} V_h \sqrt{2} \cos(h\omega t - \alpha_h) \tag{3.26}$$

The equation:

$$\sqrt{2} V_h \cos(h\omega t - \alpha_h) \tag{3.27}$$

refers to the harmonic h of the h^{th} harmonic component. V_h Refers to the rms value of the harmonic h; α_h refers to the phase angle with reference to the fundamental value. For voltage this term is usually set to zero. The total deviation of the waveform from the ideal sine wave can be indicated by calculating the total harmonic distortion which is calculated by the following expression:

$$THD = \frac{\sqrt{\sum_{h=2}^{H} V_h^2}}{V_1} \tag{3.28}$$

It should also be noted that odd-harmonic distortion is typically dominant in a supply voltage or load current. These harmonics usually affect the amplitude of the waveform. For the 3 phase system that will be used in the Ocean Turbine the harmonics can be found using these expressions.

$$i_a(t) = \sum_{h=0}^{H} \sqrt{2} I_h \cos(h\omega t - \beta_h) \tag{3.29}$$

$$i_b(t) = \sum_{h=0}^{H} \sqrt{2} I_h \cos(h\omega t - h\frac{2\pi}{3} - \alpha_h) \tag{3.30}$$

$$i_c(t) = \sum_{h=0}^{H} \sqrt{2} I_h \cos(h\omega t + h\frac{2\pi}{3} - \alpha_h) \tag{3.31}$$

The first step in finding the harmonics of a signal is to remove any noise that may be present in the signal. This can be done with the use of anti-aliasing filters. For the purposes of this thesis it is important that this filter be designed so that there is a sufficient margin between the highest frequency of interest and the Nyquist frequency. This will allow for a lower order filter to be used which will save cost as well as reduce the phase error in the passband. The requirements for the configuration of the filter are shown below in Figure 18.

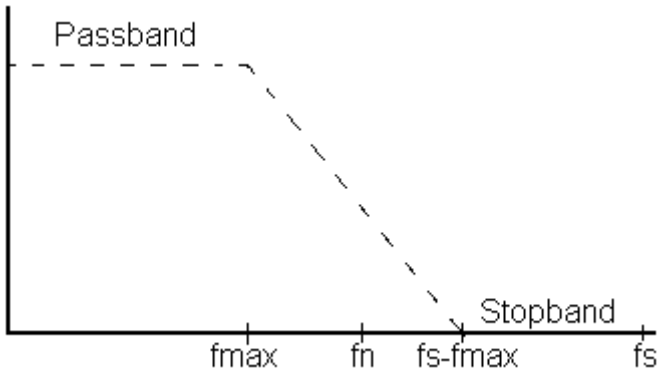

Figure 18: Frequency Characteristics of an anti-aliasing filter.

In Figure 18 fs represents the sampling frequency and fmax is the highest frequency of interest. According to IEC standards 61000-4-30 and 61000-4-7 the Fourier series shall be obtained over a rectangular window with a length equal to 10-12 cycles. To ensure that the measurement window and the power system frequency are in synch the monitoring system will use a PLL which will generate a sampling frequency that is an integer multiple of the frequency of the power system.

3.3.1.5 Unbalance

Figure 19 shows a typical 3 phase Δ connection machine. This configuration matches the configuration of the induction generator that will be used in the ocean turbine.

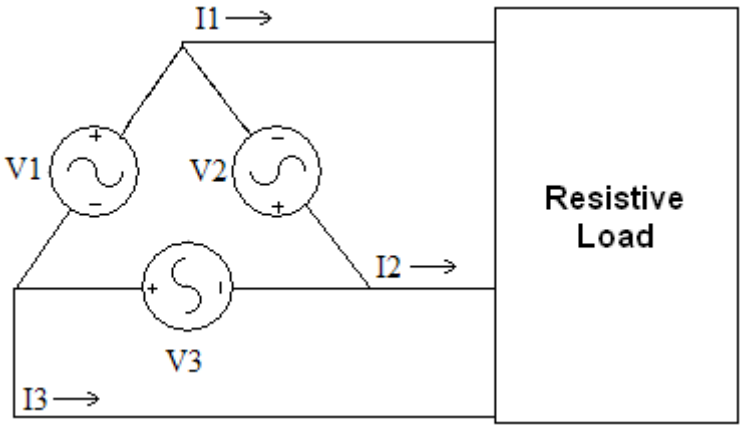

Figure 19: 3 phase Δ connection.

The voltage of a 3 phase balanced load can be described as:

- $V_1 = V\angle 0°$ (3.32)
- $V_2 = V\angle -120°$ (3.33)
- $V_3 = V\angle 120°$ (3.34)

Similarly the current is described as:

- $I_1 = I\angle 0°$ (3.35)
- $I_2 = I\angle -120°$ (3.36)

- $I_3 = I\angle 120°$ (3.37)

Unbalance in a 3 phase system is mostly due to the variation of a single load distributed over 3 phases. Even if the loads are equally distributed, the variation over time of the individual loads means that there is never a perfect balance between the load currents.[24] In the ocean turbine system the three phase power will be distributed over a single load and unbalance is a concern. The main effect of unbalance in the three phase system is a loss of power. "Rotating machines have small negative sequence impedance that is typically one-fifth of the rated impedance. If the voltage is unbalanced this will lead to a negative sequence voltage which in turn yields a negative sequence current which will in turn heat the machine. The amount of power lost by unbalance is calculated as:

$$P_{loss} = 3I^{+2}R^{+} + 3I^{-2}R^{-} \quad (3.38)$$

Where R+ and R- are positive and negative sequence resistances and I+ and I- are positive and negative sequence currents. In this situation the system would need to be derated in order to prevent the machine from overheating. This type of power loss could be signaled by a variation in the magnitude of the voltage or current. For this purpose the monitoring system includes waveform monitoring of the total three phase system as well a monitoring for each power phase. From this system a warning will be sent if the magnitude of each phase varies by more than 5%.

3.3.1.6 Power quality indices

In this section several parameters have been introduced to quantify voltage and current variations. However these parameters do not sufficiently describe the quality of the voltage or current waveforms. In order to do this there are several combinations of parameters that are used that are known as power quality indices.

Total Harmonic Distortion: The total harmonic distortion is defined as the relative signal energy present at non-fundamental frequencies. This index is used to quantify the distortion of a waveform.

Total Waveform Distortion: This index takes into account inter-harmonic distortions that may be present and more recently has been recommended by IEEE for use in quantifying waveform distortion.

$$TWD = \frac{\sqrt{V_{rms}^2 - V_1^2}}{V_1} \tag{3.39}$$

In most cases the total odd-harmonic distortion dominates. If there are high values for even or nonharmonic distortion this often indicates an abnormal state for the system.

Crest Factor: The crest factor is used in the time domain to determine how much the top of the sine wave is distorted. It can be split into two categories; the low-frequency crest factor and the high frequency crest factor. The low frequency crest factor is a measure of

the operation of electronic equipment. The high frequency crest factor is used to measure how the waveform affects the insulation aging. The relative crest factor is defined as:

$$C_r = \frac{1}{\sqrt{2}} \frac{V_{\max}}{V_{rms}} \tag{3.40}$$

While there are other Power Quality Indices these are the indices that will be most useful in measuring the waveform distortions in the system.

3.3.2 Events

Events can be classified by the duration of which they last, and the amount of residual voltage present during the occurrence. According to IEEE 1159[25]:

- An event with a residual voltage between .1.0 and 0.9 power units(pu) and a duration of 0.5 cycle and 1 minute is known as a sag.
- An event with a residual voltage less than 0.1 pu is known as an "interruption."
- An event with a residual voltage above 1.1 pu is known as a "swell."
- Events with duration between 0.5 and 30 cycles are classified as "instantaneous."
- Events with duration between 30 cycles and 3s are classified as "momentary."
- Events with duration between 3s and 1min are classified as "temporary."
- Events with durations longer than 1min are classified as "sustained."

There are three major classes of events. These are interruptions, voltage dips and transients.

3.3.2.1 Interruptions

An interruption can be defined as any situation in which the customer is no longer connected to the grid. In the application of the Ocean Turbine prototype, an interruption will occur any time the connection between the induction generator and the resistor bank is severed. There are three general causes of an interruption. The first is the operation of a circuit breaker or a fuse due to a short-circuit or earth fault in the system. The second is the operation of a circuit breaker or a fuse due to an incorrect signal tripping from one of the protection systems. The third is the intentional disconnection of the system for maintenance or repair purposes. The typical thresholds to detect an interruption are 1% and 10% of nominal voltage

3.3.2.2 Voltage dips

Most changes in the magnitude of the voltage stem from an increase or decrease in the magnitude of the current. These can be the result of short circuits, the starting of the induction motor, energizing of transformers, or the energizing of capacitor banks. It should be noted however that the energizing of capacitor banks is typically very small and can be ignored. Short circuits can stem from various sources including the breakdown of insulation between two wires or even lightning striking the machine. In order to monitor a voltage dip the residual voltage and duration of the change must be measured. Voltage dips typically have duration of less than one second and usually are very small. In order for an alarm to sound the sensors are set to pick up dips whenever the rms value drops to 10% of its value[26].

A fluctuation in the magnitude of the voltage can only be seen by monitoring the rms value of the voltage and current. If this value changes then there has been some type of event in the power system. These events can be signs that the motor is wearing and will signal that corrections to be made to the system before some major event can occur.

3.3.2.3 Transients

In power systems the term transient is used to denote any voltage or current event that is less than one half-cycle. A transient is basically a short-duration deviation from the steady state voltage or current waveform. These can be caused by lighting strikes or the opening and closing of ideal circuits. For example, in the case of a lightning strike there is a high overvoltage on the line struck which often leads to a ground fault short-circuit. This leads to a voltage dip or an interruption that lasts briefly. Transients have a very small effect on power quality and because they are of a short duration, transients need a wide bandwidth measurement circuit operating at a high sampling rate in order to be detected

3.3.2.4 Triggering

Triggering is the method used to detect events in a power system that detects the beginning and ending of a power fluctuation. This information can be used to time the duration as well as recording the waveform so that it may be analyzed later. Basically

Triggering will be used to note an event and to decide how much information about the event will be stored.

Although there are different triggering methods that can be used to monitor events, the main method used in this thesis is to monitor changes in rms or waveforms and set a threshold value. For instance, a threshold may be set at 90% of nominal voltage so that if an rms value drops below 90% of the nominal value a warning alarm will be set off. The downside to rms monitoring is that has very low accuracy in terms of the time stamp of an event.

3.4 Threshold values

This section discusses the operational thresholds of the ocean turbine system. For variations, the current and voltage magnitudes should operate within 5% of nominal values. It may operate between 5% and 10% as long as the magnitudes are in this range for less than 10 seconds. For waveform distortion electronic equipment will begin to behave erratically where a voltage waveform has a THD above 5% and when individual harmonics exceed 3%. Events on the other hand are classified by their magnitude and the length of time that they last as shown in Figure 20.

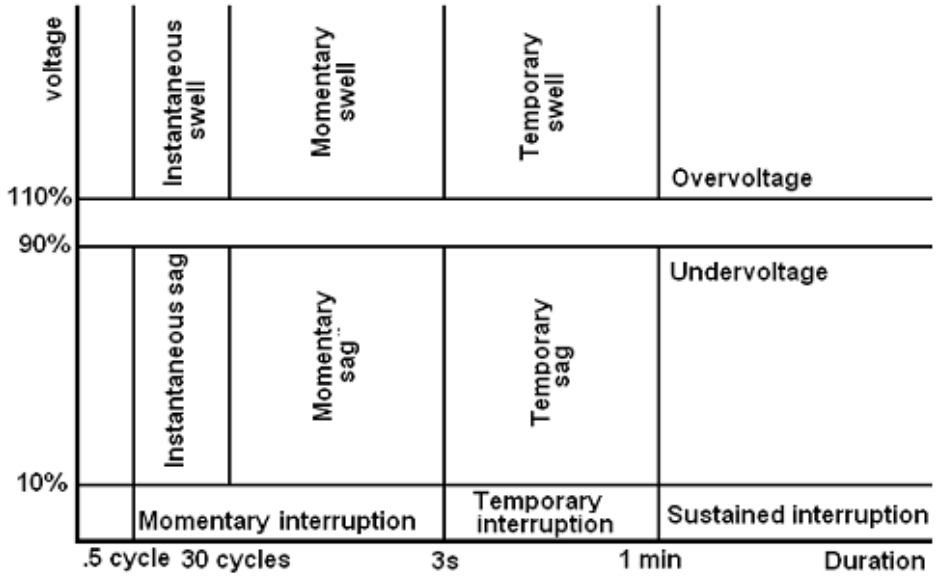

Figure 20: Event Classification.

Figure 20 is a guideline for how a warning system should be calibrated to monitor for events. When an event is detected the monitoring system should immediately begin recording data so that it can be used to determine the cause. The triggering system is discussed in detail in Chapter 4 and shows output values and warnings for all parameters shown in Table 4.

Table 4: Parameters measured in power quality analysis.

Parameter	variation warnings	events
per phase values		
rms voltage	variation of 5%	sag, swell, interruptions, transients
rms current	variation of 5%	sag, swell, interruptions, transients
apparent Power	N/A	N/A
Active Power	N/A	N/A
Reactive Power	N/A	N/A
Power factor	less than .95	N/A
THD	greater than 5%	N/A
Unbalance	phases change by 5%	N/A
Frequency Variation	variation of 5%	N/A

4 Signal processing using LabView

The NI modules discussed earlier were selected because they are compatible with NI's LabView software. This software was used in this thesis to develop signal processing algorithms for all of the power quality parameters discussed in Chapter 3. This section discusses how each parameter was calculated and shows how those calculations are implemented in LabView.

4.1 Sampling information and signal correction

Because the power systems in the United States are set at 60 Hz the fundamental frequency of the monitoring system is set to match this value. In order to provide accuracy in the calculation of harmonic distortion it is recommended that the max frequency value allowed be at least 25 times the fundamental frequency (the 25th harmonic) or 1.5 KHz. To prevent aliasing of the signal the minimum sampling frequency, or Nyquist frequency, is 2 times the max desired frequency. This means that to prevent aliasing the sampling rate must be at least 3 KHz. To improve the robustness of the system each NI module is set to sample the waveforms at 5 KHz.

The amplitude of the current signals had to be adjusted to compensate for the changes made by the current transducers. Each transducer is set to have a 4V output for a 50A input. This means that the magnitude of the signal:

$$|V_{out}| = .08|I_{in}| \tag{4.1}$$

To compensate for this the current signals are divided by .08 before they are filtered by the IIR filter discussed in the following sections. It should also be noted that due to the configuration of the current transducers on the board the current signals for phase 2 and positive DC will be negative when read by the input modules. To alleviate this problem each signal is inverted by LabView.

4.2 Three-phase measurements of rms and power

4.2.1 Calculating rms

The magnitude of the 3-phase current and voltage is found first by calculating the rms value of each phase over a window of 12 cycles as prescribed by IEC 61000-4-30.

The digitized signal is first broken into its discrete values according to the sample window. Once the samples are taken they are manipulated by squaring each value and adding them together. The total is then divided by the number of samples and the square root of the total is taken according to the equation for calculating rms discussed in Chapter 3. The rms value of the waveform is then returned for further processing.

The rms value of the amplitudes from the three phases is then calculated as:

$$V_{rms} = \sqrt{\frac{1}{3}(V_a^2 + V_b^2 + V_c^2)} \tag{4.2}$$

Figure 25 shows how these values are displayed in the LabView environment.

4.2.2 Finding the power factor from the DFT

As discussed earlier in this thesis the phase angle of each waveform is found by obtaining the fundamental component of the waveform by means of the discrete Fourier transform (DFT) algorithm. To do this, in general each waveform is sampled at regular time intervals T to produce the sample sequence:

$$\{x(nT)\} = x(0), x(T),...x[(N-1)T] \tag{4.3}$$

of N sample values, where n represents the sample number from n=0 to n = N-1. The DFT of X (nT) is then defined as the sequence of complex values:

$$\{X(k\Omega)\} = X(0), X(\Omega),..., X[(N-1)\Omega] \tag{4.4}$$

in the frequency domain where Ω is the first harmonic frequency and:

$$X(k) = \sum_{n=0}^{N-1} x(nT)e^{-jk\Omega nT}, k = 0,1,...., N-1 \tag{4.5}$$

The DFT X (kΩ) has real and imaginary components so that for the kth harmonic

$$X(k) = R(k(\theta)) + jI(k(\theta)) \tag{4.6}$$

From this equation the associated phase angle for each X (k) is found from the equation:

$$\phi(k) = \arctan[I(k(\theta))/R(k(\theta))] \tag{4.7}$$

Each waveform is sampled over 12 cycles and the phase angle is the average of the calculated phase angles for that sample time. Similarly to the total rms values of each waveform, the total three phase angle is found by taking the average phase of all three waveforms. The three phase PF is then calculated as:

$$PF = \cos\left(\frac{1}{3}(\phi_a + \phi_b + \phi_c)\right) \tag{4.8}$$

In LabView this process is implemented by first sampling the waveform. The sample sequence is then passed through a block which calculates the Fourier transform of the sampled data. The transformed data is then separated into its real and imaginary components. This data is then passed to another block that calculates the phase of the sample window according to the equations discussed above. The phase angle is then passed to another block that calculates the power factor. The output of this system is shown in Figure 25.

4.3 Measuring frequency

In LabView each waveform is sampled over a 12 cycle period. The algorithm then counts the number of zero crossings and divides by the time and returns the measured frequency of the signal. This value is then displayed in the LabView environment shown in Figure 25.

4.4 Measuring waveform distortion

As discussed in Chapter 3 the first step in measuring the waveform distortion is to get rid of any noise that may be in the waveform data. The filter used in this system was developed based on the configuration shown in Figure 21.[27]

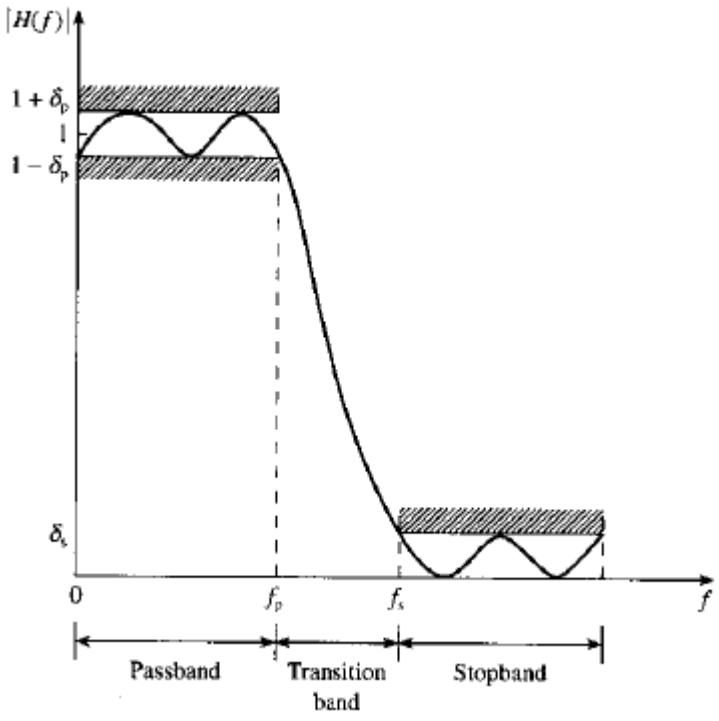

Figure 21: Tolerance scheme for a low-pass filter.

In Figure 21, δ_P and δ_S represent the pass-band and stop-band deviations from normal. The pass-band ripple and stop-band attenuations are calculated as:

$$A_s(\text{Stopband attenuation}) = -20\log_{10}\delta_s \tag{4.9}$$

$$A_p(\text{Stopband attenuation}) = -20\log_{10}(1+\delta_p) \tag{4.10}$$

For this application an infinite impulse response (IIR) Butterworth filter was chosen and developed using the FDATool program in Matlab. The frequency response of this filter is described as:[28]

(4.11)

$$|H(\omega)|^2 = \frac{1}{1+\left(\frac{\omega}{\omega_p^p}\right)^{2N}}$$

where N is the filter order and ω_P^P is the 3dB cutoff frequency of the low-pass filter. For this filter the attenuation for the cutoff frequencies is set to 3dB and the order is also set to 3. The frequency response of this filter is shown in Figure 22.

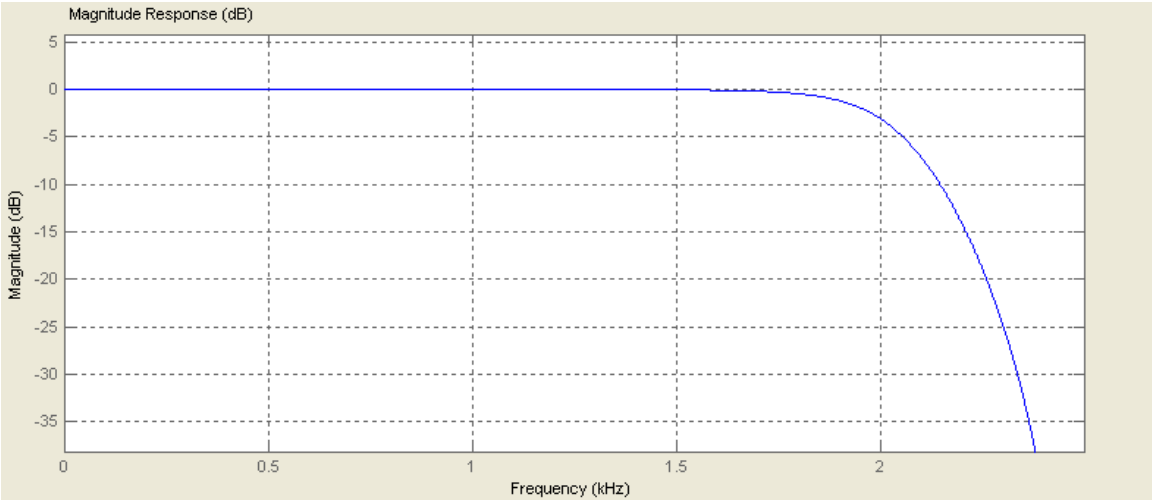

Figure 22: Magnitude Response of IIR filter.

Figure 22 shows that all frequencies up to the 1.5 KHz that we are interested in will pass through the filter so that the harmonics can be measured up to the 25th harmonic of the fundamental frequency. This filter is also ideal because it is a low order filter and can be run in real time which is important in this application as power data needs to be monitored in real time. The waveform response of this filter as implemented in LabView is shown in Figure 23.

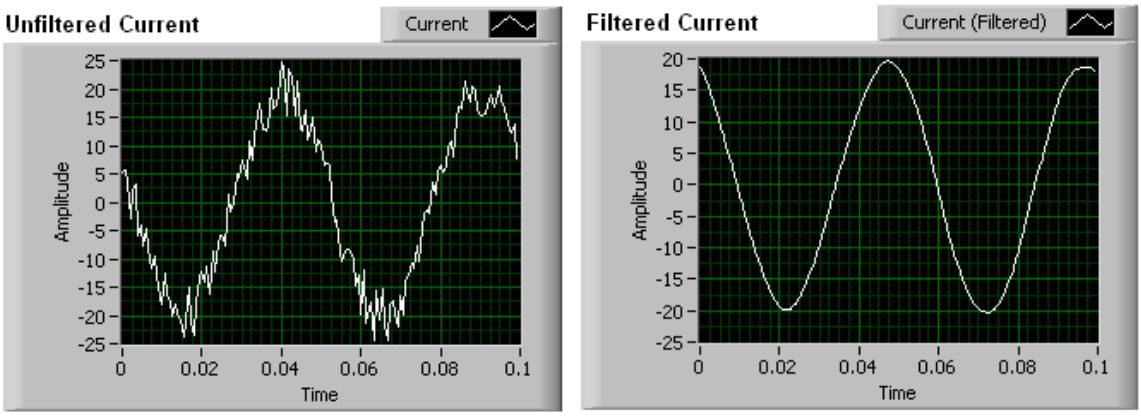

Figure 23: Waveform output of IIR filter.

For this test the input current signal was set to amplitude of 20A and a noise signal of 5A was added to it. The test was repeated using various current, noise and frequency amplitudes and for each test the filter returned the original signal. Figure 23 shows that the IIR filter used successfully filters out the noise and returns the original signal. This filter is placed between the input signals from the NI input modules and the signal processing algorithms so that all data will exclude any noise that the signals may inherit from outside sources.

To calculate the waveform distortion the DFT of the signal is taken only this time the waveform spectrum is plotted and the total harmonic distortion is calculated according to the equations discussed in Chapter 3. In the LabView environment the total harmonic distortion is returned as well as the amplitude of each individual harmonic along with the fundamental frequency. These values are displayed for each individual waveform as well as the total 3 phase harmonic distortion for the voltage and current. The 3 phase values are found by calculating the THD from the highest value per harmonic according to the following equation.

$$THD = \frac{\sqrt{\sum_{h=2}^{H} \max(V_{ha}, V_{hb}, V_{hc})}}{\max(V_{1a}, V_{1b}, V_{1c})} \tag{4.12}$$

These displays are also shown in Figure 26.

4.5 Events

In LabView all events are monitored by the process of triggering. If one of the monitored values falls below the nominal rated value then a warning light will turn on. It is important to note that there will be no other action taken by this system. The purpose of this system is solely to monitor power quality. Each event is monitored according to its description in Chapter 3. In the case of an event LabView begins collecting the data from the waveform in question. The data is stored in binary format which can be read by another LabView program. The location of this file can be defined by the user within the

host power monitoring program. The data will stop being collected as soon as the event has passed. A discussion of each alarm in the LabView environment appears in the following section.

4.6 Measuring DC power

The purpose of measuring DC power is to verify that the amount of power that actually reaches the load in the prototype system is comparable to the power delivered by the ocean turbine. The AC drive in the electrical system will convert the three phase AC power from the turbine into single phase DC power. The DC voltage and current signals are monitored by the NI 9239 device. In order to use this device the output voltage is stepped down on the sensor board by a factor of 100. This is found by the equation:

$$V_{out} = \frac{R2}{R1 + R2} \tag{4.13}$$

Where R1 = 1MΩ and R2 = 10.2KΩ. This gives a correction value of 99.03. To account for this value the signal for DC voltage is multiplied by 99.03 before it is processed. The output power over the resistor is then simply calculated in Watts as:

$$P = VI \tag{4.14}$$

4.7 The LabView environment.

The LabView algorithms discussed above display their respective values in the LabView environment. For each phase the voltage and current waveforms are displayed as shown in the Figure 24.

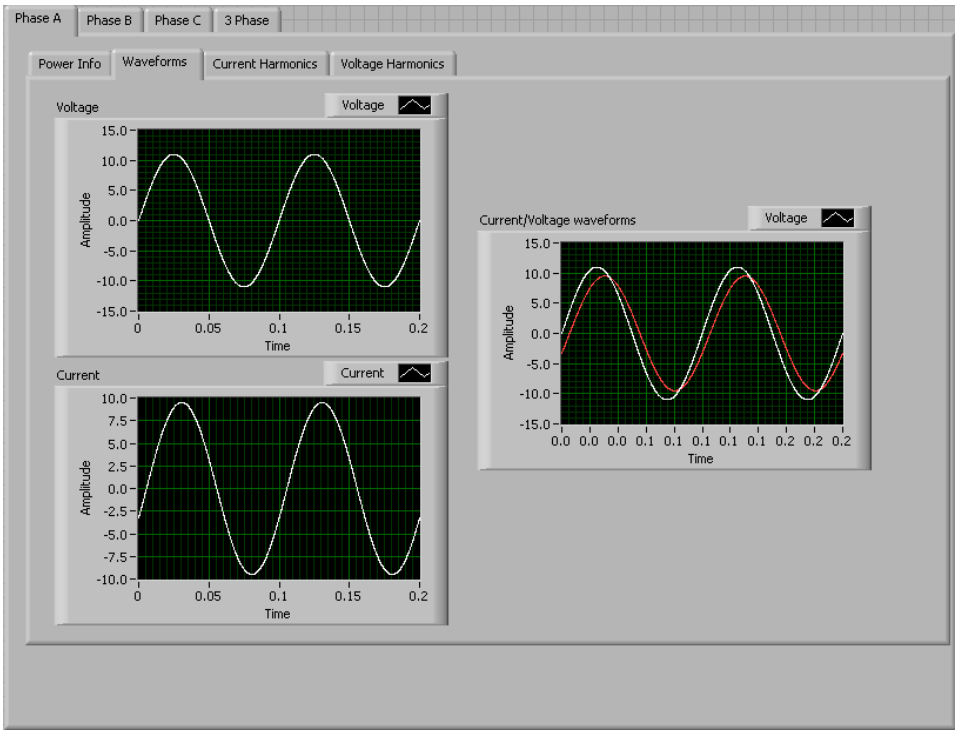

Figure 24: LabView environment showing waveforms.

Figure 24 shows the overall setup of the LabView environment which shows the measured power quality values. The outside box has a tab for each phase as well as a tab that shows the combined three phase values. The inner tabs show that values for each specified phase. These include a plot of each current and voltage waveform, a tab that shows all of the measured power info and a tab that shows the harmonics for the current

and voltage waveform of each phase. Each tab is discussed in this section. In Figure 24 the waveforms of phase A are shown separately and then together in order to visually illustrate the phase angle.

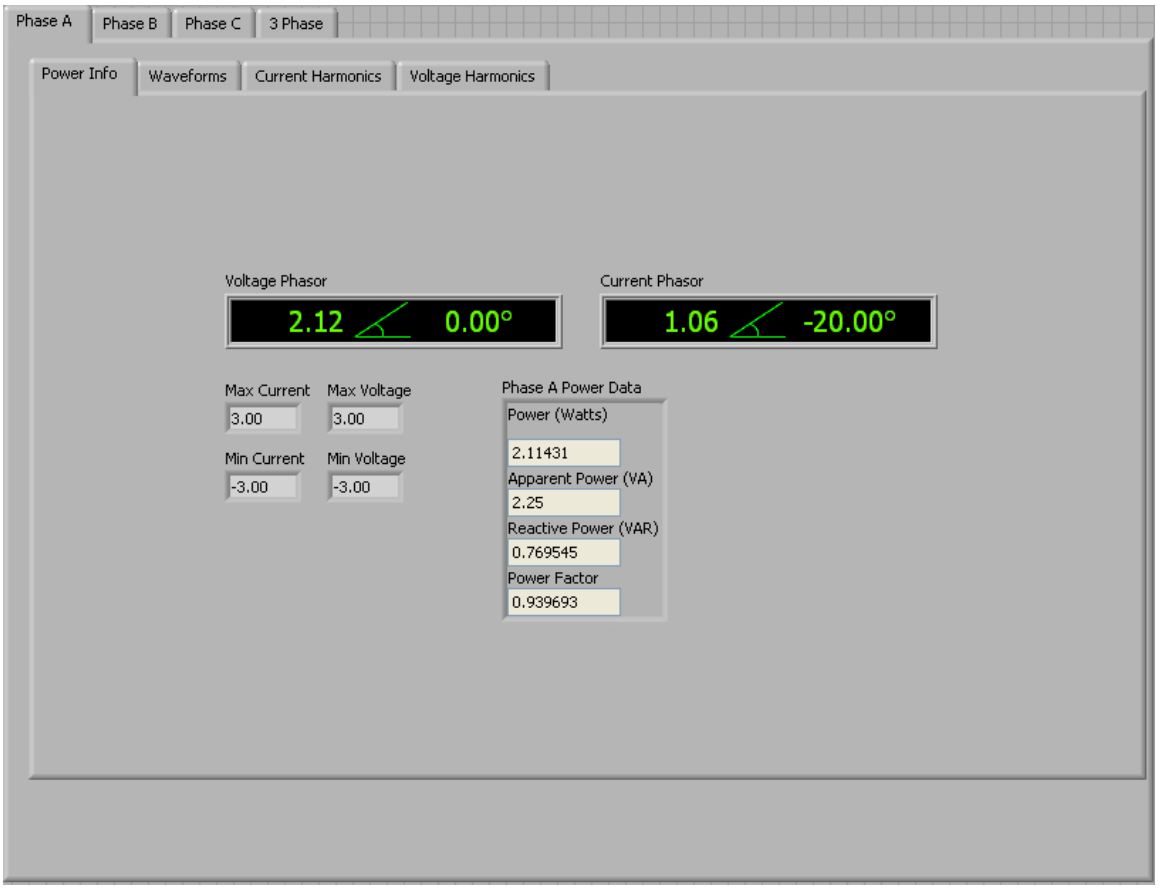

Figure 25: LabView display of power values.

In Figure 25 the phasors for the voltage and waveforms are displayed. The phasor includes the rms value of each waveform as well as the phase angle between them. The algorithms are specified to set the voltage phase to 0 degrees and to measure the current phase with respect to the voltage phase. In this case the current waveform is lagging the voltage waveform by twenty degrees.

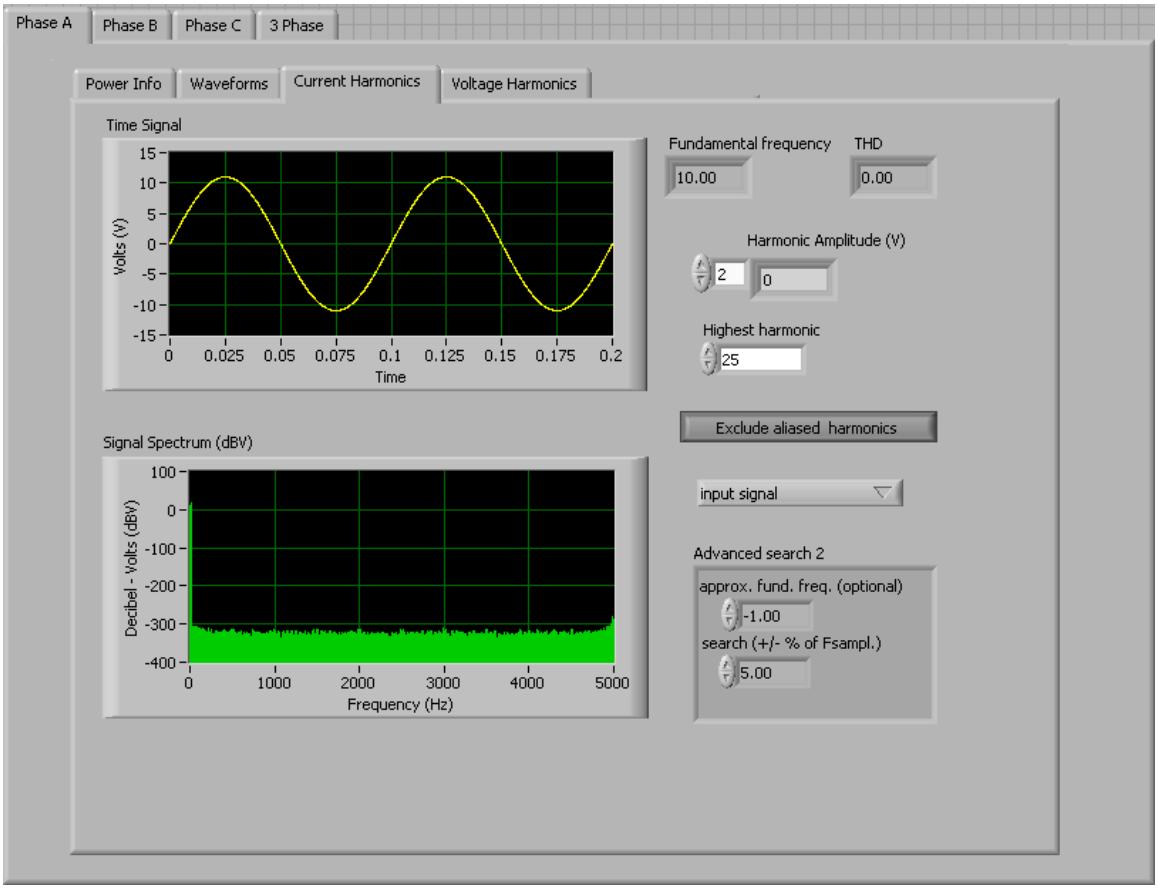

Figure 26: LabView environment showing harmonics.

In Figure 26 the harmonic data for each waveform are shown. The top image shows the waveform in the time domain and the bottom image shows the waveform in the frequency domain. This image also shows the magnitude of each harmonic of the waveform. On the right are displayed several values of the waveform. The fundamental frequency shows the measured fundamental frequency of each waveform. The THD represents the amount of harmonic distortion present in the signal. This is shown as a value and should be multiplied by 100 in order to calculate the percent of the waveform that is distortion. Below these is the harmonic amplitude monitor. This calculates the magnitude of each harmonic up to the highest specified harmonic.

The three phase tab contains all of the values that were discussed here except that it will show the total three phase output of each parameter. Also included on this tab is a phase diagram that shows each current and voltage phasor in graphical format.

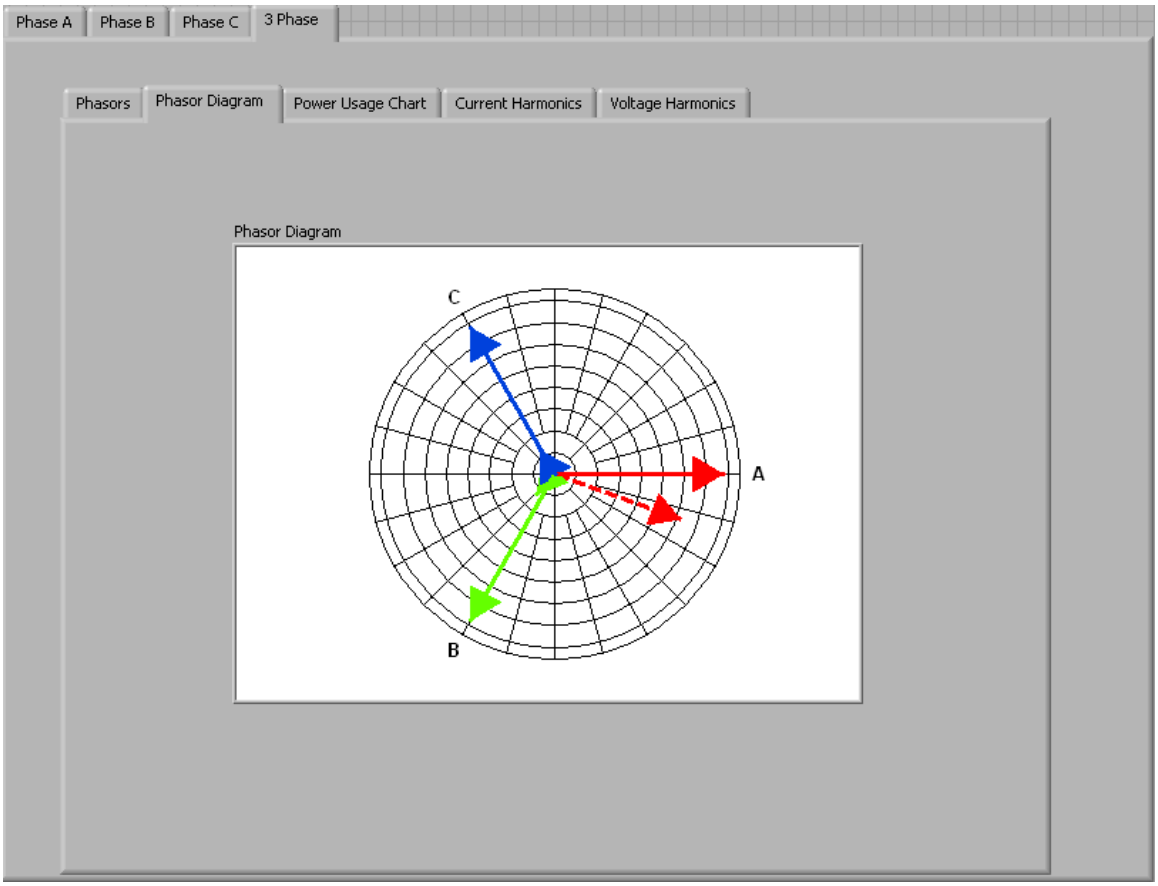

Figure 27: LabView representation of phasor diagram.

Figure 27 shows the phasor diagram of the voltage and current waveforms. It expresses the magnitude of each as well as their phase angle compared to each other. This diagram is used to show unbalance in the system. Also included in the three phase tab is a chart that shows graphically all of the power values.

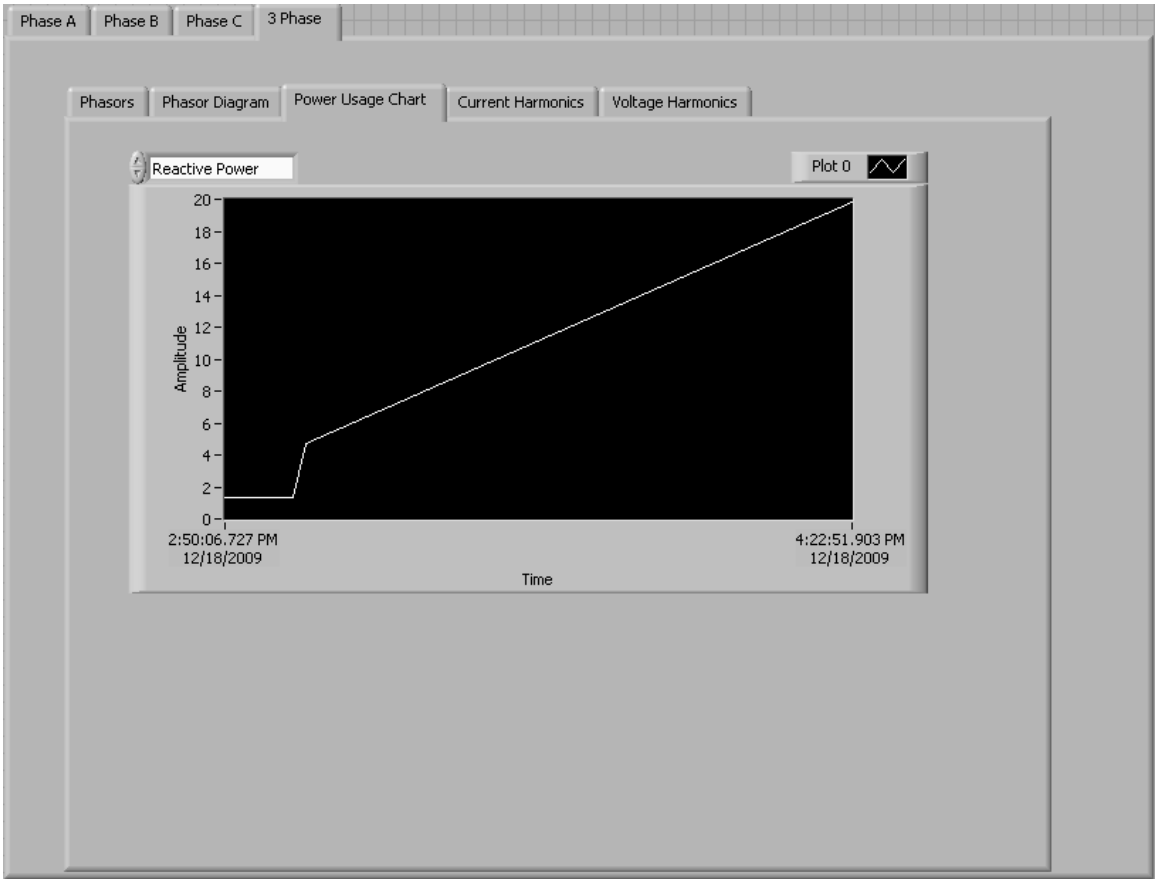

Figure 28: Graphical representation of power values.

If a fault occurs in the system the chart in Figure 28 will make it easy to identify how power values have changed over time. In this graph the phase angle was decreased to show that the reactive power will increase as the angle between voltage and current decreases.

The last graphical display developed for the ocean turbine power quality monitoring system is the warning tab. The implementation of the warning system is shown below in the Figure 29.

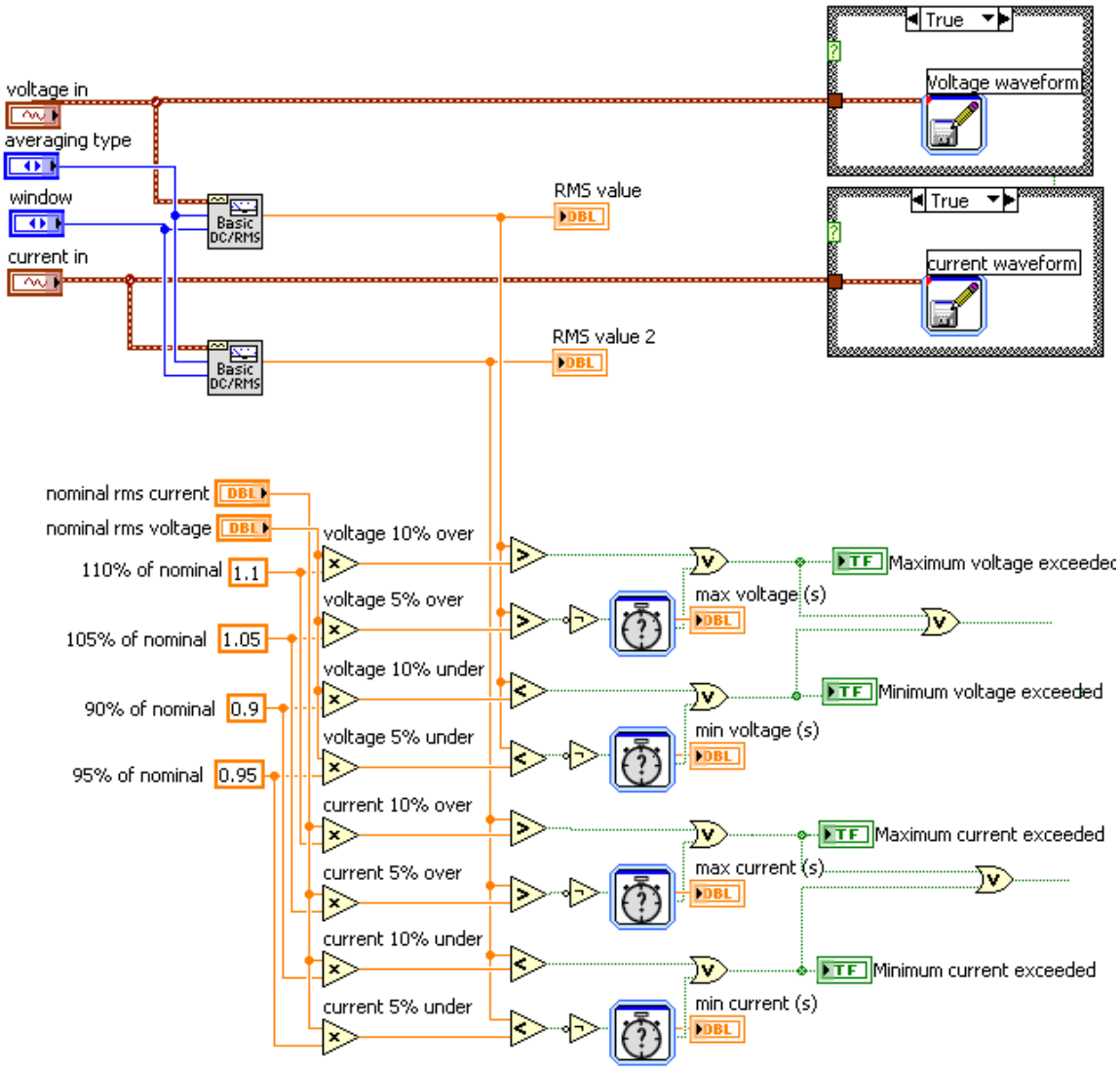

Figure 29: Variation sensor.

Figure 29 shows the first part of the warning system. In this visual instrument (VI) the rms values of each waveform are measured by the methods previously discussed. The rms values are then compared to the nominal rms values for the voltage and current produced by the induction generator. If these values are exceeded by 5% but less than 10%, a timer is started. If the variation lasts for 10 seconds a warning light will appear. This light will also appear if the rms values change by more than 10% of normal or if it

falls to 10% of the nominal value. These alarms are shown above as "Maximum/Minimum current/voltage exceeded." When any of these alarms are tripped the corresponding waveform is then recorded in a file that is specified in the module. These waveforms can then be read by another program and the output file can be defined according to the user. Also when any of the alarms are tripped a signal is sent to the second part of the alarm system which is shown in the Figure 30.

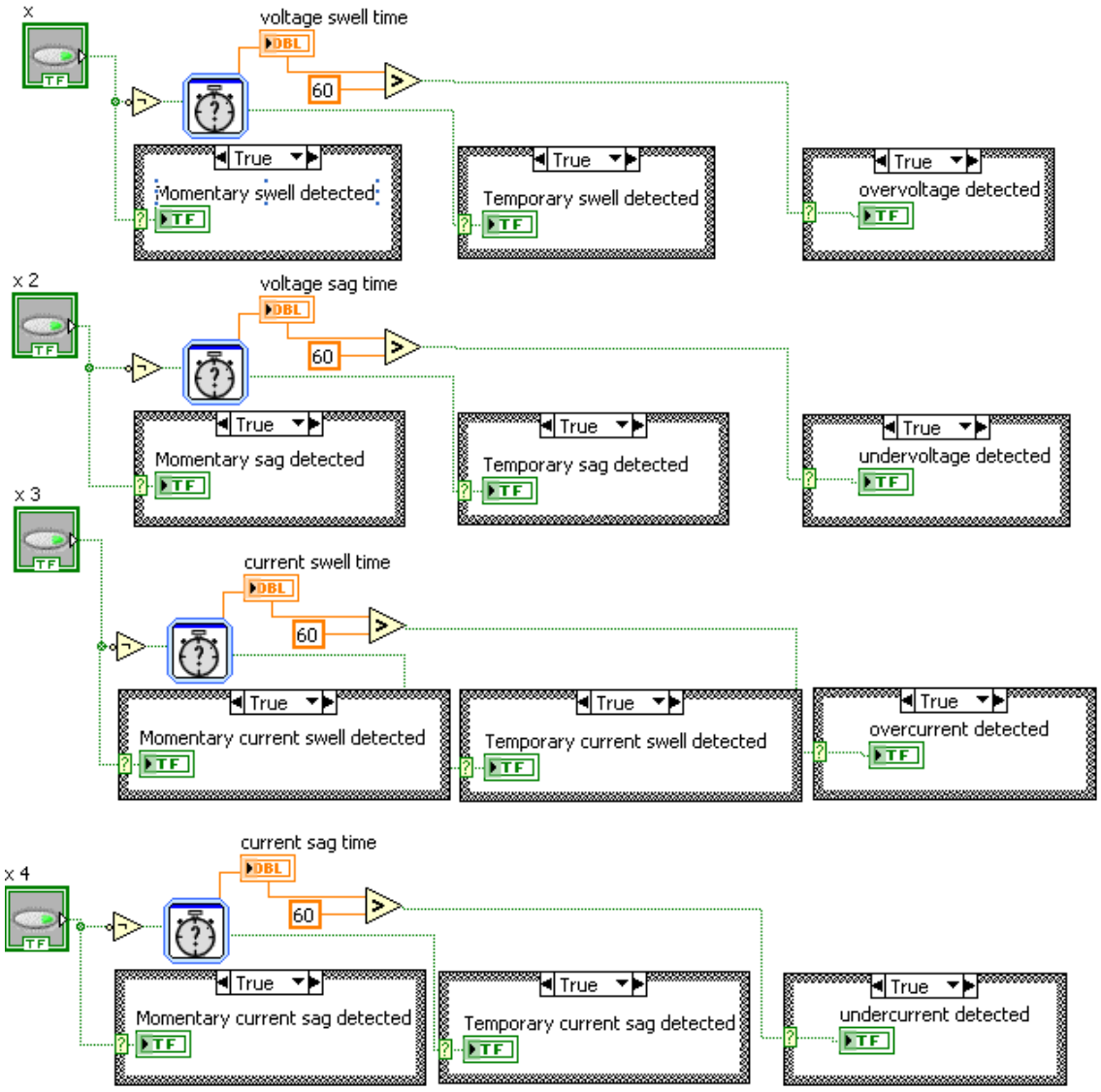

Figure 30: Event classification system.

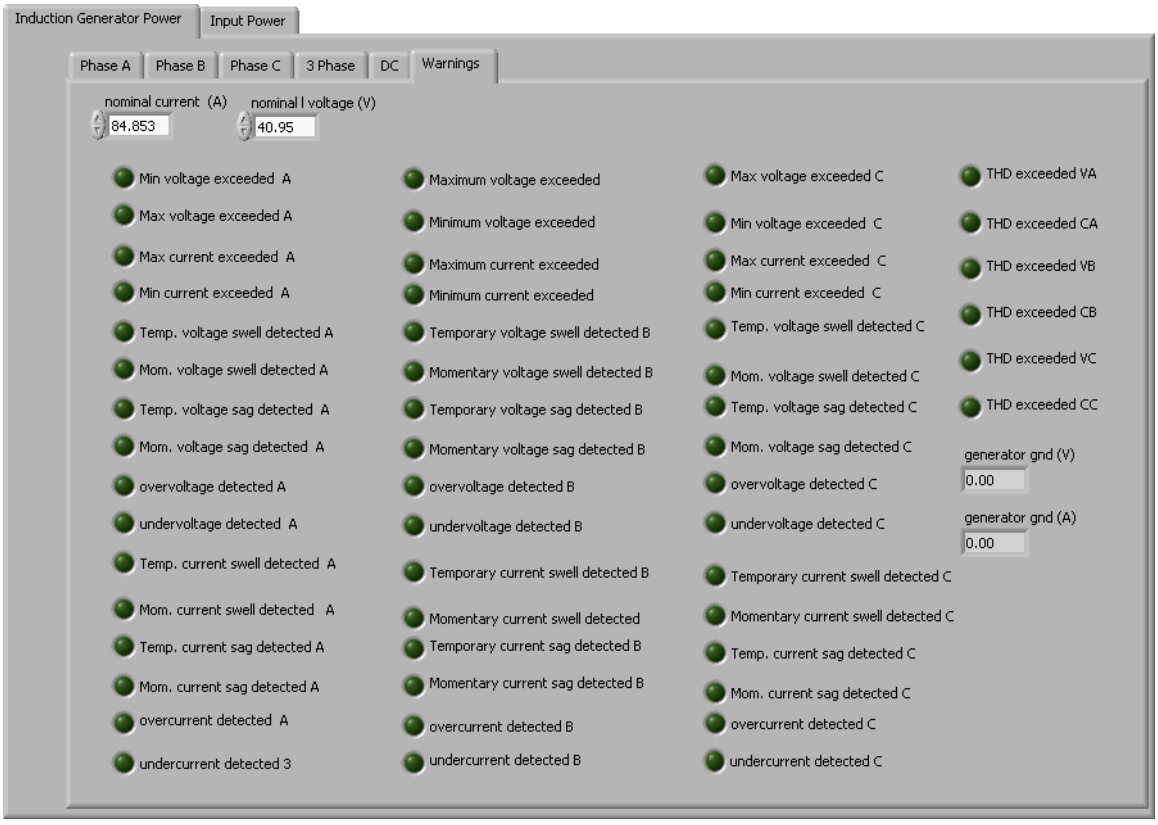

Figure 31: Error warning tab.

The error warning tab is designed to send a warning whenever power quality levels fall below specified levels. The first 3 warnings will only light up when a power quality event is in progress. When this occurs a file is created that collects waveform data for as long as an event is present in the power system. As soon as an event has passed these warnings will turn off and the file will be saved and closed. The last column is placed in order to inform the user that a power quality error has occurred and that data should be analyzed. This warning light must be reset by the user. A set of warnings is setup for each phase so that any power quality errors may be traced to the source. On the 3 phase tab a window has also been created to show that there are errors within the system.

5 Verification of power quality monitoring system

To demonstrate that this system accurately measures the quality of power generated by the turbine, a number of tests were performed to test the accuracy and stability of the monitoring system. The first step was to test the sensor boards that were developed to support the power quality sensors. Once these were verified the next step was to analyze the signal processing algorithms that are implemented in LabView. The process of these validation tests as well as the results of each is discussed in this section.

5.1 Analysis of the power quality sensor board

5.1.1 Measurement test

To verify that the sensor board functions properly it was necessary to test each current and voltage sensor that would be connected to the NI input modules. To test each of these the test bench shown in the Figure 32 was used.

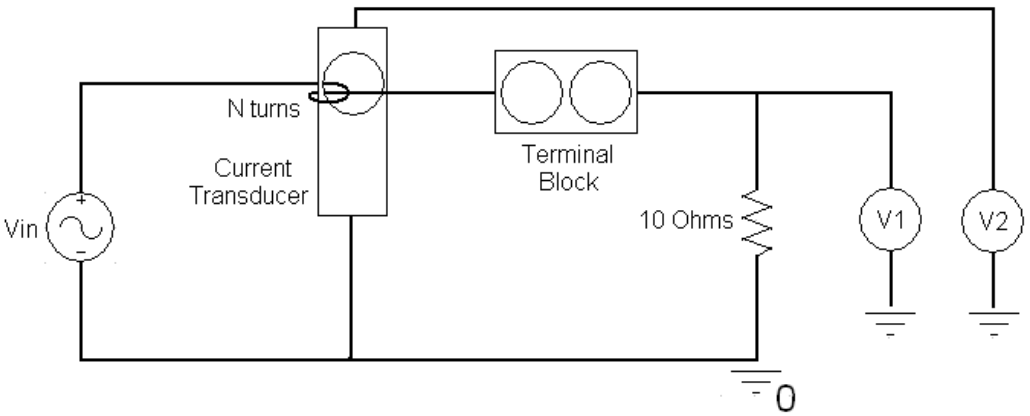

Figure 32: Test setup #1 for sensor board.

To test each sensor a line was wired through each current transducer and then connected to a section of the terminal block. Another line was wired from the other side of the terminal block to a 10 Ω resistor and to the negative terminal of the voltage source. The amount of current sent through the line was controlled by varying the input voltage. The amount of current could then be calculated according to Ohm's law shown here.

$$\text{Ohm's Law: } I = \frac{V}{R} \tag{5.1}$$

To test the current sensors at higher currents the test wire was wrapped around the current transducer according to the desired value of current. If the supply current was 1 A then the current transducer would sense a current of N Amps where N is the number of turns. If the input is 2A then the current sensor would sense a current of 2N Amps. By using this method the current sensors were able to be tested up to the maximum expected values of 60A.

V1 represents the current sensor outputs J3 and J5 on Figure 33. These connectors feed the current signal to the NI 9239 input module discussed in Chapter 2. In this test each set of points (signal, ground) were tested to ensure that they functioned according to specifications for a number of values. Similarly V2 represents the voltage outputs J4 and J6. Each set of points is wired to the signal lines from the terminal block which is represented as J2 in the following diagram. The signals are then connected to the NI 9225 module discussed in Chapter 2. In this way the voltage of each phase is read directly from the phase wire. Again each set of points was tested to ensure that they accurately monitor

the voltage waveforms. In this test the voltage was tested for 2 different values while the current was tested for 5 different values.

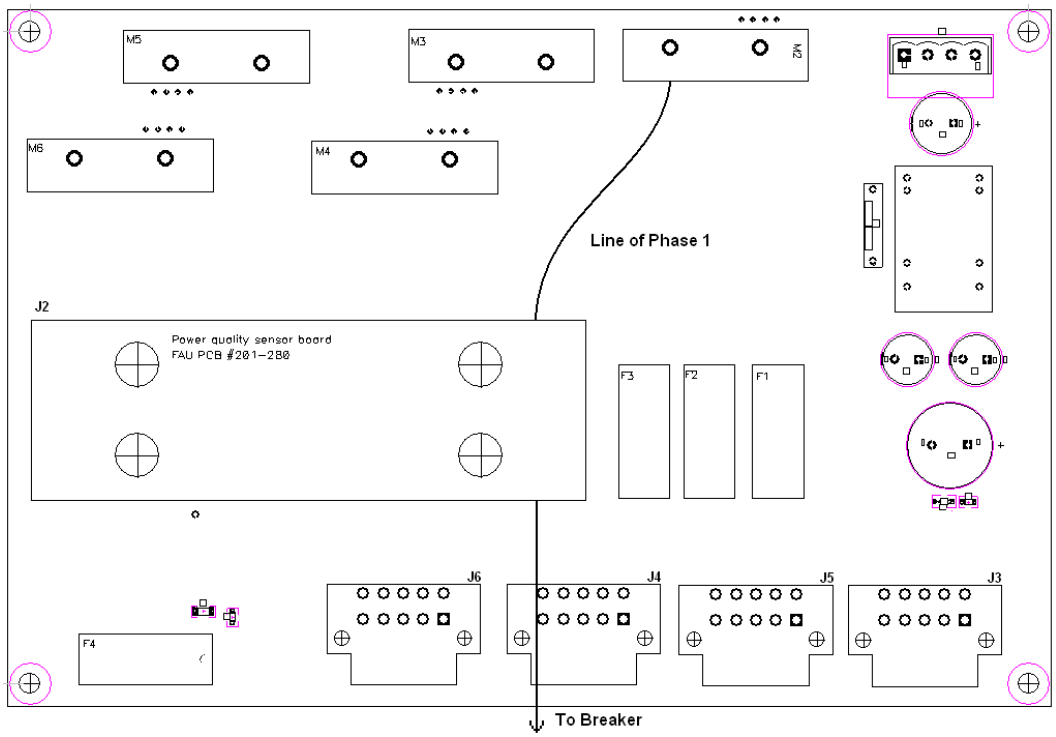

Figure 33: Test configuration on sensor board.

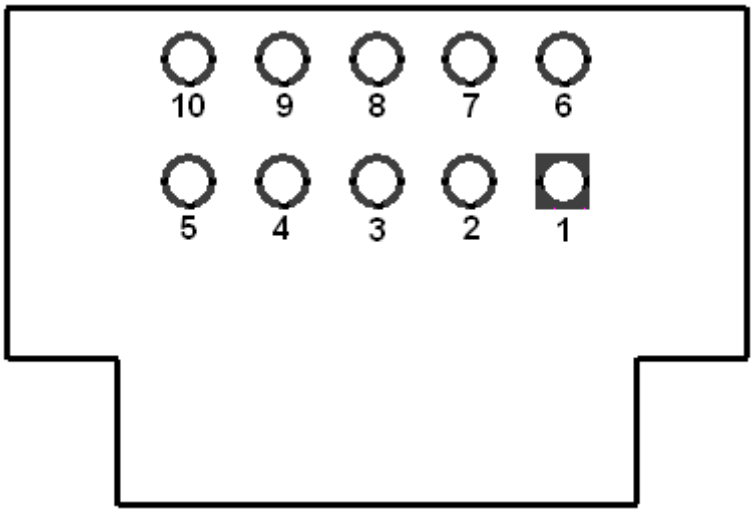

Figure 34: Signal connector pin configuration.

Figures 33 and 34 show the setup for testing the first current transducer, labeled as M2. For this input the current is read across pins 1 and 6 of the connectors J3 and J5. In the same way the voltage is read from pins 1 and 6 of the connectors J5 and J6.

For M2 the output voltage is plotted as a function of the input current.

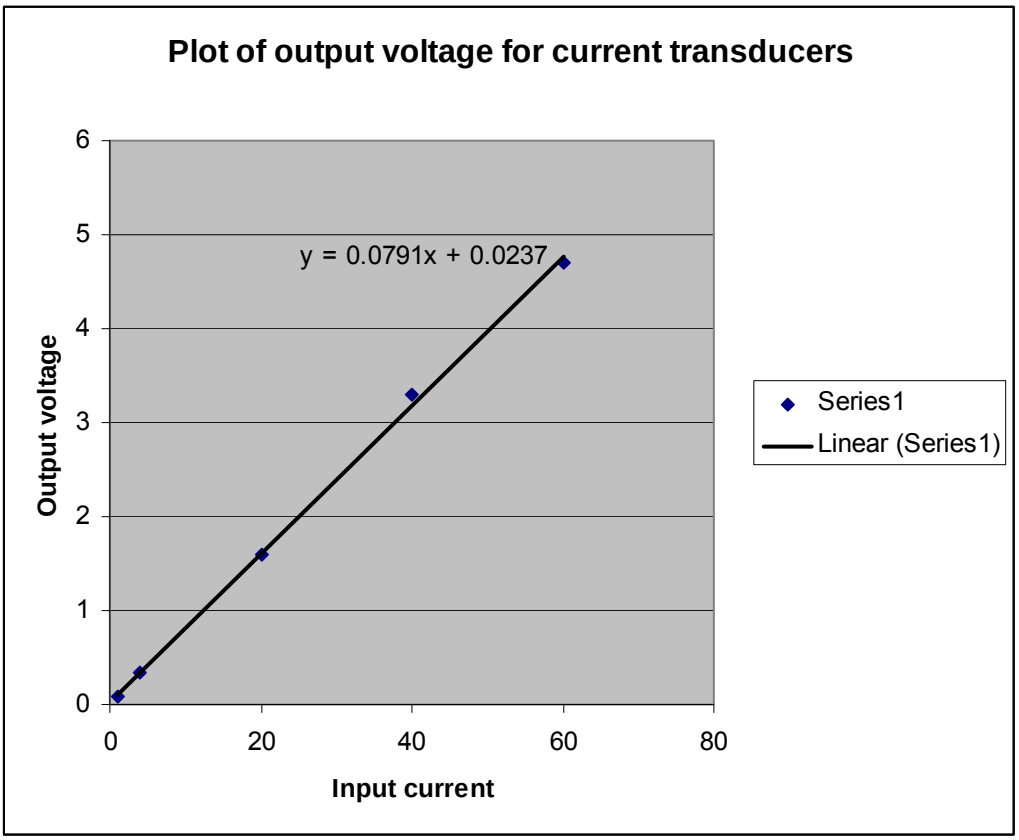

Figure 35: Data plot for phase 1 sensor.

The current transducers are manufactured to change the input current by a factor of .08. Figure 35 shows that the slope of the line of regression for the data is .0791. The error between this value and the expected value is 1.25%. This error is expected due to inefficiencies in the voltmeters that were used in this test. This figure and Table 5

demonstrate that the sensor board can be used to accurately measure the voltage and current waveforms produced by the ocean turbine system.

Table 5: Measured values for current and voltage sensors.

Input values	Output values per phase (V)					
Current (A)	Phase 1	Phase 2	Phase 3	Neutral	DC positive	DC negative
1	0.07	-0.08	0.08	0.08	-0.079	0.08
2	0.31	-0.32	0.31	0.32	-0.31	0.32
20	1.58	-1.61	1.59	1.6	-1.59	1.6
40	3.19	-3.22	3.2	3.2	-3.19	3.22
60	4.8	-4.83	4.8	4.8	-4.78	4.82
Voltage (V)						
10	10.2	10.1	10	10.2	10.1	10
40	40.1	39.9	40.1	39.8	40	40.2

Table 5 shows the measured values of each current and voltage sensor for the given input. It is important to note that the due to the configuration of the current sensors the values of phase 2 and DC positive are negative. This table verifies that the sensor board operates according to specifications and will accurately measure the power quality of the ocean turbine.

5.1.2 Frequency analysis

5.1.2.1 Test setup

The NI modules used in this system have a maximum sampling rate of 50 KHz. To ensure that the sensor boards could operate within this frequency a test of the gain of each device was developed. This test was also used to measure the time response of the current

sensors to changes in the magnitude of each device. To run this test the following configuration was used.

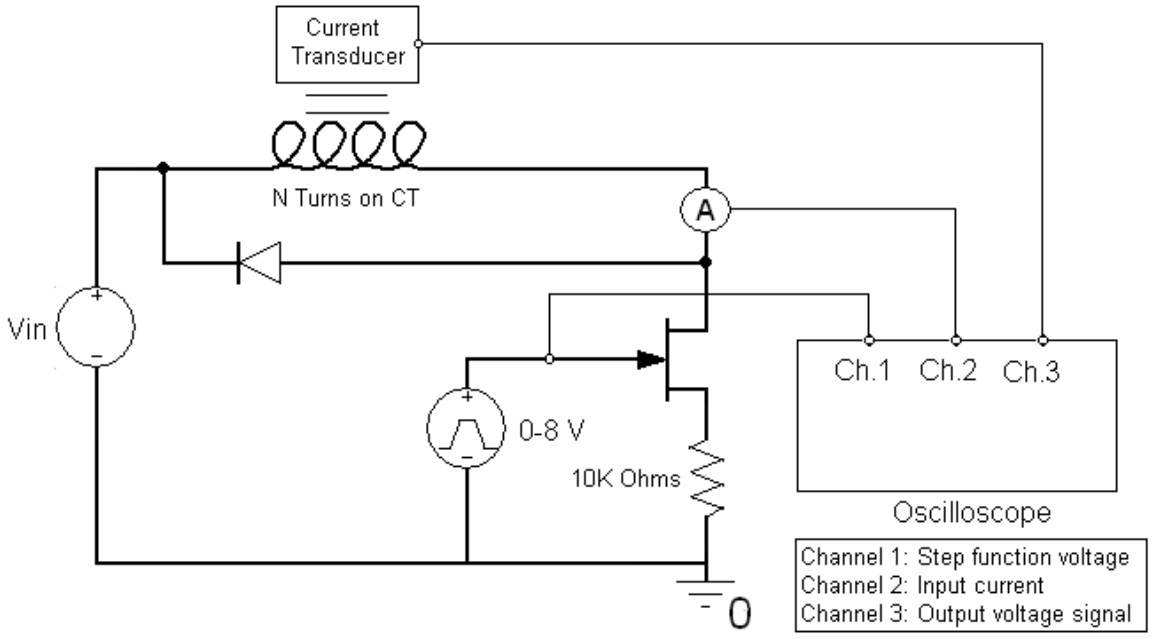

Figure 36: Frequency test configuration.

To measure the frequency response the same basic setup was used that was applied to the DC test. In this configuration however a mosfet was placed in series with the current transducer. A signal generator was then connected to the gate of the mosfet so that a square wave signal could be sent through the current transducers in order to measure the step response of the sensor board. This was done because there was no AC power source available that could be used to test this board. A diode was also added so that any induced current by the wiring configuration could be dissipated while the mosfet is off.

In the monitoring system the NI modules discussed in Chapter 2 will be used to collect data. However at the time of these tests the modules were unavailable so an oscilloscope

was used instead. In this test bench there are three signals that are sent to the scope. Channel one measures the square wave that is sent to the mosfet. This signal is used to measure the step response of the system by comparing the output waveforms to the square wave introduced by the mosfet. The second signal comes from a probe that measures the current in the line by the use of a Hall Effect sensor. Channel 2 of the scope measures the current that is sent through the current transducers. Channel 3 of the scope collects the data from pins 1 and 6 of J3 on the sensor board. This is the output voltage measured by the current transducers. This test was performed by measuring the output signal for input values of 5, 25 and 50 A. These values were accomplished by wrapping the signal wire around the current transducer 5 times and applying 1, 5 and 10 Amps. The waveforms of each are shown below in Figures 37-39.

5.1.2.2 Magnitude results

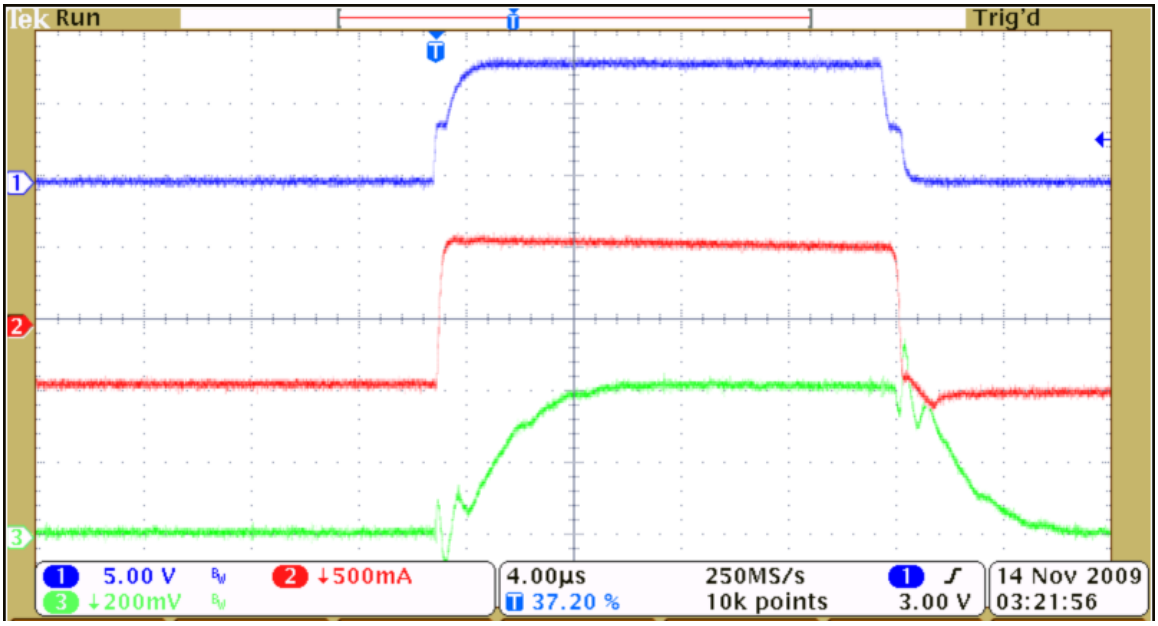

Figure 37: Current waveforms for 5A input.

Figure 37 shows the three waveforms for an input current of 5A. The lower left hand of the images shows the value of each division for each waveform. For waveform 1 the value given to each division is 5 V. In the figure waveform 1 stretches about 1.7 divisions which correspond to a magnitude of 8 V for the input signal. Channel 3 has a magnitude of .4 volts which is the expected value for the input current level of 5A. For channel 2 the measured input current is shown to be 1A but the wire is wrapped around the current transducer 5 times so that the transducer returns an output voltage that corresponds to 5A rather than the input of 1A shown here.

This verifies the results of the previous tests which show that the sensors accurately measure the voltage and current of the input signal. It is also important to note that the response time of the output voltage to a change in the input current is too small to measure and that the rise time of the output voltage signal is 257.9μS. This value will be even smaller when the system is measuring sinusoidal signals from the ocean turbine. These values are also small enough that the measurement system can be considered to be running in real time.

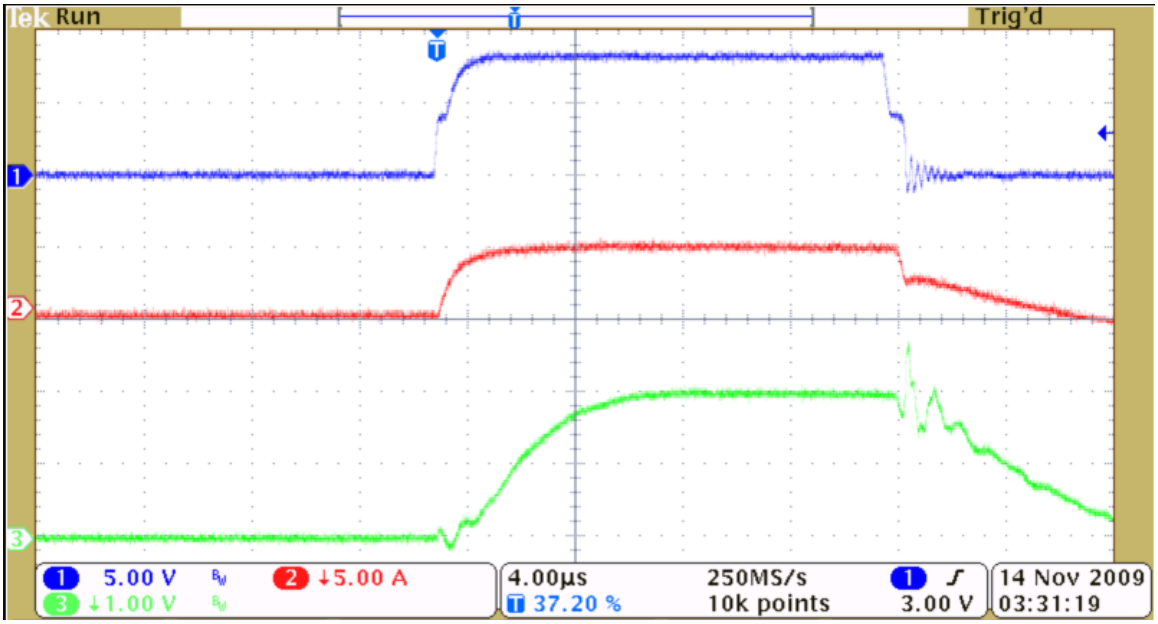

Figure 38: Current waveforms for 25A input.

Figure 38 shows the response of the system when the input current is stepped up to 25 A. Again the measured input current is shown as 5A but the current transducer measures a value of 5*5 = 25A. This value corresponds to the output voltage shown in channel 3 of 2V.

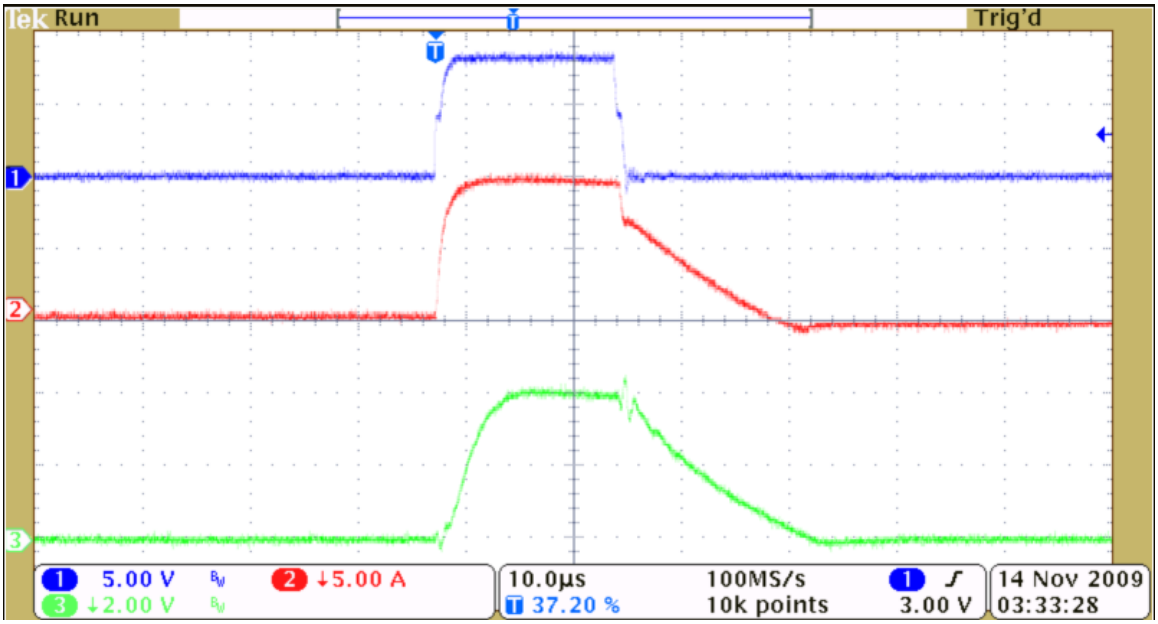

Figure 39: Current waveforms for 50A input.

Figure 39 shows the response of the system when the input current is again stepped up, this time to 50 A. The measured input current is shown as 10A but in this configuration the current transducer measures a value of 5*10 = 50A. This value corresponds to the output voltage shown in channel 3 of 4V.

5.1.2.3 Frequency analysis

The last test performed on the sensor board was to measure the frequency response of the system for each value of current. The purpose of this test is to verify that the sensors can measure a high frequency signal and still return accurate data. It is also important that the response of the gain of the sensors not change if the magnitude of the current changes. To verify the gain of the system for each input current needed to be measured and compared to the other current values. If the gain signal is the same for each value of input current

then the system will work regardless of the frequency of the input signal. This is especially important for calculating the harmonic distortion of the waveforms. To ensure that the waveform could be measured up to the 50 KHz that the modules are capable of, the input frequency was set to 300 KHz to give some room for error.

The output waveforms from the current transducers can be described as shown in Figure 40.

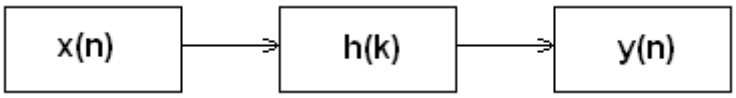

Figure 40: Correlation function.

In this diagram x(n) represents the input signal to the current transducer and h(k) is the impulse response of the current transducer that transforms the current into a voltage waveform. The output signal is represented by y(n). Because this system is linearly time invariant with an input of x(n) (digitized signal) the output of the system in the time domain is given by:

$$y(n) = \sum_{k=-\infty}^{\infty} h(k)x(n-k) \tag{5.2}$$

The sampled waveforms shown in Figures 37-39 each contain over 10,000 points. Because it would be impossible to make this calculation for all of the data points it is necessary to use another means to find the function h (k). To do this the data was transformed into the frequency domain by using the DFT. In the frequency domain the output of the system is given by:

$$y(j\omega) = h(j\omega)x(j\omega) \tag{5.3}$$

From this equation the gain of the system is simply calculated as:

$$h(j\omega) = \frac{y(j\omega)}{x(j\omega)} \tag{5.4}$$

The desired bandwidth of this system is 50 KHz which is set by the limits of the NI modules. To verify that the system works properly the sampling frequency was set to 1MHz. This ensures that any values that appear above the 50 KHz will be seen. The data processing for this test was performed using Simulink.

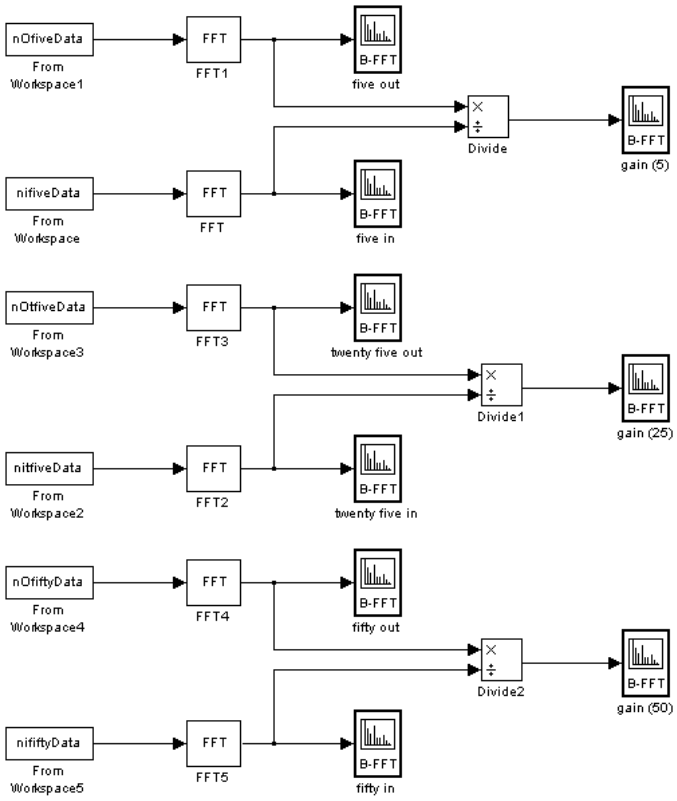

Figure 41: Simulink model for verifying frequency response.

To ensure accuracy in the results the set of values for 25A and 50A were normalized to the 5 A values. This was done by dividing the input currents by 5 and 10 respectively and the output currents by the same values. The FFT was then taken of each waveform and the gain h(k) was then calculated and plots of each were developed.

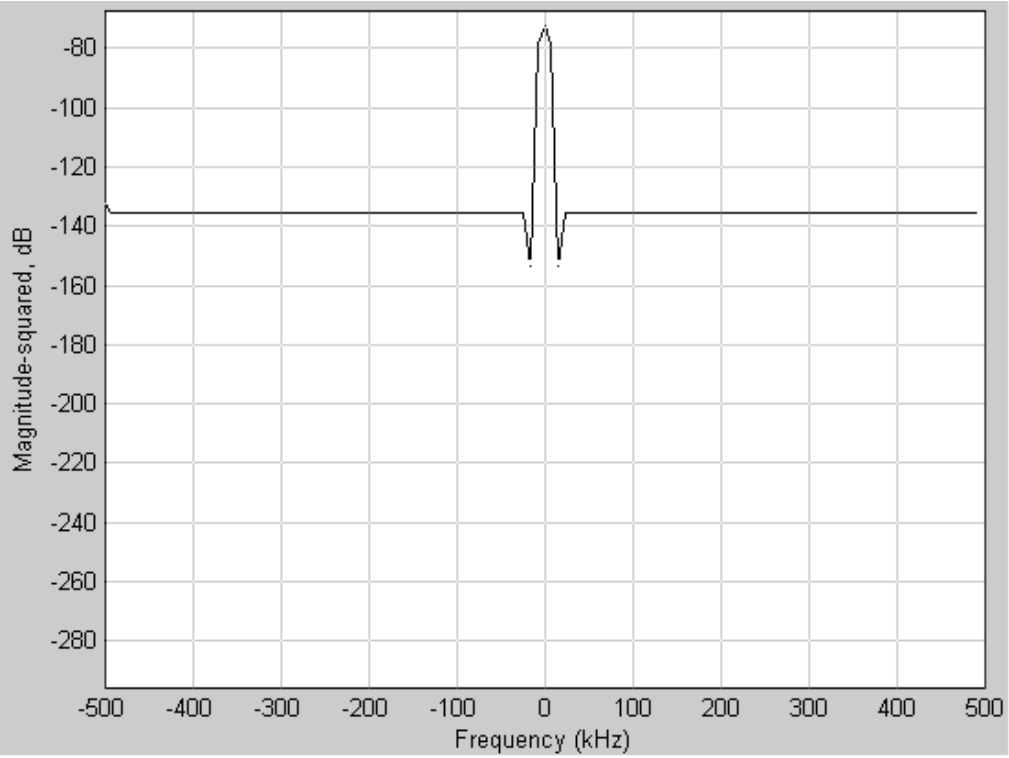

Figure 42: Frequency response of h(k) at 5A.

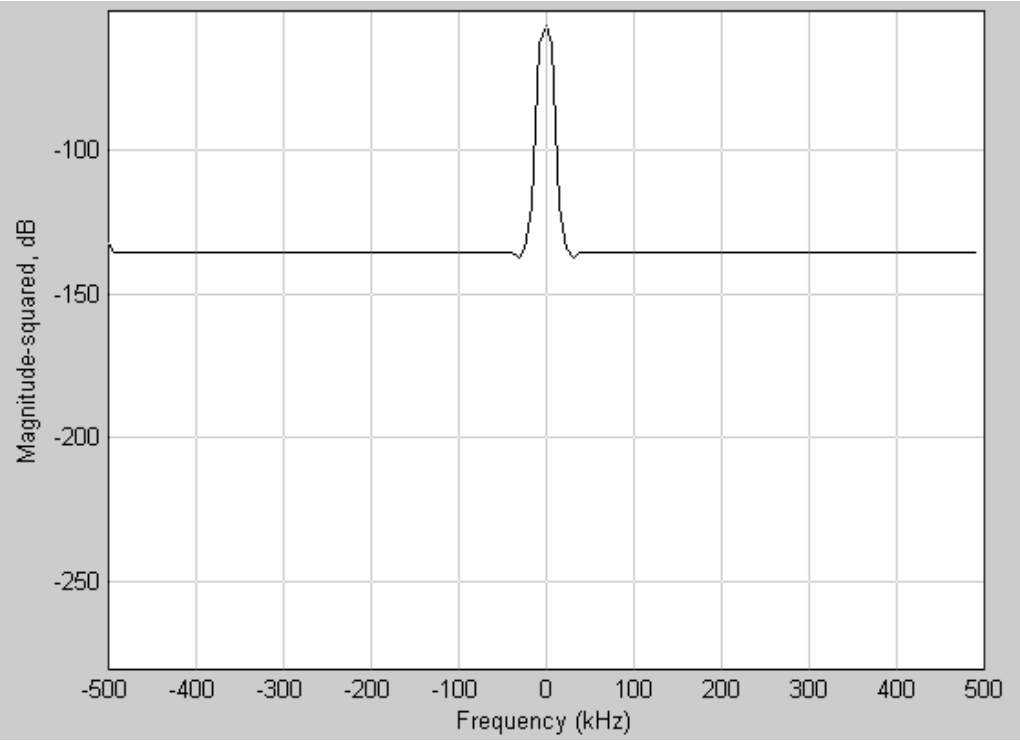

Figure 43: Frequency response of h(k) at 25 A.

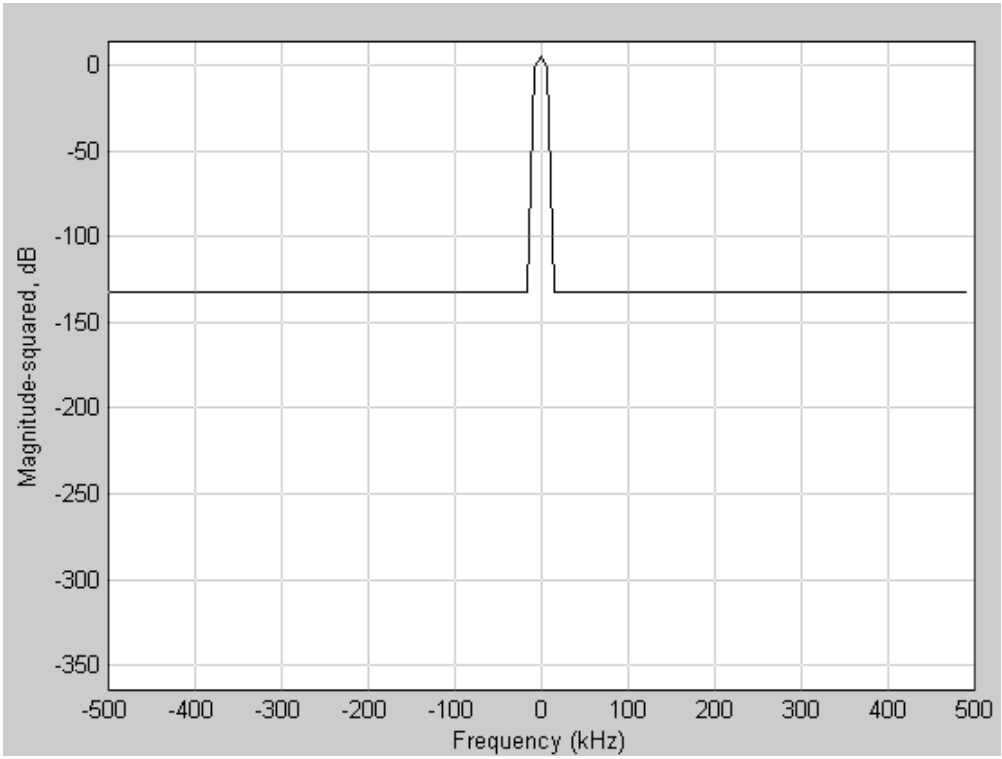

Figure 44: Frequency response of h(k) at 50A.

These 3 figures show that the h(k) responds right at the 30KKz level that the signal was input into and that the response is identical for all 3 current levels.. These figures show that the bandwidth of the current sensors is at least equal to the band width of the NI modules and that these instruments are capable of accurately measuring the voltage and current waveforms produced by the ocean turbine system.

5.2 Analysis of signal processing

5.2.1 Simulation results

In order to test the power quality monitoring system a three phase power generator was simulated as well as a DC power supply. The characteristics of these simulated signals, including frequency, amplitude and noise present, were controlled in order to test and improve the power quality monitoring system.

5.2.1.1 RMS

Because the magnitudes of the tones are known, the rms value for the current and voltage can be calculated simply by:

$$rms = \frac{magnitude}{\sqrt{2}} \tag{5.5}$$

To test the LabView algorithms for calculating the rms values, 2 waveforms were simulated as shown in the following diagram.

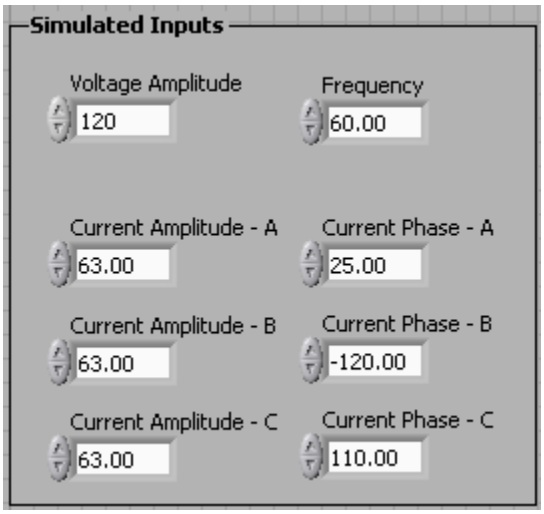

Figure 45: Test signal setup.

From Figure 45 the amplitude of the input voltage waveform is 120V and the amplitude of the current waveform is 63 A. These waveforms were then fed into the LabView algorithms for calculating power quality values. The output rms values are shown in Figure 46.

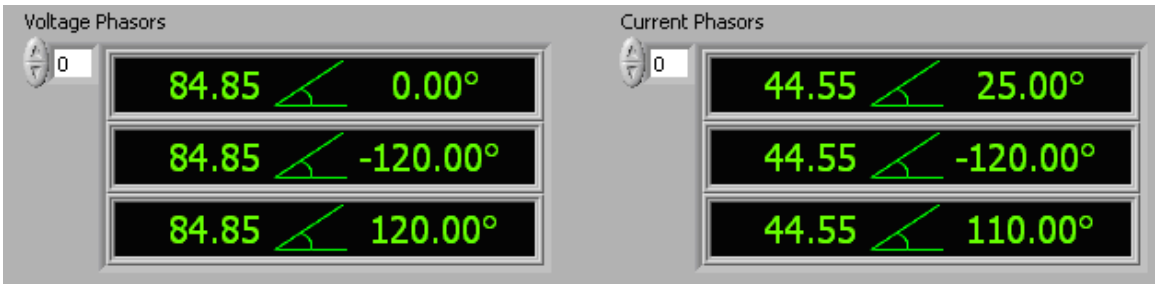

Figure 46: Measured rms values of test voltage and current.

These values can be checked using the equation for rms values discussed previously. The voltage is calculated as

$$V_{rms} = \frac{120}{\sqrt{2}} = 84.85V \tag{5.6}$$

and the current is calculated as:

$$I_{rms} = \frac{60}{\sqrt{2}} = 44.55A \tag{5.7}$$

Based on these values and the values shown in Figure 46 the algorithms are accurate in measuring the rms value of each waveform input. These tests were also run with noise added to the signal. The signals plus noise were then sent to a filter and the rms measurements were taken. The results were the same as those shown here.

5.2.1.2 Phase and power values

In Figure 45 the configuration of the input signals is shown. This shows the current of phase A to be out of phase from the voltage by a factor of 25 degrees while phase B is out of phase from the phase B voltage by 0 degrees and the current of phase C is out of phase of the phase C voltage by 10 degrees. From Chapter 4 the PF of each phase is calculated as

$$PF = \cos\phi \tag{5.8}$$

where φ is the phase angle between the voltage and current waveforms. In this case the power factor for each phase is:

Table 6: Measured Power Factor.

Measured Power Factor		
Phase 1	Phase 2	Phase 3
0.906	1	0.98

The total power factor is found by taking the average of the three phases added together. In this case the total power factor is .9637 which is the measured value shown in figure 50.

The three phase power of the ocean turbine system is calculated using several steps. The first is to measure the amplitude of each waveform. This includes the waveform for voltage and currents for all three phases. The rms value of each is then calculated by dividing the amplitude by the square root of 2. The power values are then calculated by:

$$\text{Apparent Power: } S = V_{rms} * I_{rms} \tag{5.9}$$

$$\text{Active Power: } P = V_{rms} * I_{rms} * Cos(\phi) \tag{5.10}$$

$$\text{Reactive Power: } Q = V_{rms} * I_{rms} * Sin(\phi) \tag{5.11}$$

The total three phase power is then calculated by adding the power of each phase together.

$$\text{Total power: } P_{total} = P_A + P_B + P_C \tag{5.12}$$

The power values are calculated in the power quality monitoring system by reading each waveform into LabView. The calculations have been programmed into LabView and are displayed as in the following diagram.

To test these values the signals were input as shown in Figure 45 and each value was measured accordingly. The measured power values are shown here in the Figure 47.

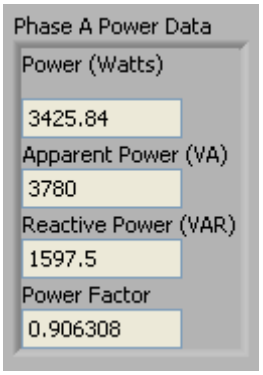

Figure 47: Measured values of phase A.

To verify the accuracy of these measured values they can be compared to the calculated power values of the waveform. This was done for all three phases as shown here.

Table 7: Phase A calculated values.

Calculated values (Phase A)	
V	120 V
I	63 A
Phase	25 degrees
S	3780 VA
P	3425.8 W
Q	1597.5 VAR

It is shown that the calculated values match the measured values and verifies that the calculations for phase A work correctly.

The calculations are repeated her for phase B and C of the test signals.

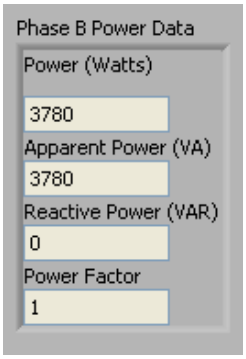

Figure 48: Measured values of phase B.

Table 8 Phase B calculated values.

Calculated values (Phase B)	
V	120 V
I	63 A
Phase	0 degrees
S	3780 VA
P	3780 W
Q	0 VAR

It is shown that the calculated values match the measured values and verifies that the calculations for phase B work correctly.

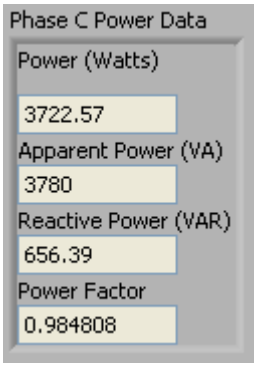

Figure 49: Measured values of phase C.

Table 9: Phase C calculated values.

Calculated values (Phase B)	
V	120 V
I	63 A
Phase	10 degrees
S	3780 VA
P	3722.57 W
Q	656.39 VAR

It is shown that the calculated values match the measured values and verifies that the calculations for phase C work correctly.

Figure 50 shows the measured values of the total three phase power of the system.

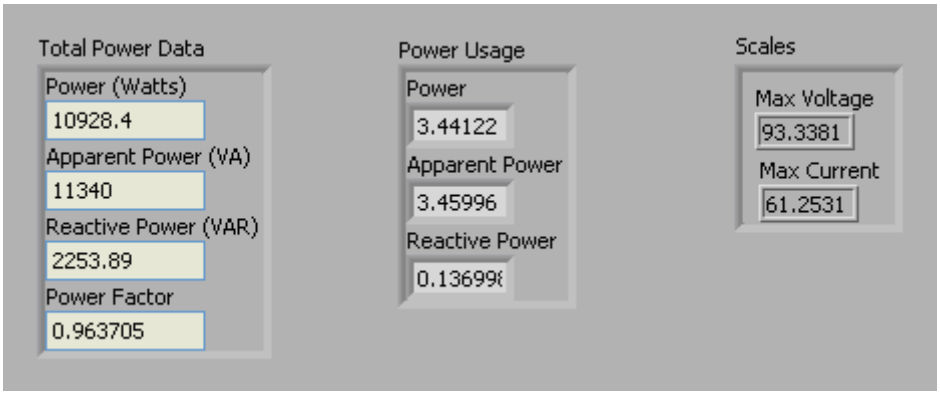

Figure 50: Measured 3 phase power values.

Again, these values can be verified by comparing them to the calculated 3 phase power for the given input configuration. The calculated values are:

$$S = 3780 + 3780 + 3780 = 11340 \text{ VA} \tag{5.13}$$

$$P = 3425.84 + 3780 + 3722.57 = 10928.4 = 3722.57 \text{ W} \tag{5.14}$$

$$Q = 1597.5 + 0 + 656.39 = 2253.89 \text{ VAR} \tag{5.15}$$

These values match the values shown in figure 50 and verify that the LabView algorithms for measuring power values function as specified.

5.2.1.3 Measuring frequency

As discussed above, the zero crossing method described above is used to calculate the frequency of each power waveform. To test this algorithm the frequency of each waveform was varied and the output was compared to the input. Table 10 shows the input

and output values that were measured. This table verifies that the frequency monitoring algorithms used in the monitoring system accurately measure the frequencies of each input waveform, although it should be noted that it is unclear how these algorithms will react to fast variations in the frequencies of the measured waveform.

Table 10: Frequency measurement Values.

Phase A					
in	60	62.3	65	70	125.3
out	60	62.3	65	70	125.3
Phase B					
in	60	62.3	65	70	125.3
out	60	62.3	65	70	125.3
Phase C					
in	60	62.3	65	70	125.3
out	60	62.3	65	70	125.3

5.2.1.4 Measuring THD

To test the THD algorithms noise was added to each waveform at varying harmonics. The resulting waveform and controls are in Figure 51.

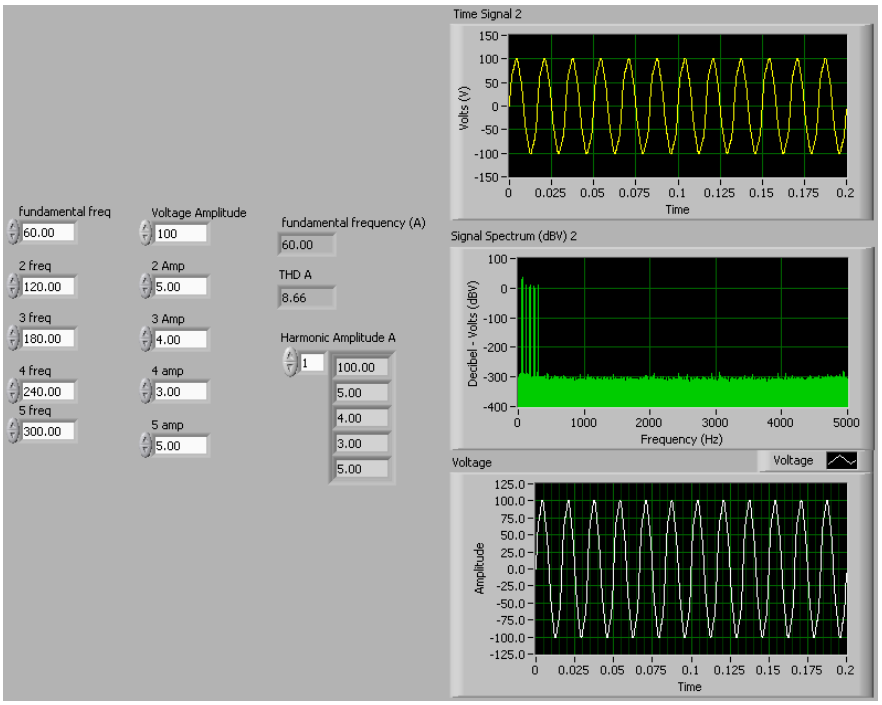

Figure 51: THD test data.

From section three the equation for calculating the THD is given as:

$$THD = \frac{\sqrt{\sum_{h=2}^{H} V_h^2}}{V_1} \tag{5.16}$$

Using the values in Figure 51:

Vh = 100, V1 = 5, V2 = 4, V3 = 3, and V4 = 5. Plugging these values into the equation for THD gives:

$$THD = \frac{\sqrt{25+16+9+25}}{100} = .0866 = 8.66\% \tag{5.17}$$

This calculated value matches the value of the THD that is shown in the Figure 51 of 8.66%. This verifies that the THD algorithms accurately measure and calculate the harmonic distortion of each waveform and can be used as part of the power quality monitoring system.

5.2.2 Experimental results

The above section has demonstrated that the power quality system developed as part of this work accurately measures and quantifies power quality indices. The next step in the verification of this system is to experimentally show that the system is capable of collecting and manipulating data from the actual turbine power system. Unfortunately the dynamometer was not complete at the time this thesis was completed. However the motor that is being used to simulate the Gulf Stream Current in the dynamometer project was at the time operational. This section describes the experimental data that was collected from this motor and demonstrates that the system may be used to monitor power quality in the ocean turbine prototype.

5.2.2.1 Setup and test procedures

To monitor the motor side of the dynamometer the power quality sensor board was installed to measure the power between the motor and the drive. The NI input modules were then wired to the sensor board so that the data could be read by the cRIO controller

and then manipulated using LabView. The motor was then run at varying rpm's and the power quality indices were measured for each rpm value.

5.2.2.1.2 Notes about installation of cRIO device

It should also be noted that the cRIO device will obtain a new ip address each time it is powered on. When this occurs the ip address used in LabView needs to be changed to match the new address. To ip address of the virtual controller can be viewed by opening the project window in LabView which is shown here.

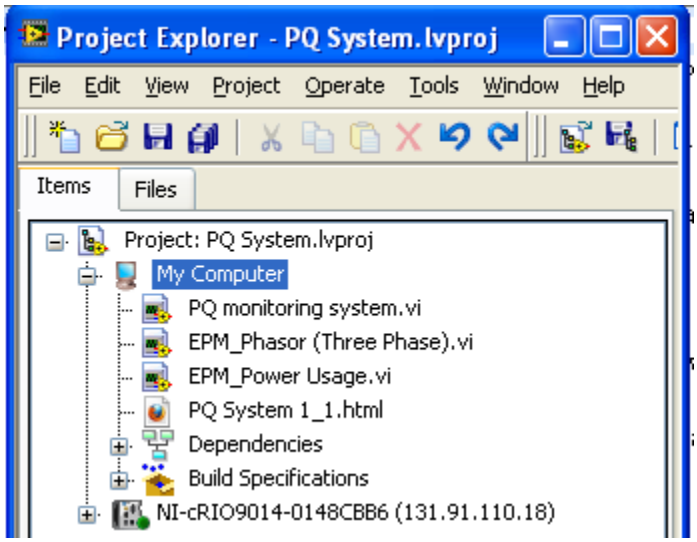

Figure 52: Project Explorer window.

The virtual ip address is circled in the figure above. To view the ip address of the actual controller the Tools/Measurement and Automation Explorer tab should be selected. In this window the controller will be listed under the remote systems tab. By selecting the controller the network settings will appear and the ip address will be listed. If the ip

address listed here does not match the address on the virtual controller the virtual controller address will have to be changed. To do this, right click on the virtual controller in the project explorer window and select properties. Under the general tab the address shown in the network settings window should be entered as the ip address.

It is also important to note that in order to change the scan engine settings of the cRIO device that the device has to be disconnected and then reconnected in order for the changes to be implemented. This again can be done by right clicking on the controller in the project explorer window and selecting connect/disconnect.

5.2.2.2 RMS values for current and voltage

It should be noted that there was no load on the motor when these tests were run. The result is that the voltage and current have no distinct measurable waveforms. Because of this fluctuation the power values calculated as well as the rms voltage cannot accurately be measured. For the purpose of this test we expect to see a constant rms current while the rms voltage will rise in parallel with an increase in the rpm of the motor. The rms current level is actually measured by the drive and the experimental value can be measured against the value calculated by the drive. The operational current is shown by the drive to fluctuate between 31 and 41 amps.

Figure 53: Experimental values of rms voltage and current.

Figure 53 shows the measured rms current and voltage values measured between the AC motor and the drive while the motor was running at 10 Hz. Table 11 shows the rms values for each speed of the motor. From this table it can be verified that the current remains constant around 32 amps and the voltage increases with the increase of the rotational speed of the motor. The difference in voltage can be accounted for by the varying of the waveform due to distortion.

Table 11: Measured rms values.

Measured rms values

Hz	Volts	Current
10	115.56	33.34
20	136.65	42.41
30	167.78	36.39
40	192.86	34.03
50	224304	34.71

5.2.2.3 Waveforms and THD results

The voltage waveforms can be described as "hash[29]" which would be caused by the switching of the pulse width modulation that is controlled by the drive. Because of this the expected waveforms of the voltage will have no waveform at all while the current waveform would be filled with distortion. This is consistent with the acquired waveforms that are shown here.

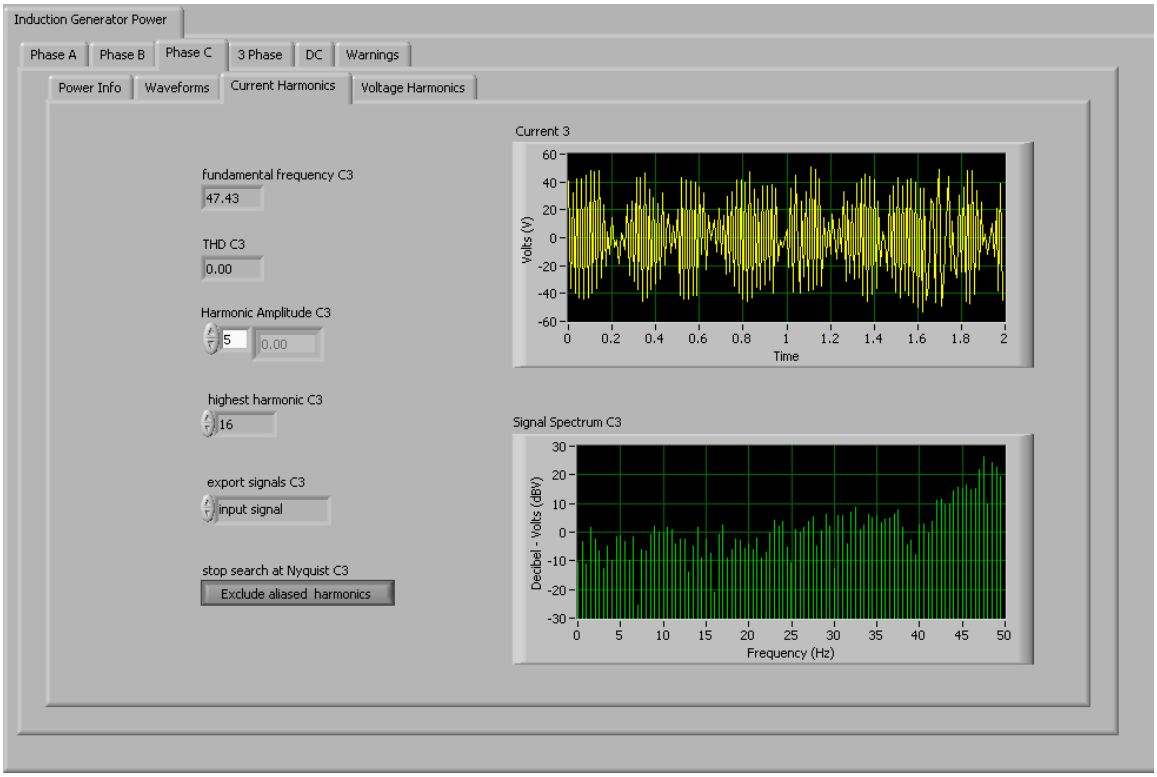

Figure 54: Experimental current waveform.

Figure 53 shows the time waveform as well as the signal spectrum of the current waveform. While this is somewhat expected it is impossible to know if this is an accurate reading without testing the motor with a load on it. It is also important to note that because of the amount of distortion in the signal that the THD reading is also not accurate.

5.2.2.4 Warning system

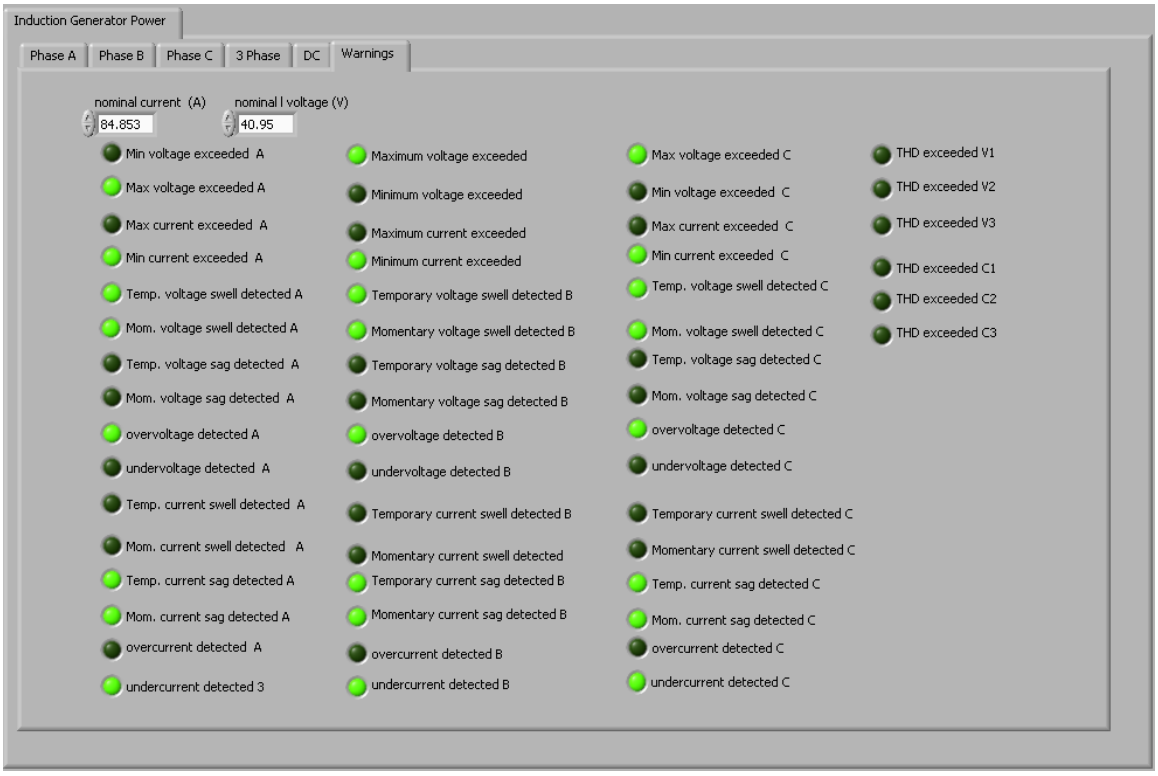

Figure 55: Warning system results.

While the experimental results were not able to completely validate the voltage and THD calculations it did provide a chance to experimentally test the warning system. Figure 54 shows the results after two minutes of testing. Note that the recommended values for voltage and current for this test were 40.95V and 84.853A. These values were arbitrarily chosen. After 5 seconds the momentary voltage lights came on. After 10 seco0nds the temporary warning lights were activated and after 1 minute the overvoltage/undercurrent detected lights were activated. This is consistent with the event classifications discussed in Chapter 3. This verifies that the warning system operates according to specifications.

6 A model of the ocean turbine electrical system

6.1 Motivation

Power quality monitoring includes an understanding of how certain changes in the system will affect the overall operation. These changes could include variations in the environment in which the system sits, wearing of the motor windings or any number of faults that may occur. In order to understand how the system will operate in such a dynamic environment a model of the power system was developed using P-Spice. This model actually is built to simulate the function of the dynamometer but can be used to simulate various scenarios that the turbine may encounter when deployed in the Gulf Stream.

6.2 Model development

As shown in Figure 2, the ocean turbine electrical system is made up of 4 key components. These are the:

- AC voltage source
- Resistor load bank
- AC variable speed drive
- 3 phase induction machine

In order to create a model of the system of each these components first had to be modeled in the P-Spice environment.

6.2.1 AC voltage source

The AC voltage source is set to model the power source that will be used to initially power the ocean turbine to begin rotation of the blades. In the dynamometer setup at FAU's SeaTech campus this power source is the FPL power grid. As such the model for this source is an AC signal with amplitude of 120V running at a frequency 0f 60Hz.

6.2.2 Resistor load bank

The load bank resistor is simply modeled as a resistor with a value of 1MΩ. This was done to model the large load of the resistor bank that converts the electrical energy into heat.

6.2.3 The AC variable speed drive

The main purpose of the AC drive is to control the amount of voltage across the load bank resistor. However, the AC drive also will be used to control the rotational speed of the ocean turbine propeller. This is done by changing the frequency of the rotating magnetic field which in turn will change the speed of the rotor shaft. In order to change the frequency of the magnetic field the AC signal that controls the magnetic field of the

induction machine is converted to a DC signal by a rectifier. The signal is then sent to an inverter which changes the signal back to AC but with a frequency defined by the drive. In order to model this process a circuit model was created for an inductor and a rectifier according to the schematic shown in Figure 3. The models for the rectifier and the inverter as well as their input/output waveform are discussed below.

6.2.3.1 The inverter

The circuit model and the P-Spice equivalent of an inverter are found in the following figures. In this model the full-bridge inverter was used because it supplies twice the output voltage as the half bridge and requires less paralleling of devices at high power level. This gives more accurate results with what is expected from the actual drive. The circuit diagram is found in Figure 51 and was taken from the "Power Electronics" Textbook.[30]

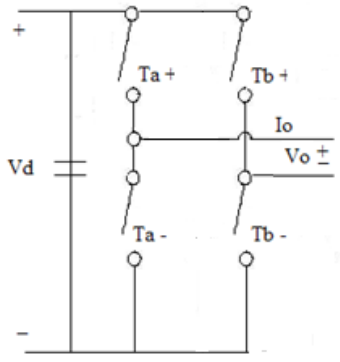

Figure 56: P-Spice model of an inverter.

Because the electrical system is going to be switching back and forth from DC to AC power the inverter switching scheme was designed to produce a square wave. This is accomplished by setting the switches so that while Ta + and Tb – are in the on state, Ta – and Tb + are off. This reverses when the switches are flipped. The output voltage is regulated by the input DC voltage as shown below:

$$V_o = \frac{4}{\pi} V_d \quad 30 \tag{6.1}$$

P-Spice Model

Figure 57 shows the P-Spice implementation of the full-bridge inverter. In order for the current through the inductor to return to 0 amps in each cycle, the duty cycle of the inverter is set to 20%. It operates at a period of 100us. The input and output waveforms for this device are also shown below.

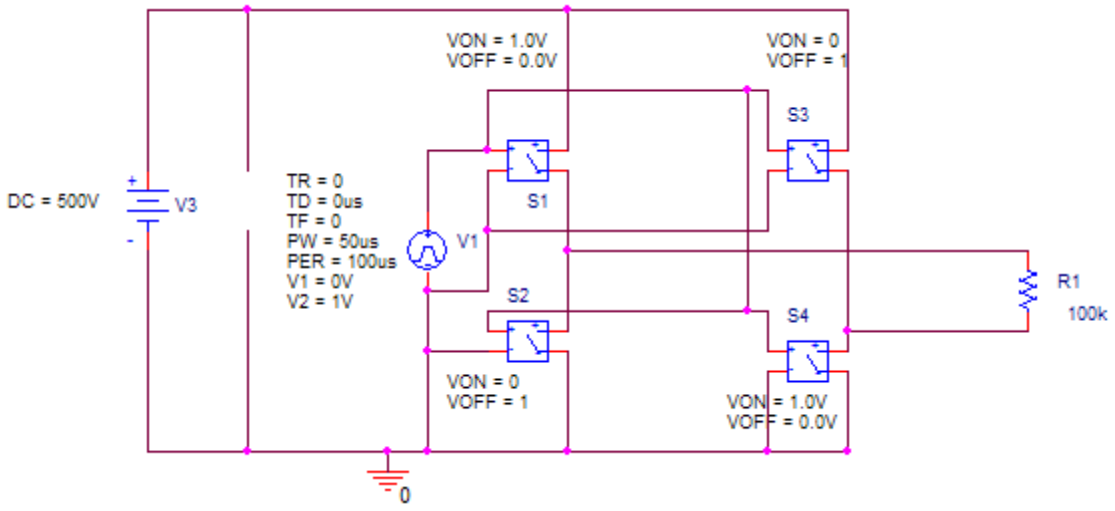

Figure 57: P-Spice model of a full bridge inverter.

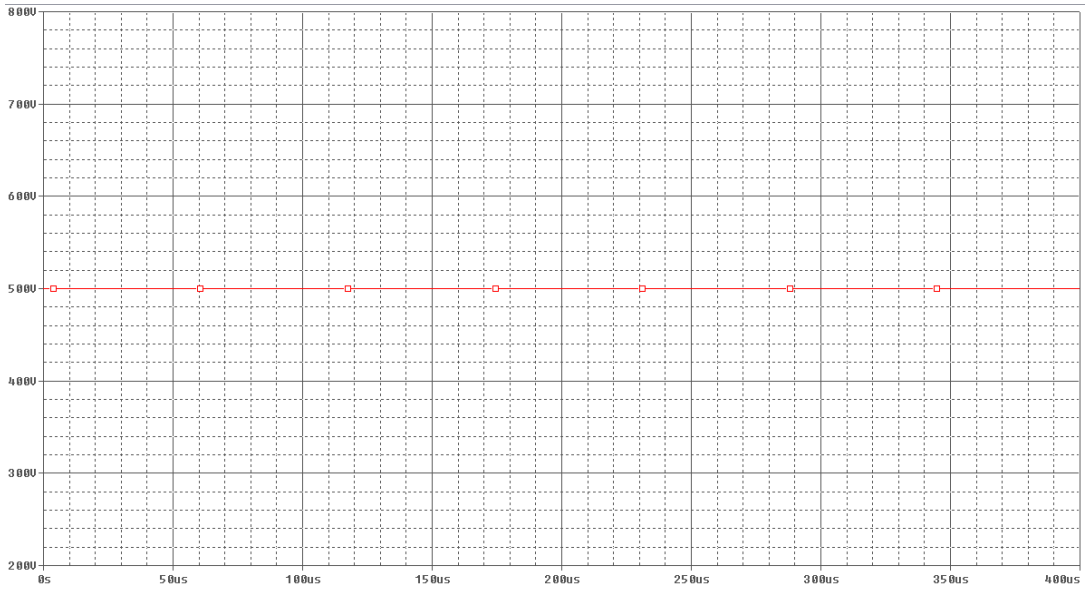

Figure 58: Input voltage to the inverter.

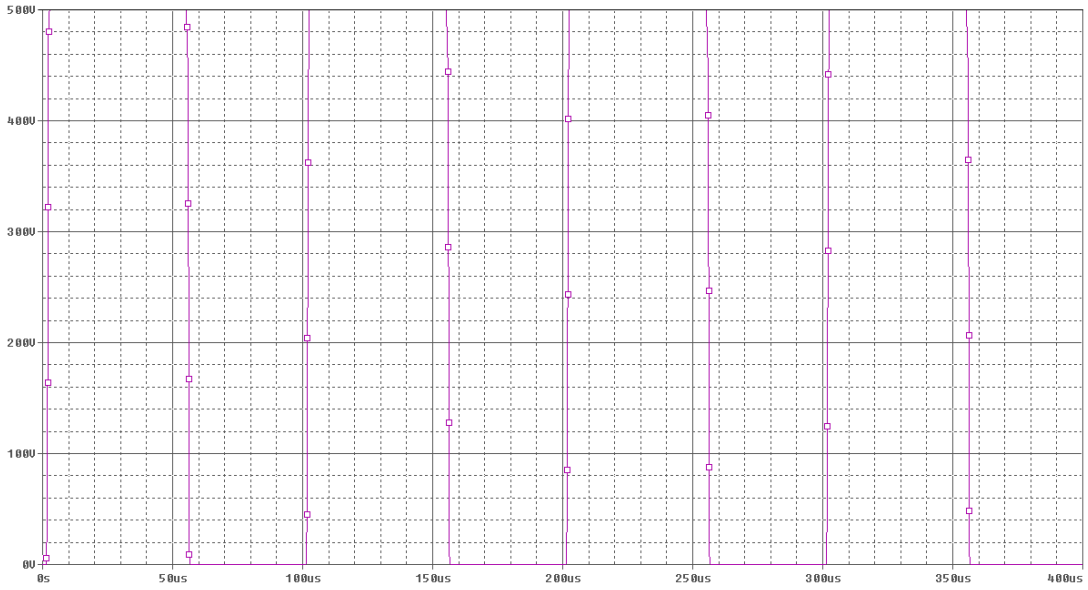

Figure 59: Output voltage of inverter.

From these figures one can see that the model of the inverter successfully changes an AC signal to a DC signal.

6.2.3.2 The rectifier

Figure 60 depicts the P-Spice model for the rectifier. The diodes block the negative current and allow only the positive current through. As a result the AC current from the generator is turned into a DC signal which is then passed to the load resistor.

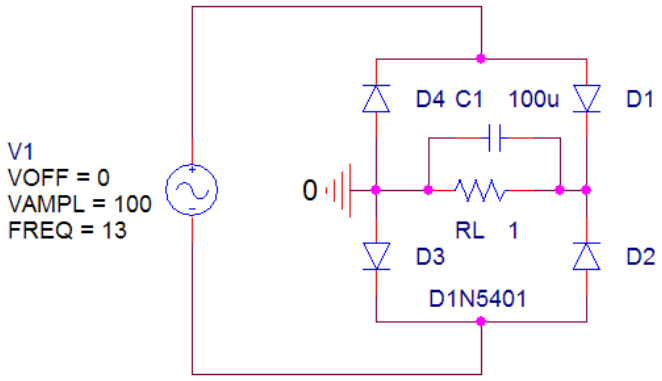

Figure 60: Circuit model of a rectifier.

The source of this model has an amplitude of 100V with a frequency of 13hz. With this input it is expected that the voltage across the load resistor R1 will be a sine wave that goes between zero and 81 volts.

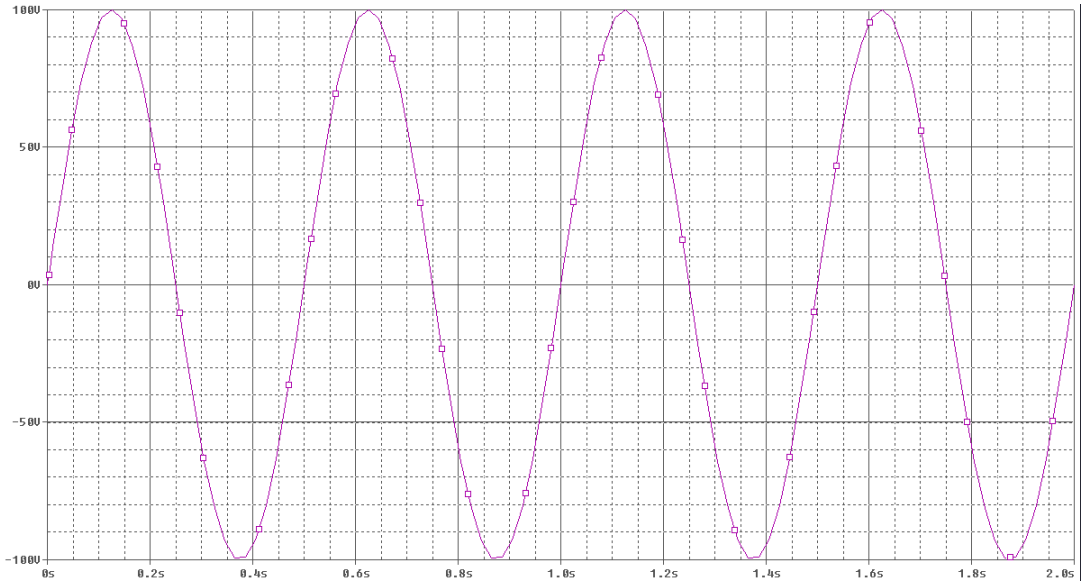

Figure 61: Input voltage for the rectifier.

From the waveform shown below one can see that the ouput amplitude is actually 96 Volts. The difference is due to the resistance of the diodes in the rectifier circuit.

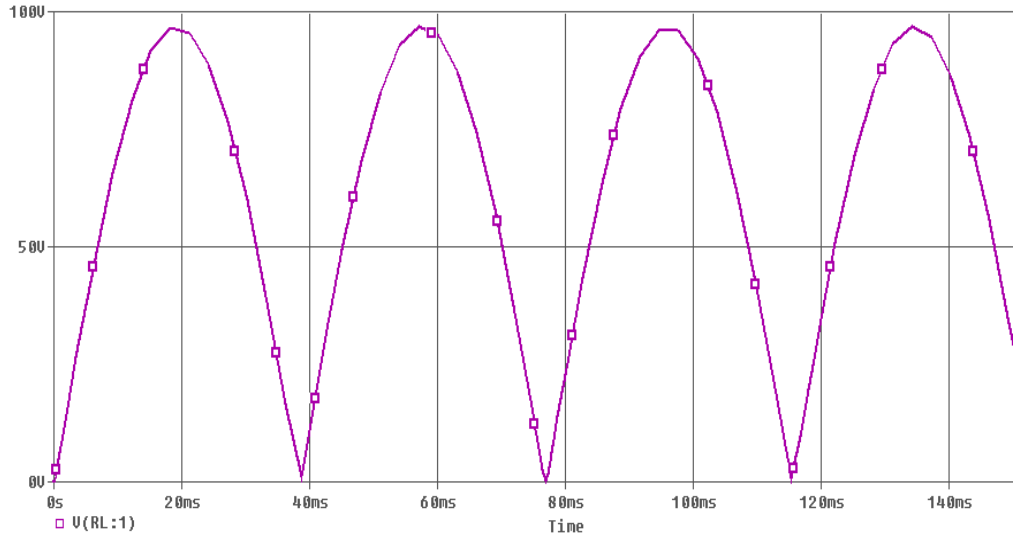

Figure 62: Output voltage from the rectifier.

6.2.4 The induction generator

In order to simplify calculations, in analysis and design of induction motors, the "per-phase equivalent circuit" shown in Figure 58 is often used. In the circuit, R_s and R_r represent the stator and rotor resistances. The inductances of the induction machine are represented as Ls, Lr and Lm where Ls is the inductance of the stator coil, Lr is the inductance of the rotor coil and Lm represents the magnetizing inductance of the motor. The values of these parameters can be found by using a locked rotor and no-load test. However in this case these parameters have been supplied by the manufacturer. They are found below in Table 12.

Table 12: Sumimoto induction machine parameters.

Parameter	Value
Stator Resistance (Rr)	0.1675 ohms
Rotor Resistance (Rs)	0.0998 ohms
Stator Leakage Inductance	1.767 mH
Rotor Leakage Inductance	3.160 mH
Mutual Inductance	66.63 mH

Another important parameter to discuss is the slip of the induction machine. In an induction machine the rotor does not rotate synchronously to the excitation frequency of the stator. This difference is due to the need of a changing magnetic field that will induce the current through the rotor. The slip is defined as:

$$S = \frac{\omega_s - \omega_r}{\omega_s} \tag{6.2}$$

where ω_s represents the angular velocity of the stator current and ω_r represents the angular velocity of the rotor.

In the steady-state AC circuit, current and voltage phasors are used and they are denoted by the underline. From Figure 58 the following parameters can be derived.

- Power consumption in the stator = $I_s^2 R_s$ (6.3)

- Power consumption in the rotor = $\frac{I_r^2 R_r}{s}$ (6.4)

- Produced Torque (per phase) on the shaft $T_s = I_r^2 R_r \left[\frac{P}{2\omega_s} \right]$ (6.5)

  where P is the number of poles on the stator.

This single-phase equivalent model is useful for predicting steady-state performance, but it will not work well for predicting the dynamic behavior of the Sumimoto motor used in this project. Eventually, this model will have to be adjusted to account for the transient response of the system. For now the focus of the P-Spice model that is being developed to simulate the steady-state response of the Ocean Turbine electrical system.

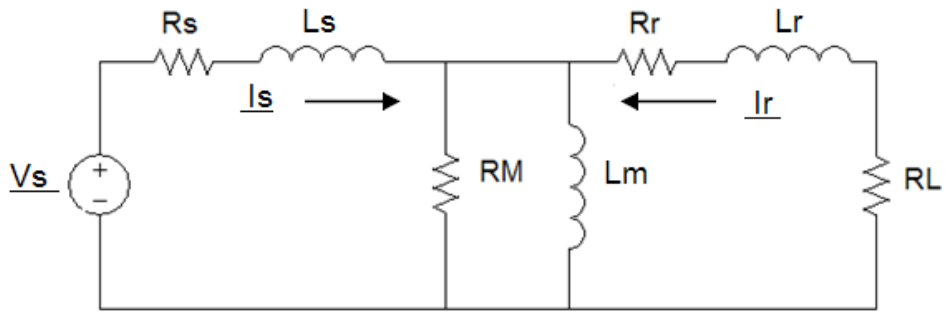

Figure 63: single-phase model of an induction machine.

P-Spice model of the ocean turbine induction generator

The P-Spice model of the induction machine is shown below in Figure 64.

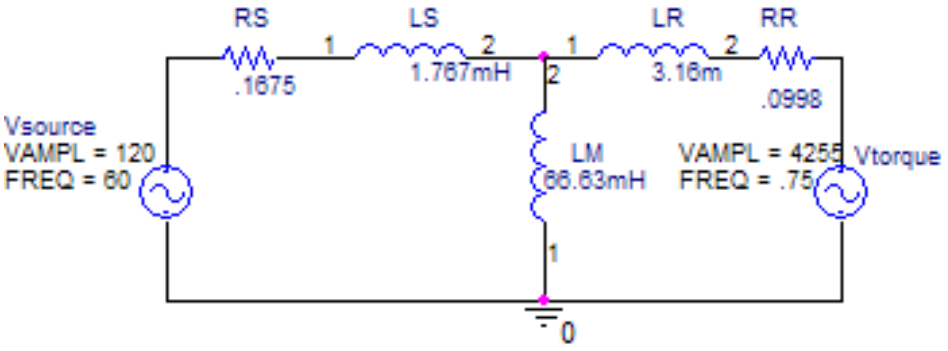

Figure 64: P-Spice model of the induction machine.

This model is built assuming the generator will produce about 20kW to the resistor bank. The Torque required for this power can be found by using the relationship between torque (T), power (P), and the shaft speed (ω).[31]

$$\text{Shaft Torque: } T = I_r^2 R_r \left[\frac{P}{2\omega_s}\right] \tag{6.6}$$

For the Ocean Turbine System:

- The number of poles P = 4
- The shaft speed $\omega_s \approx$ 45 RPM (4.7 rad/sec)
- Power = 10kW
- From these values the shaft Torque T = 4255 Nm
- The units of torque are: $\frac{kgm}{s^2}$
- The units of Voltage are: $\frac{kgm}{s^2 c}$, where C ≈ 1

Because the units of torque and voltage are the same a voltage source can be used to represent the torque on the shaft of the induction machine. This voltage is represented as Vtorque on the P-Spice model. The other values on the model were provided by the manufacturer.

Power quality can be improved in a number of ways. For example the power factor can be changed by adding a capacitor in parallel with the load. The value of the required capacitor can be found by calculating the amount of reactive power necessary to bring up the power factor. The required capacitance can then be found from the equation:

$$Q_{req} = \frac{1}{j\omega c} \tag{6.7}$$

Other power quality parameters can be corrected by changing the settings of the AC drive based upon the source and type of power quality interference. To fix these problems

different strategies can be applied using the software tools that came with the drive. Different parameters will be used on the P-Spice model in order to test the effectiveness of varying strategies in order to choose the best fit for the problem. These are some examples that can be explored further however the focus of this thesis will be in the creation of the P-Spice model.[32]

6.2.5 The induction generator in series with the rectifier

The next step is to combine the induction generator to the rectifier. A box model of the setup is shown in Figure 60. Figure 61 shows the circuit equivalent model of this setup.

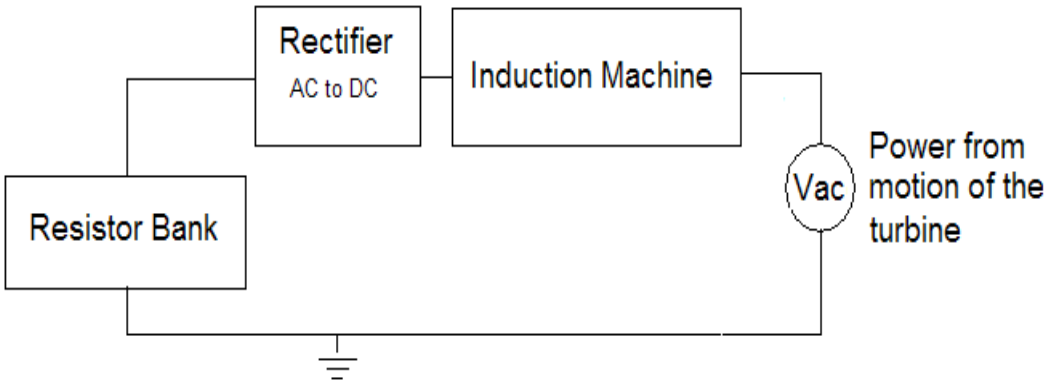

Figure 65: box model of induction generator in series with the rectifier.

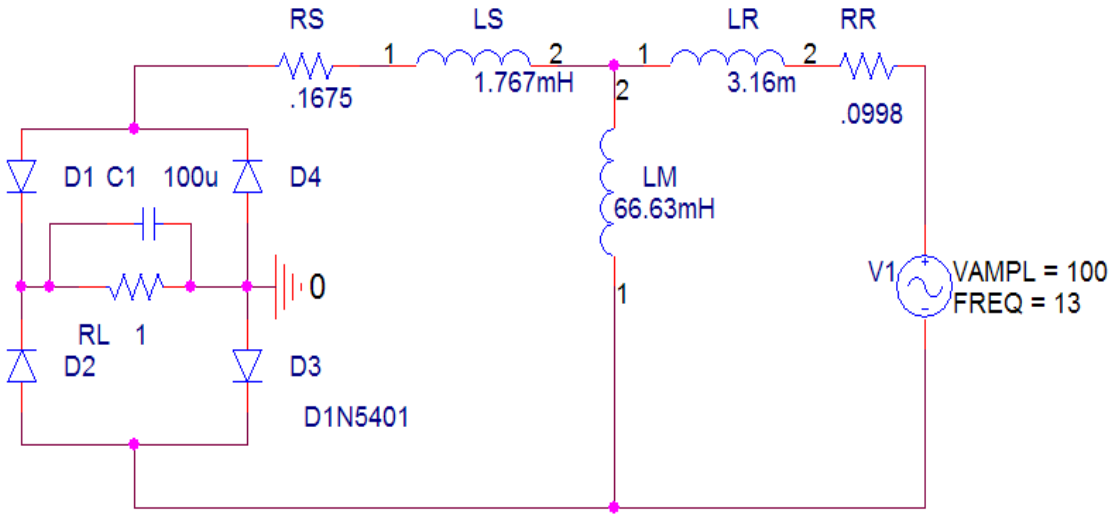

Figure 66: Circuit model of the induction generator in series with the rectifier.

The voltage across RL will be different than that shown in Figure 57 due to the extra resistance that is placed on the induction generator from the rectifier. However this should only affect the amplitude. The voltage across the load resistor in Figure 61 is shown below in Figure 62.

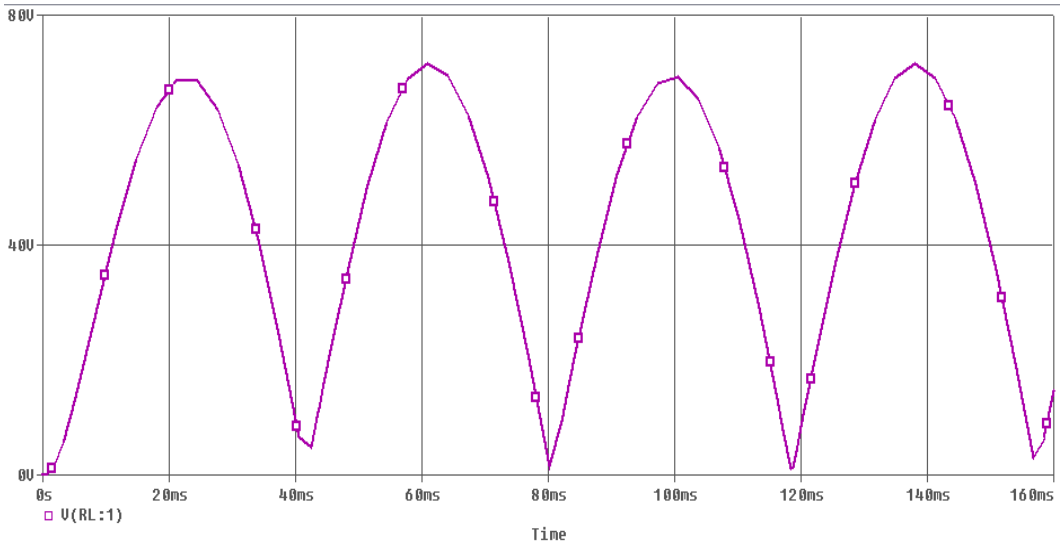

Figure 67: Voltage waveform across the load resistor.

6.2.6 The induction generator in series with the rectifier

Next the inverter was placed in series with a model of an induction motor in order to see the resulting waveform that would exist across the rotor of the induction machine. The rotor shaft is represented here as RL. Initially an AC power source will be used to power the turbine blades. This source will be rectified and then inverted in order to control the initial rotational velocity of the propeller blades. In this phase the three phase induction machine actually functions as motor. The P-Spice model of the input signal, inverter and induction motor is shown here.

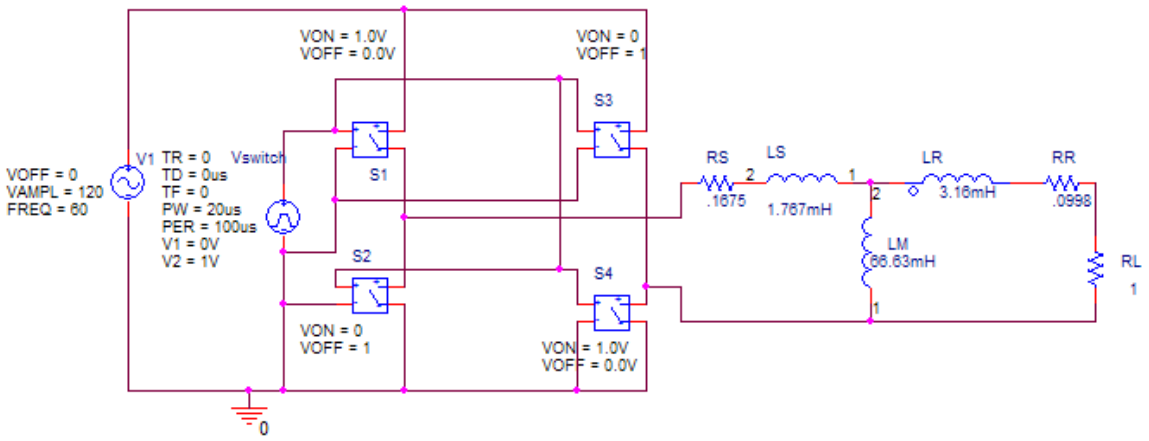

Figure 68: Circuit model of an inverter in series with the induction generator.

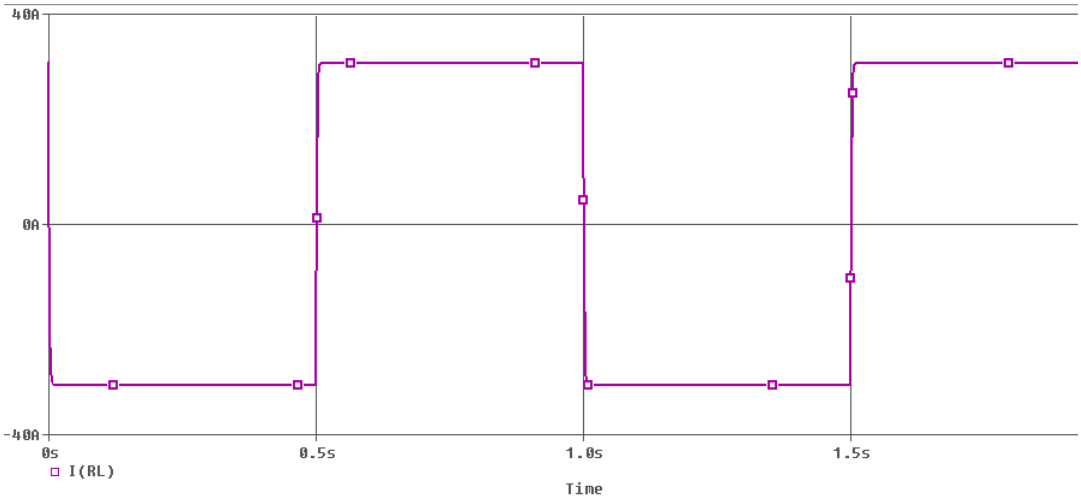

Figure 69: Waveform output from an inverter.

In Figure 69 the voltage was applied to the inverter and the induction machine. The resulting waveform across the rotor is shown here. This shows that the signal will not be degraded as it is passed through the induction machine to the rotor. The waveforms that have been discussed are identical to the waveforms that can be expected from the actual system.

6.2.7 Ocean turbine model

The final step is to put everything together in the model so that it is an accurate representation of Figure 65. The P-Spice circuit model is shown in Figure 70.

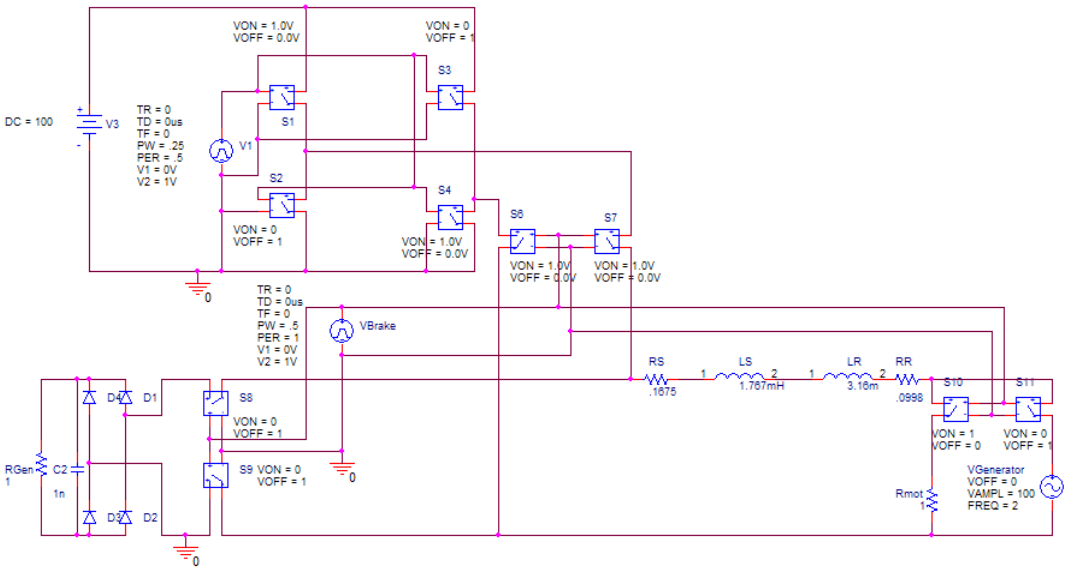

Figure 70: Full P-Spice model of the ocean turbine electrical system.

In this simulation the controller is set to switch between the induction motor and the induction generator a 2 Hz. While functioning as an induction motor the power is delivered to the resistor Rmot which represents the shaft of the induction machine. While in generator mode the power is delivered to RGen which represents the resistor bank that will be used to burn off the power created by the induction generator. The output voltage through Rmot and RGen is shown in Figure 71. One can see that while operating as a motor the output voltage is a square waveform and that while the model is functioning as a generator the voltage across RGen is DC.

Pulse width modulation needs to be applied to the input waveforms so that the square wave will look more sinusoidal. The more sinusoidal waveforms will match the waveforms that are expected in the actual turbine system

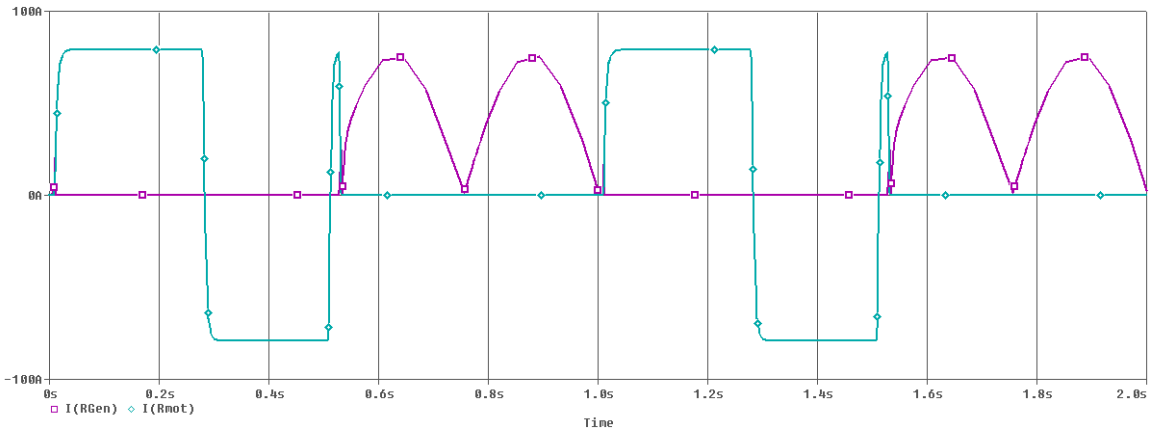

Figure 71: current across R_{mot} and R_{gen} as a function of time.

6.3 Limitations to the model

This P-Spice model represents the ocean turbine system while operating at nominal levels and accurately represents the dynamometer that will be used in testing the system. This model does not take into account variations that will occur within the system. Adjustments will need to be made in order to accurately simulate the system response to changing power levels that will occur as ocean conditions vary.

The model of the AC drive is also missing the controller function. The controller will be used to measure the rotational velocity of the propeller blades and make adjustments as necessary. As this system is defined a model of the controller will also need to be added in order to make this P-Spice model more dynamic.

7 Conclusion

The purpose of this thesis was to develop a system that would collect voltage and current waveforms from various locations in the ocean turbine electrical system. These waveforms were then to be processed in order to calculate various parameters that define the quality of power that is delivered to and generated by the ocean turbine. For this thesis work a system was developed and tested to meet these criteria.

7.1 Power quality measurement

This thesis provides the hardware devices that can be used in monitoring the quality of power generated by the ocean turbine. The devices discussed have been shown to accurately record waveforms for varying power levels as well as sampling rates. These include a power quality sensor board that contains all the sensors that are used to measure the current and voltage waveforms created in the turbine system. These signals are then passed on to NI modules that collect the waveforms and pass them tot eh LabView environment where the data can be processed. These devices have also been shown to accurately collect data for all power levels that are expected in the system.

7.2 Signal processing

From the data provided by the LabView algorithms, the power quality monitoring system discussed in this thesis delivers accurate measurements of the most important values that quantify power quality. These include statistical data on the power waveforms including rms, phase and power values as well as the calculation of frequency and total harmonic distortion. These values are important when quantifying the quality of the power that is developed by the ocean turbine. This system has also shown accuracy in identifying situations in which the level of power quality falls below set standards. The system was shown to be a valuable tool in identifying whether the ocean turbine is a viable source of energy. The system developed, can also be used for machine condition monitoring. In this case if the turbine system begins to fail, the power quality monitoring system will be able to identify these failures as a drop in power quality. When such warnings are given the system should be monitored to find any malfunctions within the turbine system.

From the results of testing, the power quality system developed has been proven to accurately assess the power quality of the ocean turbine system. This setup is recommended for use in the COET ocean turbine project as it will be able to monitor power quality and also provide some data as to the condition of the ocean turbine during operation.

7.3 Power system model

To aid in future development a model of the ocean turbine was developed. This model includes P-Spice modules of each hardware device that are implemented in the ocean turbine setup. This model has been shown to accurately represent the current, voltage and power waveforms that can be expected from the turbine for a set of given conditions. The model developed can be used to test the power response of the system for varying conditions. These conditions can include the state of the ocean current as well as the physical properties of the induction machine. The model can also be used to introduce other factors into the system such as capacitor banks that may be used for the improvement of power quality.

7.4 Future work

7.4.1 Hardware

The next step of this work will be to use the monitoring system to measure the power generated by the induction motor. The power sensor board has been installed and testing can begin as soon as the dynamometer is ready for trials. When this happens the rms voltage and current should be measured against values that are directly calculated from sensors being used in the machine condition monitoring system.

After dynamometer tests are completed the next step will be to implement the system into the turbine itself. This will involve coordination with the staff who are in charge of the safety system of the turbine. It should be noted that the sensor boards were designed with extra connectors so that the safety system could also monitor the voltage and current waveforms present in the system.

7.4.2 Software

Once the system has been implemented into the turbine data will have to be collected and processed to monitor power quality over time. Tests should also be developed to simulate varying ocean conditions in order to test the response of the ocean turbine power system to changes in the ocean environment. As these are developed the alarm system built into LabView should be expanded to include warnings about the hardware. For example if it is found that the windings of the motor begin to degrade, information about the power quality response to that degradation should be collected. From this data a warning should be created that looks for that response and can send a warning about the condition of the windings before failure occurs. This type of warning system can save time and money by identifying problems early so that they can be repaired before any major failures occur. This can be included as part of the machine condition monitoring project.

7.4.3 System Model

The monitoring system needs to be used for the collection of waveform data of the dynamometer. As this data is collected the P-Spice model will need to be adjusted so that the simulated waveforms match the measured waveforms. A controller will also need to be developed that will simulate the control response of the AC drive. This will need to be done as the drive configuration is setup for the operation of the dynamometer. Once this is done a series of tests will need to be developed that introduce faults into the system so that the response can be monitored. Again this could be included as part of the machine condition monitoring project.

8 Glossary of terms

A

Active Power: The average instantaneous power over an integer number of cycles.

B

Base Power: the sum of the rated powers of all generators connected to a system.

C

Compatibility level: A reference value used to compare equipment emission and immunity. This defines the emission and immunity limits.

Compatibility Margin: the ratio between the immunity limit and the emission limit.

Complex impedance: the ratio between complex voltage and complex current.

Current Disturbance: Term to denote that a disturbance originates with the customer and not the network. For any disturbances with the turbine they will be noted as current disturbances.

Current Quality: concerns the deviation of the actual current from the ideal current.

D

Distribution Networks: Transport the electrical energy from the transmission substations to various loads.

Disturbance: Any deviation of current or voltage from the ideal.

E

Electromagnetic compatibility: the ability of a device, equipment or system to function satisfactorily in its electromagnetic compatibility without introducing intolerable electromagnetic disturbances to anything in that environment.

Emission Limit: Lower than or equal to the compatibility level.

Emission Margin: ratio between the emission limit and the compatibility level.

Event: Sudden disturbances with a beginning and an ending.

F

Flicker: Voltage fluctuations between .5 and 25 Hz that cause variations in lighting.

Ferrules: The plastic devices used to connect two wires.

H

Harmonic Distortion: Distortion is the alteration of the original waveform. The harmonic distortion refers to the distortion of the wave due to power in the harmonics of the signal.

I

Ideal Signal: A sinusoidal waveform with constant amplitude and frequency.

Immunity Level: set higher than or equal to the compatibility level.

Immunity margin: the ratio between the immunity limit and the compatibility level.

Inertia constant: the ratio of the rotational energy at nominal speed to the base power of the generator.

Instantaneous power: the flow of energy at any moment in time.

Interference: the degradation of a device, equipment, or system caused by an electromagnetic disturbance.

Interruption: An event with a residual voltage of less than 0.1 pu.

Islanding: Occurs when a section of electrical grid becomes disconnected from the main part of the grid.

N

Nyquist Frequency: the minimum sampling frequency that will assure there is no aliasing.

P

Power Quality: refers to voltage and frequency stability as well as the absence of electrical noise. 2) the measuring and quantifying the performance of a power system. 3) a combination of voltage and current quality.

Power Quality Monitoring: the process of measuring analog currents and voltages to the statistical indices resulting from post-processing.

S

Sag: an event with a residual voltage between 0.1 and 0.9 pu and a duration between 0.5 cycle and 1 minute.

Speed Governor: a control system that delivers a signal to the power station of the generator.

Spinning Reserve: the amount of extra power that can be produced in a matter of seconds.

Stationary Signal: a signal is assumed stationary over a short period of time or block of data.

Stiffness: refers to the ability of a distribution feeder to maintain constant voltage during periods of high current.

Swell: an event with a residual voltage above 1.1 pu.

T

Total Demand Distortion (TDD): the ratio of the rms value of the total harmonic current to the rated current.

Total Harmonic Distortion: the ratio of the sum of the powers of all harmonic components to the power of the fundamental frequency. THD = (Sum of harmonics)/Power in fundamental frequency.

V

Variation: steady-state disturbances that require continuous measurements.

Voltage Disturbance: a disturbance that originates within the network. (Power Grid)

Voltage Quality: concerns the deviation of the actual voltage from the ideal voltage.

Bibliography

[1] Florida State Legislature, “2006 Florida Energy Act,” 2006, http://www.dep.state.fl.us

[2] A.M. El-Zonkoly, Power system model validation for power quality assessment applications using genetic algorithm, Expert Systems with Applications, Volume 29, Issue 4, November 2005, Pages 941-944, ISSN 0957-4174, DOI: 10.1016/j.eswa.2005.06.013.

[3] Danish Wind Industry Association “Wind Turbines and Power Quality Issues” www.windpower.org/en/tour/grid/rein.htm

[4] Justin Sobol, FPL Project Development / Renewable Energy

[5]"Basic AC Drives". Siemens. May 20, 2009 <http://www.sea.siemens.com/step/pdfs/acd_2.pdf>.

[6] "Phoenix EX". Instruction Manual. Niagara Falls: US Drives Inc., 2008.

[7] IEC standards on power: 61000-4-30

[8] Bollen, Math H.J. Irene Y.H. Gu. “Signal Processing of Power Quality Disturbances” IEEE press series on power engineering.

[9] Dugan, Roger C. Surya Santoso, Mark F. McGranaghan “Electrical Power Systems Quality”

[10] X. X. Chen. Wavelet-based methods to detect, locate, quantify, and identify slight deviations of amplitude and phase in power systems. Paper presented at the IEEE Power Engineering Society General Meeting, Toronto, July 2003.

[11] Tom Pantelakis, Electrical Engineer. Florida Atlantic University

[12] NI cRIO-9014 Data sheet: http://www.ni.com/pdf/products/us/cat_2006_8000_161_101_d.pdf

[13] Nilsson, James William. Susan A. Riedel “Electric circuits 7th edition” Pearson Education Inc. 2005

[14] Expert group study on recommended practices for wind turbine testing and evaluation, section 7: Quality of Power, Single Grid-Connected WECS pages 9-10

[15] Santoso, S.; Powers, E.J. “Power Quality assessment via wavelet transform analysis.” Paper no 95, SM 371-5 PWRD

[16] The measuring institute of wind energy institutes. “Power Performance Measurement Procedure” Version 4 November 2006

[17] National Instruments Tutorials “Measuring Power Quality values)

[18] “Power Quality of distributed wind projects in the turbine verification program” J. Green, VandenBosche, Lettenmaier, Randall. NREL/CP-500-30407 September 2001 www.nrel.gov/docs/fy01osti/30407.pdf

[19] FPL Facility Connection Requirements.

[20] V.E. Wagner (Chair). Effects of harmonics on equipment-report of the IEEE task force on the effects of harmonics on equipment. *IEEE Transactions on Power Delivery,* 8(2): 672-680, April 1993.

[21] Liu Min; Li Yalu, "A Method for Calculating Total Harmonic Distortion of Digital Sinusoidal Waveform," *Electronic Measurement and Instruments, 2007. ICEMI 07. 8th International Conference on* vol., no., pp.3-947-3-951, Aug. 16 2007-July 18 2007 URL: http://ieeexplore.ieee.org/stamp/stamp.jsp?arnumber=4351075&isnumber=4350397.

[22] Santoso, S; Powers, E.J.; Grady, W.M/, “Power quality disturbance data compression using wavelet transform methods,” *Power Delivery, IEEE Transactions* on vol.12, no3, pp.1250-1257, Jul 1997

[23] Y. Baghouz (chair), Time-Varying harmonics: Part 2-harmonic summation and propagation. *IEEE Transactions on Power Systems,* 17(1): 279-285, January 2002.

[24] A. van Jounne and B.B. Banerjee. Assessment of voltage unbalance. *IEEE Transactions in Power Delivery,* 16(4): 782-790, October 2001.

[25] [N1] Interpreting IEEE standard 519 and meeting its harmonic limits in vfd application.

[26] Xiao Xiangning; Tao shun; Tianshu, B.; Xu Yonghai, “study on distribution Reliability considering voltage Sags and Acceptable Indices,: Power Delivery, IEEE Transactions on, vol. 22, no. 2, pp. 1003-1008, April 2007

[27] S.K. Mitra. *Digital signal Processing-A Computer based approach*. McGraw-Hill, Boston, 2001

[28] Ifeachor, Emmanuel C. Barrie W. Jervis “Digital Signal Processing, a practical approach” Prentice Hall 2002

[29] Nuding, Ted. U.S. Drives, Inc. tnusdrivesinc@yahoo.com

[30] Mohan, Undeland, Robbins. "Power Elecronics: converters, applications and design."

[31] M. N. Mansouri, M. F. Mimouni, B. Benghanem, M. Annabi, Simulation model for wind turbine with asynchronous generator interconnected to the electric network, Renewable Energy, Volume 29, Issue 3, March 2004, Pages 421-431, ISSN 0960-1481, DOI: 10.1016/S0960-1481(03)00225-8. (http://www.sciencedirect.com/science/article/B6V4S-49JX7D4-1/2/99d80f47d33aae5d6fc08ba1dd53fa24).

[32] Zill, Dennis G. Michael R. Cullen "Differential Equations with Boundary-Value Problems" Cullen 5th edition 2001.

[31] Greenberg, Michael D. "Advanced Engineering Mathematics 2nd edition" Prentice Hall, Upper Saddle River, NJ 1998.

[32] Boylestad, Robert L. Louis Nashelsky "Electronic Devices and Circuit Theory ninth edition" Prentice Hall, 2006.

[33] Jacob, J. Michael "Power Electronics: Principles and Applications" Delmar Publishing 2002.

[34] Cooper, George R., Clare D. McGillem "Probabilistic Methods of Signal and System Analysis" Oxford University Press 1999.

[35] Reliability standards for the bulk electric Systems of North America. North American Electric Reliabilty Corporation, November 2009.

[36] IEEE recommended practice for monitoring electric power quality *IEEE Std ; 1159-1995 Volumes 1159-1995 of IEEE Std*, Institute of Electrical and Electronics Engineers.

[37] Ignall, Ross-Dranetz-BMI**,** Mark McGranaghan – Electrotek Concepts
Mark Figor – DHL. "Power Quality Monitoring for High Reliability Systems"
http://www.reliabilityweb.com/excerpts/excerpts/power_quality_for_high_reliability.pdf

[38] Melhorn, Christopher J. Mark F. McGranaghan. "Interpretation and Analysis of Power Quality Measurements" http://www.dranetz-bmi.com/pdf/interpret.pdf